THE ROLE OF THE A1 SUBUNIT IN THE ACTIVITY OF SHIGA TOXINS

by

DEBALEENA BASU

A dissertation submitted to the

Graduate School-New Brunswick

Rutgers, The State University of New Jersey

In partial fulfillment of the requirements

For the degree of

Doctor of Philosophy

Graduate Program in Plant Biology

Written under the direction of

Nilgun Tumer

And approved by

_____

_____

_____

_____

New Brunswick, New Jersey

[OCTOBER 2016]

ABSTRACT OF THE DISSERTATION

The role of the A1 subunit in the activity of Shiga toxins

by DEBALEENA BASU

Dissertation Director:

Nilgun Tumer

Shiga toxin (Stx) producing *E.coli* infections can lead to life-threatening complications, including hemorrhagic colitis and hemolytic uremic syndrome (HUS). Stx1 and Stx2 are AB_5 toxins consisting of an enzymatically active A subunit and a pentamer of receptor binding B subunits. Stx2-producing *E.coli* strains are more frequently associated with HUS than Stx1-producing strains. The role of the A subunits in the increased potency of Stx2 has not been fully investigated. This study using purified A1 subunits, provide the first direct evidence that the higher affinity for ribosomes in combination with higher catalytic activity towards the SRL allows Stx2A1 to depurinate ribosomes, inhibit translation and exhibit cytotoxicity at a significantly higher level than Stx1A1 in yeast and human cells. To determine if conserved arginines at the distal face of the active site contribute to the higher affinity of Stx2A1 for the ribosome, Arg172, Arg176 and Arg179 in Stx1A1 and Stx2A1 are mutated. It is seen that Arg172 and Arg176 are more important than Arg179 for depurination activity and toxicity of Stx1A1 and Stx2A1.

Mutation of at least two of the three arginines is required to significantly reduce depurination by Stx2A1 *in vitro* and in cells in yeast and mammalian cells. Conserved arginines at the distal face of the active site are critical for interactions of Stx1A1 and Stx2A1 with the stalk, while a conserved arginine at the active site is critical for non-stalk specific interactions with the ribosome. Mutations at conserved arginines at either site reduced ribosome interactions of Stx1A1 and Stx2A1 similarly, indicating that they do not contribute to the higher affinity of Stx2A1 for the ribosome. Interchanging residues E60 and 61 in Stx1A1 and Y60 and Q61 in Stx2A1 that are located away from the active site and ribosome stalk binding site, resulted in small but significant increase in depurination level of E60Y/E61Q for Stx1A1 and a decrease in depurination level of Y60E/Q61E of Stx2A1 *in vivo* in yeast. A larger difference may be observed if more than two residues are simultaneously altered to change the electrostatic charge distribution of Stx1A1 and Stx2A1 sufficiently.

DEDICATION

This thesis is dedicated to my pillars of strength, my parents Sadhana Basu & Dilip Kumar Basu and my grandfather Bholanath Ghosh, whose love, encouragement and support have made this document possible.

ACKNOWLEDGEMENTS

I would first like to express my sincere gratitude to my advisor, Prof. Nilgun Tumer, who supported me with her patience, motivation, enthusiasm, and knowledge of science. Her guidance pushed me to strive for excellence in research. I would also like to thank my thesis committee members, Prof. James White, Prof. Faith Belanger, and Prof. Nancy Woychik for their encouragement, insightful comments and questions. I am thankful to Prof. Derek Gordon and the Department of Genetics for supporting this thesis through 4 years of teaching assistantship.

I am grateful to my fellow students and lab members who I've worked beside over the course of my doctoral research for providing many stimulating and intellectual discussions, assistance with research and making my work and stay enjoyable. A special thank you to Xiao-Ping, for her constant advice and guidance, John for being the most helpful human being, Mike for all his patient mentorship, and Jenny for her help and intellectual discussions. I am especially indebted to Anwar, Qing, and Yijun for growing up and growing old with me in the lab, Dan and Matt for all the interesting conversations, and Kerrie whose support, intelligence, and compassion have been incredible. A special thank you to Helen and Monica whom I had the pleasure of mentoring and who made my daily job extremely pleasurable. Special thanks also goes out to Sakthi Poobala Chandran for being a constant companion and the best apartment-mate through the ups and downs during my Ph.D.

Last, but not the least, I am eternally thankful to my family – my sisters, Dipanwita Basu and Debomita Basu, and my brother-in-laws, Avik Ghosh, Ashish Ambwani, and Shirsho Biswas for setting the bar of excellence so high and for their absolute love and encouragement. My Ph.D. would have been a lot more difficult without my husband, Shaurjo Biswas, who has been a pillar of strength and outrageously loving and supportive, putting up with my crazy work hours, cooking the most delicious food, and helping and supporting during good times and bad.

TABLE OF CONTENTS

LIST OF FIGURES

SUPPLEMENT

LIST OF TABLES

SUPPLEMENT

CHAPTER 1: Introduction

RIBOSOME INACTIVATING PROTEINS

Ribosome inactivating proteins (RIPs) are a class of proteins that irreversibly damage the ribosome catalytically, by modifying the large rRNA and inhibiting translation (Nielsen and Boston 2001, Stirpe 2004). RIPs are present throughout the plant kingdom, including in cereals such as wheat and barley. These proteins are thought to be produced for defense against invading pathogens (Peumans, Hao et al. 2001). They also occur in certain fungi and bacteria (Nielsen and Boston 2001). The enzymatic activity of RIPs involves *N*-glycosidation to remove a specific adenine corresponding to residue A_{4324} in the 28S rRNA of the large ribosomal subunit (Nielsen and Boston 2001, Stirpe 2004). This adenine lies within a 14-nucleotide region that is known as the α-sarcin/ricin loop (SRL) and is conserved in all kingdoms. A GAGA sequence, in which the first A is the RIP substrate forms the core of a putative tetraloop surrounded by a short base-paired stem. Irreversible modification of the target A residue blocks elongation factor (EF)-1- and EF-2-dependent GTPase activities and renders the ribosome unable to bind EF-2, thereby blocking translation (Nielsen and Boston 2001, Parente, Conforto et al. 2008).

CLASSIFICATION OF RIPs

The RIPs are divided into three types based on their physical properties. Type 1 RIPs such as pokeweed antiviral protein (PAP), trichosanthin and saporin are single chain, highly basic monomeric enzymes approximately 30 kDa in size (Nielsen and

Boston 2001, Stirpe 2004, Chan, Chu et al. 2007). They are relatively non-toxic to cells and animals although they inhibit cell-free protein translation. They are commonly found in vegetables such as tomato, spinach and pumpkin as well as in stable crops like wheat, barley and maize (Prestle, Schönfelder et al. 1992, Ishizaki, Megumi et al. 2002, Barbieri, Polito et al. 2006). Type 2 RIPs on the other hand consist of an A chain and variable number of B chains. The A chain, is the active chain, while the B chain can bind receptors on the surface of eukaryotic cells and mediate retrograde transport of the A-chain to the cytosol. Potent toxins like ricin, abrin and Shiga toxin fall into this category (Nielsen and Boston 2001, Stirpe 2004). While ricin has a 32 kDa A chain and a 34 kDa B chain, Shiga toxins have a 32 kDa A chain and five 7.7 kDa B chains. Type 3 RIPs are synthesized as inactive precursors (proRIPs) that require proteolytic processing events to occur between amino acids involved in formation of the active site. These RIPs are much less prevalent than type 1 or type 2 RIPs. Such types of RIPs have been isolated from maize and barley. Because of their potent and selective toxicity, RIPs have garnered interest as biological weapons, and for use in antiviral and anticancer therapy (Nielsen and Boston 2001, Stirpe 2004).

SHIGA TOXINS

Shiga toxin producing *E.coli* (STEC) strains such as *E.coli* O157:H7 as well as other serotypes are the major causative agents of severe gastroenteritis, which can lead to life-threating complications including hemorrhagic colitis (HC) and hemolytic uremic syndrome (HUS) (Boerlin, McEwen et al. 1999, Scallan, Hoekstra et al. 2011). HUS is the most common cause of renal failure in children in the US (Siegler and Oakes 2005).

The recent multi-state outbreak of *E.coli* O157:H7 in the US and a HUS outbreak in Germany in 2011 highlight the public health impact of this pathogen (Bielaszewska, Mellmann et al. 2011, Frank, Werber et al. 2011, Karch, Denamur et al. 2012, Kaper and O'Brien 2014). STEC strains produce Shiga toxin 1 (Stx1) and/or Shiga toxin 2 (Stx2) or variants of either toxin. *E. Coli* O157:H7 strains carrying Stx2 are more virulent and are more frequently associated with HUS (Pickering, Obrig et al. 1994, Nataro and Kaper 1998, Manning, Motiwala et al. 2008). However the molecular basis for the higher potency of Stx2 is unknown. Although extensive research is being undertaken to develop effective vaccines and therapeutics to protect against HUS, there are no current therapies available. In order to develop inhibitors against Shiga toxin, there is a need for better understanding of their underlying mechanism of toxicity.

Shiga toxin (Stx) from *Shigella dysenteriae* and Stx1 (Stx1) and 2 (Stx2) from Shiga toxin-producing *Escherichia coli* (STEC) are a family of structurally and functionally related proteins (Bergan, Lingelem et al. 2012, Kaper and O'Brien 2014). Stx, Stx1 and Stx2 are ribosome inactivating proteins (RIPs), a class of proteins that irreversibly damage the ribosome catalytically by modifying the large rRNA and inhibiting protein synthesis (Nielsen and Boston 2001, Stirpe 2004, Zhabokritsky, Kutky et al. 2010, May, Yan et al. 2013, Stirpe 2013). RIPs are *N*-glycosidases that remove a specific adenine from the highly conserved α-sarcin/ricin loop (SRL) in the 28S rRNA of the large ribosomal subunit. Irreversible modification of the target adenine blocks elongation factor (EF)-1- and EF-2-dependent GTPase activity and renders the ribosome unable to bind EF-2, thereby blocking translation (Clementi, Chirkova et al. 2010, Shi, Khade et al. 2012) .

STRUCTURE OF SHIGA TOXINS

Stx derives its name from the dysentery causing bacteria, *Shigella dysenteriae*, which was first described by Kiyoshi Shiga in 1898. While Stx from *S. dysenteriae* differs from Stx1 by one amino acid (Strockbine, Jackson et al. 1988, Johannes and Römer 2010), Stx1 and Stx2 have only 56% amino acid similarity and are antigenically distinct (Strockbine, Marques et al. 1986, Calderwood, Auclair et al. 1987, Jackson, Neill et al. 1987). STEC can produce either one type of toxin or a combination of variants of one or both types of toxin (Karch, Tarr et al. 2005). Stx1 and Stx2, which are also referred to as Stx1a and Stx2a, are type II RIPs (Scheutz, Teel et al. 2012), which consist of a catalytically active A chain associated with a pentamer of B subunits responsible for the binding of the Shiga toxins to their common cellular receptor, globotriaosylceramide (Gb3) (Stein, Boodhoo et al. 1992, Fraser, Chernaia et al. 1994). The B subunits (7.7 kDa each) form a central pore which harbors the C-termini of the A subunit (Fraser, Fujinaga et al. 2004). The crystal structure of the Stx1 B subunit pentamer, bound with Gb3 shows that each B monomer contains three distinct binding sites for the glycan component of Gb3, referred to as P^k trisaccharide, α-D-Gal*p*-(1-4)-β-D-Gal*p*-(1-4)-β-D-Glc*p*-(1-O) for a total of 15 sites (Ling, Boodhoo et al. 1998). Of these 3 binding sites (labeled 1-3), site 2 has the highest occupancy of electron density defining the position of the trisaccharide, while site 1 has the lowest (Ling, Boodhoo et al. 1998, Shimizu, Sato et al. 2007). The only known exception to this Gb3-dependence of Shiga toxins is for the Stx2 variant Stx2e, which exhibits specific affinity for globotetraosylceramide (Gb4) (DeGrandis, Law et al. 1989, Samuel, Perera et al. 1990), although Stx1 and Stx2 can bind to Gb4 weakly (Nakajima, Kiyokawa et al. 2001). Recently, the crystal structure of Stx2 bound

to a P^k derivative has been published. This structure showed that only two of three previously identified binding sites on the B_5 pentamer was functional in Stx2, indicating that there are differences in receptor binding between Stx1 and Stx2a (Jacobson, Yin et al. 2014).

The A subunit of Shiga toxin consists of A1 and A2 chains which are bound together by a disulphide bond between C242 and C261 forming a loop (van Deurs and Sandvig 1995). The X-ray crystal structures of *Shigella* Stx and Stx2 are highly similar (Fraser, Chernaia et al. 1994, Fraser, Fujinaga et al. 2004). However, structural differences have been identified between Stx1 and Stx2. In Stx1, part of the active site is blocked by the A2 chain, while it is accessible in Stx2 (Fraser, Fujinaga et al. 2004). The active site of Stx2 is accessible to the adenine substrate and Stx2 cleaves the adenine when it is crystallized in the presence of adenosine (Fraser, Cherney et al. 2006). In the crystal structure, the A subunit in Stx2 is in a different orientation with respect to the B subunit, which may affect receptor affinity of Stx2. The C-terminus of Stx2 extends through the pore formed by the B pentamer, which is thought to interfere with receptor binding (Fraser, Fujinaga et al. 2004). However, it is not known if the A subunits contribute to the interaction of the holotoxins with the receptor and whether the A subunit interferes with Gb3 binding. Stx1 and ricin have been shown to interact with human neutrophils, which do not express Gb3 or Gb4, through their A subunit without inducing their internalization (Arfilli, Carnicelli et al. 2010). TLR4 has recently been identified as the receptor that recognizes the A subunits of Stx1 and Stx2 in human neutrophils (Brigotti, Carnicelli et al. 2013).

Once the toxins bind the globotriaosylceramide (Gb3) receptor, they are endocytosed by a clathrin-dependent or independent pathway (Sandvig and van Deurs 2005, Bergan, Lingelem et al. 2012). They then undergo retrograde transport to the Golgi apparatus and then to the endoplasmic reticulum (ER). The active A1 subunit is cleaved enzymatically from the A_2-B5 complex (van Deurs and Sandvig 1995). The cleavage occurs between R251 and M252 in Shiga toxin and Stx1 and between R250 and A251 in Stx2 by the furin protease. After cleavage, the A1 fragment remains bound to the A2 fragment through the disulphide bond. The A1 chain is then released from the A2-B_5 complex by reduction of the disulfide bond in the ER and undergoes retrotranslocation from the ER into the cytosol where it depurinates the ribosome and inhibits protein synthesis (Sandvig and van Deurs 2005, Bergan, Lingelem et al. 2012).

CATALYTIC ACTIVITY AND CYTOTOXICITY OF STX1 AND STX2

Differences in cytotoxicity

An extensive review on the pathophysiology of Stx-related disease in different animal models can be found in and is briefly described here (Mayer, Leibowitz et al. 2012). Epidemiological studies suggest that majority of the HUS-associated fatalities are caused by *E.coli* O157:H7 strains carrying Stx2 (Pickering, Obrig et al. 1994, Nataro and Kaper 1998, Manning, Motiwala et al. 2008). Previous studies using Shiga toxins have shown that while Stx2 is more potent in animal models, Stx1 is more toxic to Vero cells (Tesh, Burris et al. 1993, Siegler, Obrig et al. 2003). The 50% lethal dose for purified Stx2 was 400-fold lower than for Stx1 in a mouse model, and only Stx2-treated mice developed renal complications and death (Wadolkowski, Sung et al. 1990, Tesh, Burris et

al. 1993). However, animal models have limitations compared with the observations from humans and do not replicate the disease in humans. Nonhuman primate models (Baboon) showed renal damage consistent with HUS upon intravenous injection of the toxins. Treatment of non-human primates with four doses of 25 ng/kg Stx2 caused HUS, while an equal dose of Stx1 had no effect (Siegler, Obrig et al. 2003). In another study comparison of the effects of the two toxins showed interesting differences, including different proinflammatory responses and different timing with delayed organ injury after Stx2 challenge (Stearns-Kurosawa, Collins et al. 2010). Baboons treated with Stx1 developed HUS within 2 to 3 days, while those with Stx2 took longer (3-5 days), indicating the role of other factors in producing delayed renal injury upon challenge by Stx2. Furthermore, Stx1 incited a stronger proinflammatory response earlier, while the proinflammatory response induced by Stx2 was gradual and delayed by several days (Stearns-Kurosawa, Collins et al. 2010). A subsequent study using baboon models showed that both Stx1 and Stx2 could affect kidney function. Although Stx2 was found to cause more severe damage to the kidney than Stx1, the damage inflicted on the kidney by Stx1 was significant (Stearns-Kurosawa, Oh et al. 2013).

In comparison to animal models studies in Vero cells suggested that the cytotoxicity of Stx1 is 10-fold greater than Stx2 (Tesh, Burris et al. 1993). The basis for the differential toxicity of Stx1 and Stx2 in animal models versus mammalian cell lines is unknown. Shiga toxins trigger endothelial damage in kidney and brain by targeting Gb3. However, differences have been observed in the sensitivity of endothelial cells to Stx1 and Stx2. The current knowledge of endothelial cell damage caused by Stx1 and Stx2 is reviewed in (Bauwens, Betz et al. 2013). Stx2 had a higher potency for human renal

microvascular endothelial cells (HRMEC) than to human umbilical vein endothelial cells (HUVEC), where toxicity of Stx1 and Stx2 was similar (Louise and Obrig 1995). These results indicated selective sensitivity of renal endothelial cells to Stx2 although the renal endothelial cells possessed fewer Gb3 receptor binding sites for Stx2 than Stx1(Louise and Obrig 1995). The Stx receptor distribution in the different renal cell populations and the sensitivity of the different kidney cell types to Stx1 and Stx2 is reviewed in (Bergan, Lingelem et al. 2012). Comparison of cellular injury induced by Stx1 and Stx2 in human brain microvascular endothelial cells (HBMEC) and HUVEC derived EA.hy 926 macrovascular endothelial cells indicated that these cell lines had differential susceptibility to the toxins. HBMEC cells were over 1000-fold more susceptible to Stx2, while EA.hy 926 cells were around 10-fold more susceptible to Stx1 (Bauwens, Bielaszewska et al. 2011). Stx1 caused both necrosis and apoptosis, while Stx2 induced mainly apoptosis in both cell lines (Bauwens, Bielaszewska et al. 2011). The basis for the differential susceptibility of endothelial cells to Stx1 and Stx2 is not well understood. Holotoxin stability, enzymatic activity and receptor affinity were proposed as potential factors contributing to the differential toxicity. In addition, the cytotoxicity comparisons between Stx1 and Stx2 in animals and cells are critically dependent on the specific batches of toxin used and can vary accordingly.

The B subunits of Stx1 and Stx2 have been hypothesized to play an important role in mediating the differences in potency. The B subunits of Stx1 and Stx2 display differences in receptor recognition, as well as in the number of potential binding sites (Flagler, Mahajan et al. 2010, Fuller, Pellino et al. 2011). Studies in Vero cells demonstrated that Stx1 has a higher affinity for the Gb3 receptor (Head, Karmali et al.

1991, Tesh, Burris et al. 1993, Lingwood 1996, Zumbrun, Hanson et al. 2010). Using purified Gb3, it was shown that Stx1 has a 10-fold higher affinity for Gb3 compared to Stx2 (Head, Karmali et al. 1991). It has been suggested that Stx1 might bind to Gb3 variants in the lung, preventing it from reaching more susceptible organs such as the kidneys, whereas Stx2 binds preferentially to Gb3 variants in kidney. As a result Stx1 shows decreased binding to kidney cells that are the main targets for lethality in mice (Rutjes, Binnington et al. 2002). Analysis of binding kinetics to the glycolipid receptor analog using surface plasmon resonance (SPR) showed that Stx1 bound to the receptor analog better than Stx2 and had faster association and dissociation rates (Nakajima, Kiyokawa et al. 2001). These results suggested that the differences in binding kinetics and affinity of the B subunits for the Gb3 receptor might be responsible for the greater toxicity of Stx1 to Vero cells.

The B subunits of Stx1 and Stx2 also display differences in structural stability (Karve and Weiss 2014). The B pentamer of Stx1 was more stable than the B pentamer of Stx2 and bound the receptor with higher affinity than the B pentamer of Stx2 (Karve and Weiss 2014). Moreover, while Stx1B subunits were able to bind glycolipids only as a stable pentamer, Stx2B subunits bound to glycolipids in lower oligomeric states (Karve and Weiss 2014). These results suggested that differences in receptor affinity and receptor binding preferences might contribute to the differential toxicity of Stx1 and Stx2 by affecting their targeting to susceptible tissues.

Stx A/B subunit chimeras, where the A and B subunits of the two toxins have been interchanged, have been used to study the contribution of the individual A and B subunits to toxicity (Head, Karmali et al. 1991). The holotoxin as well as the chimeric toxins were

used in mouse and in Vero cells to differentiate the roles of the subunits in toxicity (Head, Karmali et al. 1991, Tesh, Burris et al. 1993). However, the chimeric toxins were usually found to be less stable than the holotoxins due to incorrect folding (Head, Karmali et al. 1991) or showed equivalent cytotoxicity (Ito, Yutsudo et al. 1988). Chimeric toxins, created by operon fusions displayed cytotoxicity intermediate to Stx1 and Stx2 (Shimizu, Sato et al. 2007) or did not produce a functional chimera (Weinstein, Jackson et al. 1989). Therefore, clear conclusions regarding the role of each subunit in toxicity could not be deduced from these studies. A recent study used the A_2 subunit along with the B subunit to increase the stability of the chimeric toxin (Russo, Melton-Celsa et al. 2014). The binding of the chimeric toxins to the Gb3 receptor and their translocation through the monolayers of the polarized HCT-8 cells were dependent on the origin of the B subunit, and the chimeric toxin with the Stx1B subunit had a higher affinity for the receptor than the Stx2B chimera. The toxicity of the chimeric toxins to Vero and HCT-8 cells indicated the importance of the origin of the B subunit although the B subunit accounted for less than 50% of the differential toxicity for Vero cells (Russo, Melton-Celsa et al. 2014). Perhaps, due to the instability of the chimeric toxins at pH 3, the oral administration of the chimeric toxin where the A subunit was from Stx1 in mice required at least 10 times more toxin as compared to native Stx2, while Stx1 or the chimeric toxin where the A subunit was from Stx2 failed to show any mortality in mice, even at a very high concentration. This study highlighted the importance of the B subunit in the differential toxicity of Stx1 and 2. The differential lethality in mouse was thought to take place at the level of toxicity to the kidney (Russo, Melton-Celsa et al. 2014). However, although *in vivo* results indicate that the B subunits are involved in differences

in the severity of the intoxication, they do not rule out a potential role for the A subunits in the differential toxicity of Stx1 and Stx2. The critical question regarding why Stx2 is more potent than Stx1 *in vivo* still remains unanswered.

Differences in catalytic activity

The A subunits of Shiga toxins and ricin play a critical role in the toxicity of each toxin. They have the same catalytic activity and show conservation in amino acids at the active site. Mutagenesis studies identified Glu167, Arg170, Tyr77, Tyr114, Trp203 and Arg205, which are critical for the catalytic activity and are conserved between Stx1 and Stx2 (Hovde, Calderwood et al. 1988, Jackson, Deresiewicz et al. 1990, Yamasaki, Furutani et al. 1991, Deresiewicz, Austin et al. 1993, Skinner and Jackson 1997, Di, Kyu et al. 2011). Current knowledge about the mode of action of the A subunits is obtained from studies with either cultured cell lines or *in vitro* systems. *In vivo* studies at the molecular level or at the level of the whole organism are limited due to the extreme cytotoxicity of these toxins and the lack of available model systems. Using the yeast, *Saccharomyces cerevisiae* as a model, we identified the amino acids critical for the cytotoxicity of Stx1A and Stx2A and showed that the activity of the A subunits can be differentiated (Di, Kyu et al. 2011). The results showed that Asn75 and Tyr77 were more critical for the depurination activity of Stx2A, while Arg176 was more critical for the depurination activity of Stx1A. Analysis of solvent accessible surface areas indicated that Asn75 and Tyr77 were more exposed in Stx2A, while Arg176 was more exposed in Stx1A (Di, Kyu et al. 2011). Arg176 was subsequently shown to be critical for ribosome binding of Stx1A1 (McCluskey, Bolewska-Pedyczak et al. 2012), suggesting that there may be differences in the ribosome binding of Stx1A1 and Stx2A1.

Several studies used cell-free translation inhibition assays to compare the enzymatic activity of the A subunits of Stx1 and Stx2 (Tesh, Burris et al. 1993, Siegler, Obrig et al. 2003). The A subunits displayed similar translation inhibitory activities (Head, Karmali et al. 1991, Tesh, Burris et al. 1993, Brigotti, Carnicelli et al. 1997), leading to the conclusion that the enzymatic activities of the A subunits are not responsible for the toxicity differences between Stx1 and Stx2. As a result the role of the A subunit in the differential potency of Stx1 and Stx2 has not received much attention. Since translation inhibition is a downstream effect of depurination, these assays did not directly compare the catalytic activity of Stx1A1 and Stx2A1 on the ribosome. Further, while in some studies the holotoxin was used (Tesh, Burris et al. 1993), in others the holotoxin was activated by digestion with trypsin to release the A1 chain from the A2-B_5 complex and/or by chemical treatment with DTT to break the disulfide bond between the A1 and the A2 chains (Siegler, Obrig et al. 2003, Chiou, Li et al. 2011). These methods frequently yield variable amounts of activated protein and can cause degradation, preventing comparison of enzymatic activity directly (Chiou, Li et al. 2011). Therefore, due to technical limitations, the role of the A1 subunit in increased potency of Stx2 has not been fully investigated and a direct comparison of the catalytic activity has not been carried out.

The unanswered questions regarding the relative catalytic activity of RIPs highlight the importance of quantitative assays, which allow direct comparisons of the depurination activity. Our group developed a quantitative real-time PCR (qRT-PCR) assay that can directly measure the catalytic activity of the RIPs on ribosomes *in vitro* or in yeast and in mammalian cells *in vivo (Pierce, Kahn et al. 2011, May, Li et al. 2012)*. The qRT-PCR

assay exhibited a much wider dynamic range than the previously used primer extension assay and increased sensitivity (Pierce, Kahn et al. 2011). Sturm and Schramm described a quantitative enzyme coupled luminescence assay to examine the kinetics of depurination by RIPs. In this assay, adenine released by depurination is converted to AMP by adenine phosphoribosyl transferase (APRTase) and then to ATP by pyruvate orthophosphate dikinase (PPDK). The light generated by ATP via firefly luciferase is detected using a luminometer (Sturm and Schramm 2009). The qRT-PCR and the enzyme coupled luminescence assay have been used to examine the activity of the ricin toxin A chain (RTA) and its mutants (Li, Kahn et al. 2013). A highly sensitive and quantitative assay using SPR was developed by our group to examine the interactions RIPs with ribosomes (Chiou, Li et al. 2008, Li, Chiou et al. 2009, Chiou, Li et al. 2011, May, Yan et al. 2013). The development of these assays will allow direct comparisons of the binding and depurination kinetics of the A1 subunits of Shiga toxins and will help determine whether the A1 subunits of Stx1 and Stx2 have a significant role in their differential toxicity.

RIBOSOME INTERACTIONS

Although the SRL is the primary substrate for all RIPs, ribosomal proteins play an important role in of the depurination of intact ribosomes by RIPs. While the K_m of RTA for rat ribosomes and naked 28S rRNA are similar, RTA depurinates ribosomes almost 10^5-fold greater than the naked 28S RNA (Endo, Tsurugi et al. 1988), suggesting that not only the target RNA sequence, but also the structure of the ribosome plays a significant role in the catalytic activity of RIPs.

Previous studies have shown the importance of the ribosomal phosphoproteins (P) of the P-protein stalk for the depurination activity of the RIPs(Endo, Tsurugi et al. 1988, Chiou, Li et al. 2008, McCluskey, Poon et al. 2008, Li, Chiou et al. 2009, Chiou, Li et al. 2011, McCluskey, Bolewska-Pedyczak et al. 2012). Ricin has been shown to crosslink to the stalk protein P0 and the ribosomal protein L9 (Vater, Bartle et al. 1995). Trichosanthin (TCS), which is a type-1 RIP, has been shown to interact with P0, and P1 proteins of the ribosomal stalk using yeast-two hybrid analysis and by *in vitro* binding assays (Chan, Hung et al. 2001). The last 11 residues of P2, which are conserved in P0, P1 and P2 have been found to be critical for the interaction with trichosanthin (TCS) (Chan, Chu et al. 2007). The crystal structure of TCS complexed to a peptide corresponding to the C-terminal domain (CTD) of human P2, SDDDMGFGLFD, showed that the conserved DDD motif at the N-terminal region of this peptide interacts with the positively charged K173, R174, and K177 residues in TCS, while the C-terminal region is inserted into a hydrophobic pocket (Too, Ma et al. 2009). Using yeast mutants deleted in the stalk proteins (ΔP1 and ΔP2) and highly sensitive SPR and depurination assays, our group provided the first evidence that the ribosomal stalk proteins are essential for the cytotoxicity of RTA *in vivo* and that the ribosomal stalk is the main landing platform for RTA on the ribosome. (Chiou, Li et al. 2008) We subsequently showed that multiple copies of the stalk proteins accelerate the recruitment of RTA to the ribosome for depurination (Li, Grela et al. 2010).

The ribosomal P-protein stalk is a lateral flexible protuberance of the large ribosomal subunit, which recruits translational factors to the ribosome and participates in the GTPase activation by EF-Tu and EF-G. The eukaryotic P protein stalk consists of 11

kDa P1 and P2 proteins bound to a larger P0 protein. P1 and P2 dimerize via their helical N-terminal domains, whereas the highly conserved C-terminal tails of P1 and P2 interact with the translational GTPases (tGTPases) (Bargis-Surgey, Lavergne et al. 1999). Although the stalk is relatively conserved in eukaryotes there are some notable differences between the stalk structure in mammals and in yeast. The human ribosomal stalk contains two identical heterodimers of P1 and P2 bound to P0 assembled into a pentameric complex (Wool, Chan et al. 1991, Grela, Bernadó et al. 2008). In contrast the yeast pentameric stalk consists of four different proteins P1α, P1β, P2α, P2β (Planta and Mager 1998) which form two different heterodimers (Tchórzewski, Boguszewska et al. 2000), P1α-P2β and P2α-P1β, bound to P0 (Hagiya, Naganuma et al. 2005, Krokowski, Boguszewska et al. 2006). The human P1 has 40-47% sequence identity with P1α and P1β and human P2 has 53-56% sequence identity with P2α and P2β (Ballesta and Remacha 1996, Grela, Krokowski et al. 2010). The prokaryotic equivalent of P1 and P2 are L12 proteins bound to a smaller P0 equivalent L10 (Gonzalo and Reboud 2003). In bacteria, the stalk structure can be a pentamer or heptamer (Diaconu, Kothe et al. 2005), while in archaea the ribosomal stalk is a heptamer (Maki, Hashimoto et al. 2007). Although the eukaryotic and prokaryotic stalk proteins are analogous in function, there is no sequence homology between these related proteins (Wool, Chan et al. 1991, Grela, Bernadó et al. 2008).

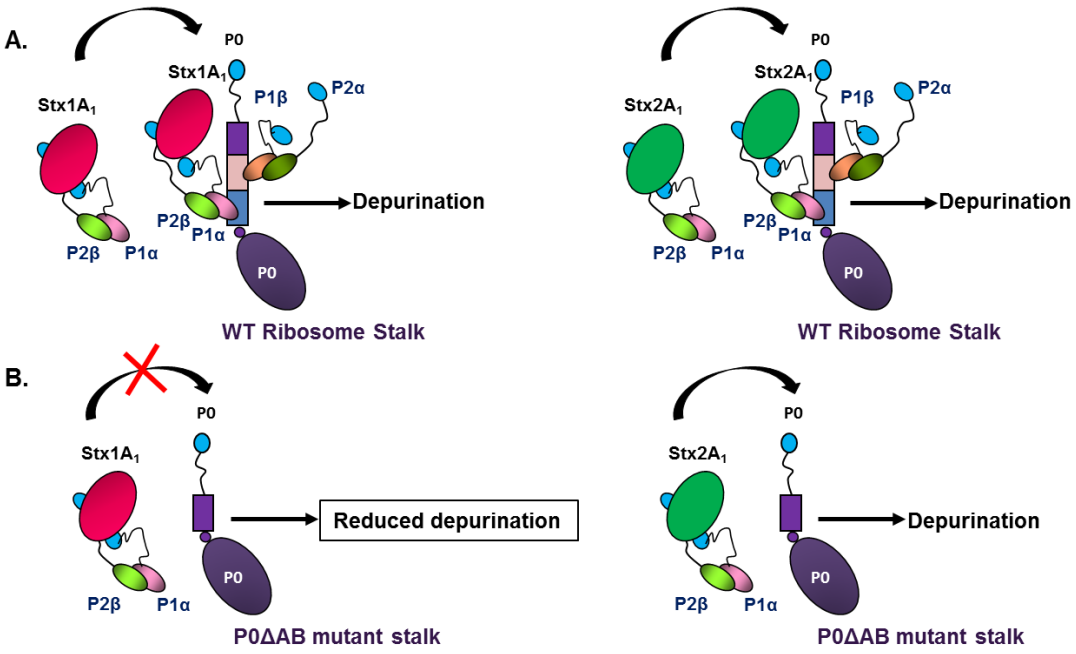

FIG 1.1. Model illustrating the interaction of Stx1A1 and Stx2A1 with the stalk mutants in the presence of purified P1α/P2β *in vitro*. (A) Both Stx1A1 and Stx2A1 are able to interact with free P1α/P2β as well as ribosome bound P1α/P2β to depurinate the ribosome. (**B**) In the P0ΔAB mutant, as the binding sites for P1/P2 dimers are deleted, free P1α/P2β proteins are not able to bind to the ribosomal stalk. Stx1A1 shows reduced depurination activity indicating its dependence on the ribosomal stalk. Stx2A1 has little or no effect on depurination suggesting that it is less dependent on P1/P2 than Stx1A1.

Using yeast-two-hybrid and pull-down experiments in HeLa cells, it was demonstrated that the A1 chain of Stx1 interacts with the P0, P1 and P2 proteins of the P-protein stalk (McCluskey, Poon et al. 2008). Removal of the last 17 amino acids of P1 or P2, but not P0 abolished the interaction between Stx1A1 and the human ribosomal stalk proteins, suggesting that the conserved CTD of P1/P2 proteins allows Stx1 to access the

SRL (McCluskey, Poon et al. 2008). To determine if Stx1A and Stx2A require the ribosomal stalk for depurination *in vivo*, we examined their depurination activity and cytotoxicity in the yeast P protein deletion mutants (Chiou, Li et al. 2011). Our results showed that ribosomal stalk is important for both toxins to depurinate the ribosome *in vivo*. Cytoplasmic stalk proteins were critical for Stx1A and Stx2A to access the SRL *in vivo* (Fig. 1.1A). However, Stx1A and Stx2A differed in depurination activity towards ribosomes when P1/P2 binding sites on P0 were deleted. P1/P2 proteins facilitated depurination by Stx1A only if their binding sites on P0 were intact (Fig. 1.1B). In contrast, Stx2A was less dependent on the stalk proteins for activity than Stx1A and could depurinate the ribosomes with a defective stalk better than Stx1A. These results suggested that cytosolic P1/P2 proteins deliver the toxins to the ribosome to create a toxin pool near the SRL (Chiou, Li et al. 2011).

The A1 chain of Stx1 was shown to interact with the ribosomal stalk proteins P0, P1, and P2 via the conserved CTD of P2 through hydrophobic and cationic surfaces on the toxin. Point mutations at arginines (Arg172, Arg176, Arg179, and Arg188) on Stx1A1 perturbed the interaction between the toxin and the P2 peptide(McCluskey, Bolewska-Pedyczak et al. 2012). Using a combination of SPR and yeast-two hybrid analysis, these arginines were shown to be critical for the interaction of Stx1A1 with the P2 peptide. The interactions with the P2 peptide were electrostatic and hydrophobic and took place at a site that was distinct from the active site. Since these residues are conserved between Stx1A1 and Stx2A1, it was proposed that Stx2 interacts with the ribosome in a similar manner (McCluskey, Bolewska-Pedyczak et al. 2012).

The arginine residues, which were critical for binding to the stalk proteins in Stx1A1 (McCluskey, Bolewska-Pedyczak et al. 2012) and RTA (Li, Kahn et al. 2013) were on the opposite face of the active site, suggesting that both toxins interact with the ribosome in a similar manner. Analysis of the interaction of RTA with wild type and mutant yeast ribosomes deleted in stalk proteins by SPR showed that this interaction did not fit the 1:1 interaction model (Li, Chiou et al. 2009). RTA interacted with wild type ribosomes by electrostatic interactions, which followed a two-step binding model. The two-step model is characterized by two different types of interactions with the ribosome, a saturable stalk dependent interaction with rapid association and dissociation rates and a much slower non-saturable stalk independent interaction with slower association and dissociation rates. The faster stalk dependent interaction was stronger than the slower stalk independent interaction. Further, the yeast mutant ribosomes lacking an intact stalk interacted with RTA by a 1:1 interaction model, which mirrored the slower interaction with wild type ribosomes (Li, Chiou et al. 2009). According to the two-step interaction model shown schematically in Fig. 1.2, in the first step RTA/Stx1A1 molecules are first concentrated on the surface of the ribosome via slow non-specific electrostatic interactions and are guided to the stalk. In the second step, rapid, more specific electrostatic interactions occur between the stalk-binding surface of RTA/Stx1A1 and the CTD of the stalk proteins. In the third step, the ribosomal stalk delivers RTA/Stx1A1 to the SRL by a conformational change of the flexible hinge region and allows RTA/Stx1A1 to depurinate the SRL at a very high rate. Consistent with this model, the interaction between RTA and the isolated native pentameric stalk complex from yeast fit well with a single step interaction model (Li, Grela et al. 2010).

The enzyme coupled luminescence assay showed that the K_m values and catalytic rates (k_{cat}) of the ribosome binding mutants of RTA for an SRL mimic RNA were similar to wild type RTA, indicating that their catalytic activity was not altered (Li, Kahn et al. 2013). However, their K_m was higher and their k_{cat} was lower towards ribosomes, indicating that the mutations affect ribosome binding and catalytic activity of RTA towards ribosomes without affecting RNA binding or catalytic activity of RTA towards naked RNA (Li, Kahn et al. 2013). Based on this data, we proposed that arginines located on the opposite face of the active site of RTA bind to the flexible P-proteins of the ribosomal stalk. Stalk binding stimulates the catalysis of depurination by orienting the active site of RTA towards the SRL and thereby allows docking of the target adenine into the active site (Li, Kahn et al. 2013). This model provided an explanation for why RTA depurinates intact ribosomes much better than free rRNA and how RTA hydrolyzes a single *N*-glycosidic bond on intact ribosomes from among the 4000 stem-loops in the large rRNA.

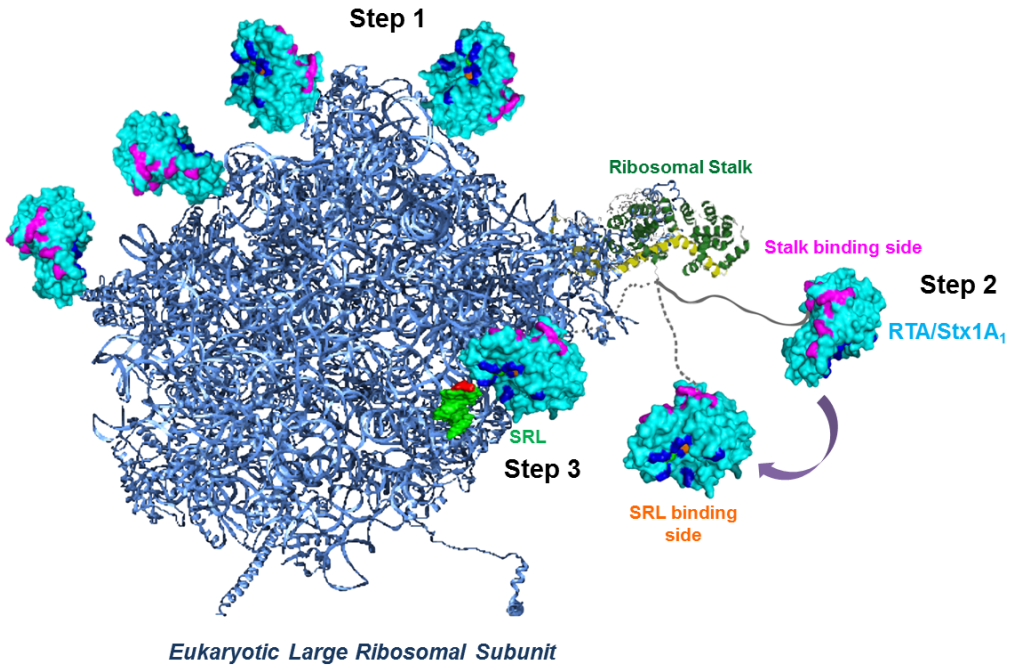

FIG 1.2. Model of how RTA/Stx1A1 access the α-sarcin/ricin loop (SRL). Eukaryotic large ribosomal subunit was created using Protein Data Bank ID: 3U5I and Protein Data Bank ID: 3U5H (blue) using the PyMOL software (The PyMOL Molecular Graphics System, Version 1.3 Schrödinger, LLC) with the SRL (green). The fitted cartoon structure of P0 fragment complexed with the N-terminal domain of P-proteins (Protein Data Bank ID: 3A1Y) from archaea is depicted as yellow and green, respectively as described. The flexible CTD domain of a P-protein is represented as a gray line. Ricin toxin A chain (RTA) (Protein Data Bank ID: 1RTC) is colored in cyan, its active site is shown in orange, RNA binding site in blue and the stalk binding site is shown in magenta. In Step 1 RTA/Stx1A1 are concentrated on the ribosome surface by nonspecific electrostatic interactions. In Step 2 RTA/Stx1A1 interact with the C-terminal domain (CTD) of P-proteins with their ribosome-binding surface, which is on the opposite side of the surface that contains the active site. The flexible hinge of P-proteins orients the active

site of RTA/Stx1A1 towards the SRL and in Step3 RTA/ Stx1A1 establish the specific contacts necessary to hydrolyze a single *N*-glycosidic bond in the SRL.

Subsequent studies showed that the ability to interact with the stalk was conserved in some RIPs, but not all RIPs (Ayub, Smulski et al. 2008). PAP, which is a type-1 RIP active against ribosomes from all five kingdoms, interacts with ribosomal protein L3 to depurinate the SRL (Hudak, Dinman et al. 1999). Since RTA, TCS and Stx1 were able to interact with ribosomal stalk, was this ability to interact with the stalk a feature of an ancestral RIP, which has been conserved in some RIPs like ricin, Shiga toxins and TCS and lost in other RIPs like PAP? Phylogenetic analysis suggested that the ability to interact with the CTD of the ribosomal stalk arose independently in different RIPs by convergent evolution (Lapadula, Sanchez-Puerta et al. 2012). Further, the ability to interact with stalk was considered an adaptive advantage and did not have strong sequence constraints, which made it easy for different proteins to acquire this feature (Lapadula, Sanchez-Puerta et al. 2012). Based on the wide distribution of RIPs in plants and their presence in some bacteria, it has been postulated that bacteria acquired an ancestral RIP domain present in plants by horizontal gene transfer. However, a recent study presented evidence for the presence of RIP genes in Fungi and Metazoa and proposed that the differential loss of paralogous genes accounted for the complex pattern of RIP genes in extant species, rather than horizontal gene transfer (Lapadula, Puerta et al. 2013).

Structural differences were shown between the structures of the CTD of bacterial and eukaryotic stalk proteins. The CTD of bacterial L12 is globular (Bernado, Modig et

al. 2010). In contrast, NMR spectroscopy showed that while the N-terminal domain of eukaryotic P1/P2 dimer is structured, the CTD is flexible and can extend away from the dimerization region (Lee, Yusa et al. 2013). It has been suggested that these structural differences in the CTD may facilitate the domain specific recognition of elongation factors. RTA is unable to depurinate intact *E. coli* ribosomes (Chan, Chu et al. 2007). Similarly, TCS can only depurinate eukaryotic ribosomes, but not bacterial ribosomes. However, TCS was able to depurinate hybrid ribosomes when the bacterial stalk proteins were replaced with the eukaryotic stalk proteins (Lee, Yusa et al. 2013). These results suggested that the CTD and the flexible linker of stalk proteins are responsible for recruiting RIPs to the ribosome (Lee, Yusa et al. 2013). Therefore, RIPs like ricin and TCS that can only depurinate eukaryotic ribosomes may have evolved to bind to the CTD of eukaryotic stalk proteins, thereby hijacking the eukaryotic stalk proteins by binding to their C-terminal consensus sequences (Choi, Wong et al. 2015).

However, some critical questions remain. Although the ribosome binding residues identified in Stx1A1 are conserved in Stx2A1, it is not known if they interact similarly with the ribosome. We have shown that there is a difference in the surface exposure of residues between Stx1A and Stx2A (Di, Kyu et al. 2011). Arg176 is more exposed in Stx1A and is more critical for the depurination activity of Stx1A than Stx2A (Di, Kyu et al. 2011). Arg176 has been shown to be important for binding of Stx1A1 to the ribosome (McCluskey, Bolewska-Pedyczak et al. 2012). It is not known if Arg176 has a similar role in binding of Stx2A1 to the ribosome. Although both Stx1A and Stx2A bind to the stalk, Stx2A is less dependent on the stalk proteins than Stx1A for its depurination activity (Chiou, Li et al. 2011). These results indicate that there are differences in the

ribosome interactions of Stx1 and Stx2, which may lead to differences in their depurination activity.

Evidence for structural differences between Stx1 and Stx2 and their importance in inactivation of the ribosome was obtained when Smith *et al*., demonstrated that monoclonal antibody (MAb) 11E10, which neutralized both the cytotoxicity and lethality of Stx2, but not Stx1, bound to three specific regions around the active site of Stx2A, but failed to bind to Stx1A (Smith, Melton-Celsa et al. 2009). The sequence of the three regions was the most divergent between Stx2 and Stx1, which explained why the antibody specifically recognized Stx2 (Smith, Melton-Celsa et al. 2009). MAb 11E10 blocked the enzymatic activity of Stx2 *in vitro* and altered its intracellular trafficking pattern, providing evidence that structural differences lead to differential effects on the catalytic activity and trafficking of Stx1 and Stx2. Another MAb, S2C4, which was able to neutralize Stx2, but not Stx1 (Jiao, Zeng et al. 2009), was predicted to bind to another region that differed in sequence between Stx2 and Stx1. This region (residues 176-188) was shown to be important for binding of Stx1A1 to the ribosomal stalk (McCluskey, Bolewska-Pedyczak et al. 2012), suggesting that structural differences between Stx1 and Stx2 may affect ribosome binding differentially. These results highlight the importance of identifying Stx2 residues, which are important in binding to the ribosome and the role of these residues on ribosome binding and depurination activity of each toxin.

Finally, in order for the toxin to depurinate the SRL specifically, it has to interact with the residues surrounding the SRL. Modeling analysis of the crystal structure of RTA and a 29-mer oligonucleotide hairpin containing the conserved GAGA loop of the SRL identified residues which may be involved in binding to the 29-mer (Olson and Cuff

1999). The amino acids at the active site are conserved between Stx1 and Stx2. However, there are conformational differences between the active sites of Stx1 and Stx2 and the active site residues are more exposed in Stx2 than in Stx1 (Di, Kyu et al. 2011). Currently it is not known if residues around the active site contribute to the catalytic activity of each toxin similarly. Analysis of depurination kinetics will shed more light on the relative role of these residues in binding to the SRL and in catalytic activity.

CONCLUSIONS

STEC are a serious cause of morbidity and mortality and a better understanding of their mechanism of virulence is of high significance. *In vivo* data indicate that the B subunits are involved in differential toxicity of Stx1 and Stx2, but do not rule out a potential role for the A subunit, suggesting that steps in addition to receptor binding and trafficking likely contribute to the differential toxicity of Stx1 and Stx2. The role of the A subunits in differential toxicity has not been fully examined. New discoveries indicate that the A subunits of Stx1 and Stx2 differ in their dependence on the ribosomal stalk proteins, suggesting that the role of the A subunits in ribosome binding, depurination activity and cytotoxicity may differ. Structural studies identified conformational differences between the active sites of the A subunits of Stx1 and Stx2. Monoclonal antibodies that selectively bind and neutralize Stx2 indicated important differences in enzymatic action and intracellular trafficking. A better understanding of the interaction of the A1 subunits of Stx1 and Stx2 with the ribosome and with the SRL, and comparative analysis of the catalysis of ribosome depurination is necessary to fully understand the factors that contribute to the higher association of Stx2 with HUS.

REFERENCES

1. Arfilli, V., D. Carnicelli, L. Rocchi, F. Ricci, P. Pagliaro, P. Tazzari and M. Brigotti (2010). "Shiga toxin 1 and ricin A chain bind to human polymorphonuclear leucocytes through a common receptor." Biochem. J **432**: 173-180.

2. Ayub, M. J., C. R. Smulski, K.-W. Ma, M. J. Levin, P.-C. Shaw and K.-B. Wong (2008). "The C-terminal end of P proteins mediates ribosome inactivation by trichosanthin but does not affect the pokeweed antiviral protein activity." Biochemical and Biophysical Research Communications **369**(2): 314-319.

3. Ballesta, J. P. and M. Remacha (1996). "The large ribosomal subunit stalk as a regulatory element of the eukaryotic translational machinery." Progress in nucleic acid research and molecular biology **55**: 157-193.

4. Barbieri, L., L. Polito, A. Bolognesi, M. Ciani, E. Pelosi, V. Farini, A. K. Jha, N. Sharma, J. M. Vivanco and A. Chambery (2006). "Ribosome-inactivating proteins in edible plants and purification and characterization of a new ribosome-inactivating protein from Cucurbita moschata." Biochimica et Biophysica Acta (BBA)-General Subjects **1760**(5): 783-792.

5. Bargis-Surgey, P., J.-P. Lavergne, P. Gonzalo, C. Vard, O. Filhol-Cochet and J.-P. Reboud (1999). "Interaction of elongation factor eEF-2 with ribosomal P proteins." European Journal of Biochemistry **262**(2): 606-611.

6. Bauwens, A., J. Betz, I. Meisen, B. Kemper, H. Karch and J. Müthing (2013). "Facing glycosphingolipid–Shiga toxin interaction: dire straits for endothelial cells of the human vasculature." Cellular and Molecular Life Sciences **70**(3): 425-457.

7. Bauwens, A., M. Bielaszewska, B. Kemper, P. Langehanenberg, G. von Bally, R. Reichelt, D. Mulac, H.-U. Humpf, A. W. Friedrich and K. S. Kim (2011). "Differential cytotoxic actions of Shiga toxin 1 and Shiga toxin 2 on microvascular and macrovascular endothelial cells." Thromb. Haemost. **105**(3): 515-528.

8. Bergan, J., A. B. D. Lingelem, R. Simm, T. Skotland and K. Sandvig (2012). "Shiga toxins." Toxicon **60**(6): 1085-1107.

9. Bernado, P., K. Modig, P. Grela, D. I. Svergun, M. Tchorzewski, M. Pons and M. Akke (2010). "Structure and dynamics of ribosomal protein L12: an ensemble model based on SAXS and NMR relaxation." Biophysical Journal **98**(10): 2374-2382.

10. Bielaszewska, M., A. Mellmann, W. Zhang, R. Köck, A. Fruth, A. Bauwens, G. Peters and H. Karch (2011). "Characterisation of the *Escherichia coli* strain associated with an outbreak of haemolytic uraemic syndrome in Germany, 2011: a microbiological study." The Lancet Infectious Diseases **11**(9): 671-676.

11. Boerlin, P., S. McEwen, F. Boerlin-Petzold, J. Wilson, R. Johnson and C. Gyles (1999). "Associations between virulence factors of Shiga toxin-producing *Escherichia coli* and disease in humans." Journal of Clinical Microbiology **37**(3): 497-503.

12. Brigotti, M., D. Carnicelli, P. Alvergna, R. Mazzaracchio, S. Sperti and L. Montanaro (1997). "The RNA-N-glycosidase activity of Shiga-like toxin I: Kinetic parameters of the native and activated toxin." Toxicon **35**(9): 1431-1437.

13. Brigotti, M., D. Carnicelli, V. Arfilli, N. Tamassia, F. Borsetti, E. Fabbri, P. L. Tazzari, F. Ricci, P. Pagliaro and E. Spisni (2013). "Identification of TLR4 as the receptor that recognizes Shiga toxins in human neutrophils." J. Immunol. **191**(9): 4748-4758.

14. Calderwood, S. B., F. Auclair, A. Donohue-Rolfe, G. T. Keusch and J. J. Mekalanos (1987). "Nucleotide sequence of the Shiga-like toxin genes of *Escherichia coli*." Proc. Natl. Acad. Sci. USA. **84**(13): 4364-4368.

15. Chan, D. S., L.-O. Chu, K.-M. Lee, P. H. Too, K.-W. Ma, K.-H. Sze, G. Zhu, P.-C. Shaw and K.-B. Wong (2007). "Interaction between trichosanthin, a ribosome-inactivating protein, and the ribosomal stalk protein P2 by chemical shift perturbation and mutagenesis analyses." Nucleic acids research **35**(5): 1660-1672.

16. Chan, S. H., F. S. J. Hung, D. S. B. Chan and P. C. Shaw (2001). "Trichosanthin interacts with acidic ribosomal proteins P0 and P1 and mitotic checkpoint protein MAD2B." European Journal of Biochemistry **268**(7): 2107-2112.

17. Chiou, J.-C., X.-P. Li, M. Remacha, J. P. Ballesta and N. E. Tumer (2011). "Shiga toxin 1 is more dependent on the P proteins of the ribosomal stalk for depurination activity than Shiga toxin 2." The international journal of biochemistry & cell biology **43**(12): 1792-1801.

18. Chiou, J. C., X. P. Li, M. Remacha, J. P. Ballesta and N. E. Tumer (2008). "The ribosomal stalk is required for ribosome binding, depurination of the rRNA and cytotoxicity of ricin A chain in *Saccharomyces cerevisiae*." Molecular microbiology **70**(6): 1441-1452.

19. Choi, A. K., E. C. Wong, K.-M. Lee and K.-B. Wong (2015). "Structures of eukaryotic ribosomal stalk proteins and its complex with trichosanthin, and their implications in recruiting ribosome-inactivating proteins to the ribosomes." Toxins **7**(3): 638-647.

20. Clementi, N., A. Chirkova, B. Puffer, R. Micura and N. Polacek (2010). "Atomic mutagenesis reveals A2660 of 23S ribosomal RNA as key to EF-G GTPase activation." Nature Chemical Biology **6**(5): 344-351.

21. DeGrandis, S., H. Law, J. Brunton, C. Gyles and C. Lingwood (1989). "Globotetraosylceramide is recognized by the pig edema disease toxin." Journal of Biological Chemistry **264**(21): 12520-12525.

22. Deresiewicz, R. L., P. R. Austin and C. J. Hovde (1993). "The role of tyrosine-114 in the enzymatic activity of the Shiga-like toxin I A-chain." Mol. Genet. Genomics **241**(3): 467-473.

23. Di, R., E. Kyu, V. Shete, H. Saidasan, P. Kahn and N. Tumer (2011). "Identification of amino acids critical for the cytotoxicity of Shiga toxin 1 and 2 in *Saccharomyces cerevisiae*." Toxicon **57**(4): 525-539.

24. Diaconu, M., U. Kothe, F. Schlünzen, N. Fischer, J. M. Harms, A. G. Tonevitsky, H. Stark, M. V. Rodnina and M. C. Wahl (2005). "Structural basis for the function of the ribosomal L7/12 stalk in factor binding and GTPase activation." Cell **121**(7): 991-1004.

25. Endo, Y., K. Tsurugi, T. Yutsudo, Y. Takeda, T. Ogasawara and K. Igarashi (1988). "Site of action of a Vero toxin (VT2) from *Escherichia coli* O157: H7 and

of Shiga toxin on eukaryotic ribosomes." European Journal of Biochemistry **171**(1‐2): 45-50.

26. Flagler, M. J., S. S. Mahajan, A. A. Kulkarni, S. S. Iyer and A. A. Weiss (2010). "Comparison of binding platforms yields insights into receptor binding differences between Shiga toxins 1 and 2." Biochemistry **49**(8): 1649-1657.

27. Frank, C., D. Werber, J. P. Cramer, M. Askar, M. Faber, M. an der Heiden, H. Bernard, A. Fruth, R. Prager and A. Spode (2011). "Epidemic profile of Shiga-toxin–producing *Escherichia coli* O104: H4 outbreak in Germany." New England Journal of Medicine **365**(19): 1771-1780.

28. Fraser, M., M. Chernaia, Y. Kozlov and M. James (1994). "Crystal structure of the holotoxin from *Shigella dysenteriae* at 2.5 A resolution." Nature structural biology **1**(1): 59.

29. Fraser, M. E., M. M. Cherney, P. Marcato, G. L. Mulvey, G. D. Armstrong and M. N. James (2006). "Binding of adenine to Stx2, the protein toxin from *Escherichia coli* O157: H7." Acta Crystallographica Section F: Structural Biology and Crystallization Communications **62**(7): 627-630.

30. Fraser, M. E., M. Fujinaga, M. M. Cherney, A. R. Melton-Celsa, E. M. Twiddy, A. D. O'Brien and M. N. James (2004). "Structure of Shiga toxin type 2 (Stx2)

from *Escherichia coli* O157: H7." Journal of Biological Chemistry **279**(26): 27511-27517.

31. Fuller, C. A., C. A. Pellino, M. J. Flagler, J. E. Strasser and A. A. Weiss (2011). "Shiga toxin subtypes display dramatic differences in potency." Infection and immunity **79**(3): 1329-1337.

32. Gonzalo, P. and J. P. Reboud (2003). "The puzzling lateral flexible stalk of the ribosome." Biology of the Cell **95**(3–4): 179-193.

33. Grela, P., P. Bernadó, D. Svergun, J. Kwiatowski, D. Abramczyk, N. Grankowski and M. Tchórzewski (2008). "Structural relationships among the ribosomal stalk proteins from the three domains of life." Journal of molecular evolution **67**(2): 154-167.

34. Grela, P., D. Krokowski, Y. Gordiyenko, D. Krowarsch, C. V. Robinson, J. Otlewski, N. Grankowski and M. Tchórzewski (2010). "Biophysical properties of the eukaryotic ribosomal stalk." Biochemistry **49**(5): 924-933.

35. Hagiya, A., T. Naganuma, Y. Maki, J. Ohta, Y. Tohkairin, T. Shimizu, T. Nomura, A. Hachimori and T. Uchiumi (2005). "A mode of assembly of P0, P1 and P2 proteins at the GTPase-associated center in animal ribosome: *in vitro* analyses with P0 truncation mutants." Journal of Biological Chemistry.

36. Head, S., M. Karmali and C. Lingwood (1991). "Preparation of VT1 and VT2 hybrid toxins from their purified dissociated subunits. Evidence for B subunit modulation of a subunit function." Journal of Biological Chemistry **266**(6): 3617-3621.

37. Hovde, C., S. Calderwood, J. Mekalanos and R. Collier (1988). "Evidence that glutamic acid 167 is an active-site residue of Shiga-like toxin I." Proc. Natl. Acad. Sci. USA. **85**(8): 2568.

38. Hudak, K. A., J. D. Dinman and N. E. Tumer (1999). "Pokeweed antiviral protein accesses ribosomes by binding to L3." Journal of Biological Chemistry **274**(6): 3859-3864.

39. Ishizaki, T., C. Megumi, F. Komai, K. Masuda and K. Oosawa (2002). "Accumulation of a 31‐kDa glycoprotein in association with the expression of embryogenic potential by spinach callus in culture." Physiologia plantarum **114**(1): 109-115.

40. Ito, H., T. Yutsudo, T. Hirayama and Y. Takeda (1988). "Isolation and some properties of A and B subunits of Vero toxin 2 and *in vitro* formation of hybrid toxins between subunits of Vero toxin 1 and Vero toxin 2 from *Escherichia coli* O157: H7." Microbial Pathogenesis **5**(3): 189-195.

41. Jackson, M., R. Deresiewicz and S. Calderwood (1990). "Mutational analysis of the Shiga toxin and Shiga-like toxin II enzymatic subunits." Journal of bacteriology **172**(6): 3346.

42. Jackson, M. P., R. J. Neill, A. D. O'Brien, R. K. Holmes and J. W. Newland (1987). "Nucleotide sequence analysis and comparison of the structural genes for Shiga-like toxin I and Shiga-like toxin II encoded by bacteriophages from *Escherichia coli* 933." FEMS Microbiology Letters **44**(1): 109-114.

43. Jacobson, J. M., J. Yin, P. I. Kitov, G. Mulvey, T. P. Griener, M. N. James, G. Armstrong and D. R. Bundle (2014). "The crystal structure of Shiga toxin type 2 with bound disaccharide guides the design of a heterobifunctional toxin inhibitor." Journal of Biological Chemistry **289**(2): 885-894.

44. Jiao, Y.-J., X.-Y. Zeng, X.-L. Guo, Z.-Y. Shi, Z.-Q. Feng and H. Wang (2009). "Monoclonal antibody S2C4 neutralizes the toxicity of Shiga toxin 2 and its variants." Prog. Biochem. Biophys. **36**(6): 736-742.

45. Johannes, L. and W. Römer (2010). "Shiga toxins—from cell biology to biomedical applications." Nat. Rev. Microbiol. **8**(2): 105-116.

46. Kaper, J. and A. O'Brien (2014). "Overview and historical perspectives." Microbiol. Spectr. **2**(2).

47. Karch, H., E. Denamur, U. Dobrindt, B. B. Finlay, R. Hengge, L. Johannes, E. Z. Ron, T. Tønjum, P. J. Sansonetti and M. Vicente (2012). "The enemy within us: lessons from the 2011 European *Escherichia coli* O104: H4 outbreak." EMBO Mol. Med. **4**(9): 841-848.

48. Karch, H., P. Tarr and M. Bielaszewska (2005). "Enterohaemorrhagic *Escherichia coli* in human medicine." Int. J. Med. Microbiol. **295**(6-7): 405-418.Karve, S. S. and A. A. Weiss (2014). "Glycolipid binding preferences of Shiga toxin variants." PloS one **9**(7): e101173.

49. Krokowski, D., A. Boguszewska, D. Abramczyk, A. Liljas, M. Tchórzewski and N. Grankowski (2006). "Yeast ribosomal P0 protein has two separate binding sites for P1/P2 proteins." Molecular Microbiology **60**(2): 386-400.

50. Lapadula, W. J., M. V. S. Puerta and M. J. Ayub (2013). "Revising the taxonomic distribution, origin and evolution of ribosome inactivating protein genes." PloS one **8**(9): e72825.

51. Lapadula, W. J., M. Sanchez-Puerta and M. Juri Ayub (2012). "Convergent evolution led ribosome inactivating proteins to interact with ribosomal stalk." Toxicon **59**(3): 427-432.

52. Lee, K.-M., K. Yusa, L.-O. Chu, C. W.-H. Yu, M. Oono, T. Miyoshi, K. Ito, P.-C. Shaw, K.-B. Wong and T. Uchiumi (2013). "Solution structure of human P1• P2

heterodimer provides insights into the role of eukaryotic stalk in recruiting the ribosome-inactivating protein trichosanthin to the ribosome." Nucleic acids research **41**(18): 8776-8787.

53. Li, X.-P., J.-C. Chiou, M. Remacha, J. P. Ballesta and N. E. Tumer (2009). "A two-step binding model proposed for the electrostatic interactions of ricin a chain with ribosomes." Biochemistry **48**(18): 3853-3863.Li, X.-P., P. Grela, D. Krokowski, M. Tchórzewski and N. E. Tumer (2010). "Pentameric organization of the ribosomal stalk accelerates recruitment of ricin a chain to the ribosome for depurination." Journal of Biological Chemistry **285**(53): 41463-41471.

54. Li, X.-P., P. C. Kahn, J. N. Kahn, P. Grela and N. E. Tumer (2013). "Arginine residues on the opposite side of the active site stimulate the catalysis of ribosome depurination by ricin A chain by interacting with the P-protein stalk." Journal of Biological Chemistry **288**(42): 30270-30284.

55. Ling, H., A. Boodhoo, B. Hazes, M. D. Cummings, G. D. Armstrong, J. L. Brunton and R. J. Read (1998). "Structure of the Shiga-like toxin I B-pentamer complexed with an analogue of its receptor Gb3." Biochemistry **37**: 1777-1788.

56. Lingwood, C. A. (1996). "Role of Verotoxin receptors in pathogenesis." Trends in microbiology **4**(4): 147-153.

57. Louise, C. B. and T. G. Obrig (1995). "Specific interaction of *Escherichia coli* 0157: H7-derived Shiga-like toxin II with human renal endothelial cells." Journal of infectious diseases **172**(5): 1397-1401.

58. Maki, Y., T. Hashimoto, M. Zhou, T. Naganuma, J. Ohta, T. Nomura, C. V. Robinson and T. Uchiumi (2007). "Three binding sites for stalk protein dimers are generally present in ribosomes from archaeal organism." Journal of Biological Chemistry **282**(45): 32827-32833.

59. Manning, S. D., A. S. Motiwala, A. C. Springman, W. Qi, D. W. Lacher, L. M. Ouellette, J. M. Mladonicky, P. Somsel, J. T. Rudrik and S. E. Dietrich (2008). "Variation in virulence among clades of *Escherichia coli* O157: H7 associated with disease outbreaks." Proc. Natl. Acad. Sci. USA. **105**(12): 4868-4873.

60. May, K. L., X. P. Li, F. Martínez‐Azorín, J. P. Ballesta, P. Grela, M. Tchórzewski and N. E. Tumer (2012). "The P1/P2 proteins of the human ribosomal stalk are required for ribosome binding and depurination by ricin in human cells." FEBS Journal **279**(20): 3925-3936.

61. May, K. L., Q. Yan and N. E. Tumer (2013). "Targeting ricin to the ribosome." Toxicon **69**: 143–151. .

62. Mayer, C. L., C. S. Leibowitz, S. Kurosawa and D. J. Stearns-Kurosawa (2012). "Shiga Toxins and the pathophysiology of hemolytic uremic syndrome in humans and animals." Toxins **4**(11): 1261.

63. McCluskey, A., E. Bolewska-Pedyczak, N. Jarvik, G. Chen, S. Sidhu and L. Johannes (2012). "Charged and hydrophobic surfaces on the A chain of Shiga-Like Toxin 1 recognize the C-terminal domain of ribosomal stalk proteins." PLoS One **7**(2): e31191.

64. McCluskey, A. J., G. M. Poon, E. Bolewska-Pedyczak, T. Srikumar, S. M. Jeram, B. Raught and J. Gariépy (2008). "The catalytic subunit of Shiga-like toxin 1 interacts with ribosomal stalk proteins and is inhibited by their conserved C-terminal domain." Journal of molecular biology **378**(2): 375-386.

65. Nakajima, H., N. Kiyokawa, Y. U. Katagiri, T. Taguchi, T. Suzuki, T. Sekino, K. Mimori, T. Ebata, M. Saito and H. Nakao (2001). "Kinetic analysis of binding between Shiga toxin and receptor glycolipid Gb3Cer by surface plasmon resonance." Journal of Biological Chemistry **276**(46): 42915-42922.

66. Nataro, J. P. and J. B. Kaper (1998). "Diarrheagenic *Escherichia coli*." Clinical microbiology reviews **11**(1): 142-201.

67. Nielsen, K. and R. S. Boston (2001). "Ribosome-inactivating proteins: a plant perspective." Annual review of plant biology **52**(1): 785-816.

68. Olson, M. A. and L. Cuff (1999). "Free energy determinants of binding the rRNA substrate and small ligands to ricin A-chain." Biophysical journal **76**(1): 28-39.

69. Parente, A., B. Conforto, A. Di Maro, A. Chambery, P. De Luca, A. Bolognesi, M. Iriti and F. Faoro (2008). "Type 1 ribosome-inactivating proteins from Phytolacca dioica L. leaves: differential seasonal and age expression, and cellular localization." Planta **228**(6): 963-975.

70. Peumans, W. J., Q. Hao and E. J. van Damme (2001). "Ribosome-inactivating proteins from plants: more than RNA N-glycosidases?" The FASEB Journal **15**(9): 1493-1506.

71. Pickering, L., T. Obrig and F. Stapleton (1994). "Hemolytic-uremic syndrome and enterohemorrhagic *Escherichia coli*." The Pediatric Infectious Disease Journal **13**(6): 459.

72. Pierce, M., J. N. Kahn, J. Chiou and N. E. Tumer (2011). "Development of a quantitative RT-PCR assay to examine the kinetics of ribosome depurination by ribosome inactivating proteins using *Saccharomyces cerevisiae* as a model." RNA **17**(1): 201-210.

73. Planta, R. J. and W. H. Mager (1998). "The list of cytoplasmic ribosomal proteins of *Saccharomyces cerevisiae*." Yeast **14**(5): 471-477.

74. Prestle, J., M. Schönfelder, G. Adam and K.-W. Mundry (1992). "Type 1 ribosome-inactivating proteins depurinate plant 25S rRNA without species specificity." Nucleic acids research **20**(12): 3179-3182.

75. Russo, L. M., A. R. Melton-Celsa, M. J. Smith and A. D. O'Brien (2014). "Comparisons of native Shiga Toxins (Stxs) Type 1 and 2 with chimeric toxins indicate that the source of the binding subunit dictates degree of toxicity." PloS one **9**(3): e93463.

76. Rutjes, N. W., B. A. Binnington, C. R. Smith, M. D. Maloney and C. A. Lingwood (2002). "Differential tissue targeting and pathogenesis of Verotoxins 1 and 2 in the mouse animal model." Kidney International **62**(3): 832-845.

77. Samuel, J., L. Perera, S. Ward, A. O'brien, V. Ginsburg and H. Krivan (1990). "Comparison of the glycolipid receptor specificities of Shiga-like toxin type II and Shiga-like toxin type II variants." Infection and immunity **58**(3): 611-618.

78. Sandvig, K. and B. van Deurs (2005). "Delivery into cells: lessons learned from plant and bacterial toxins." Gene therapy **12**(11): 865-872.

79. Scallan, E., R. M. Hoekstra, F. J. Angulo, R. V. Tauxe, M.-A. Widdowson, S. L. Roy, J. L. Jones and P. M. Griffin (2011). "Foodborne illness acquired in the United States—major pathogens." Emerging infectious diseases **17**(1): 7.

80. Scheutz, F., L. Teel, L. Beutin, D. Piérard, G. Buvens, H. Karch, A. Mellmann, A. Caprioli, R. Tozzoli, S. Morabito, N. Strockbine, A. Melton-Celsa, M. Sanchez, S. Persson and A. and O'Brien (2012). "Multicenter evaluation of a sequence-based protocol for subtyping Shiga toxins and standardizing Stx nomenclature." Journal of Clinical Microbiology **50**(9): 2951-2963.

81. Shi, X., P. K. Khade, K. Y. Sanbonmatsu and S. Joseph (2012). "Functional role of the sarcin–ricin loop of the 23S rRNA in the elongation cycle of protein synthesis." Journal of Molecular Biology **419**(3): 125-138.

82. Shimizu, T., T. Sato, S. Kawakami, T. Ohta, M. Noda and T. Hamabata (2007). "Receptor affinity, stability and binding mode of Shiga toxins are determinants of toxicity." Microbial pathogenesis **43**(2-3): 88.

83. Siegler, R. and R. Oakes (2005). "Hemolytic uremic syndrome; pathogenesis, treatment, and outcome." Current opinion in pediatrics **17**(2): 200-204.

84. Siegler, R. L., T. G. Obrig, T. J. Pysher, V. L. Tesh, N. D. Denkers and F. B. Taylor (2003). "Response to Shiga toxin 1 and 2 in a baboon model of hemolytic uremic syndrome." Pediatric Nephrology **18**(2): 92-96.

85. Skinner, L. and M. Jackson (1997). "Investigation of ribosome binding by the Shiga toxin A1 subunit, using competition and site-directed mutagenesis." Journal of bacteriology **179**(4): 1368-1374.

86. Smith, M. J., A. R. Melton-Celsa, J. F. Sinclair, H. M. Carvalho, C. M. Robinson and A. D. O'Brien (2009). "Monoclonal antibody 11E10, which neutralizes Shiga toxin type 2 (Stx2), recognizes three regions on the Stx2 A subunit, blocks the enzymatic action of the toxin *in vitro*, and alters the overall cellular distribution of the toxin." Infection and immunity **77**(7): 2730-2740.

87. Stearns-Kurosawa, D., V. Collins, S. Freeman, V. L. Tesh and S. Kurosawa (2010). "Distinct physiologic and inflammatory responses elicited in baboons after challenge with Shiga Toxin type 1 or 2 from enterohemorrhagic *Escherichia coli*." Infection and Immunity **78**(6): 2497.

88. Stearns-Kurosawa, D. J., S.-Y. Oh, R. P. Cherla, M.-S. Lee, V. L. Tesh, J. Papin, J. Henderson and S. Kurosawa (2013). "Distinct renal pathology and a chemotactic phenotype after enterohemorrhagic *Escherichia coli* Shiga toxins in non-human primate models of hemolytic uremic syndrome." Am. J. Pathol. **182**(4): 1227.

89. Stein, P. E., A. Boodhoo, G. J. Tyrrell, J. L. Brunton and R. J. Read (1992). "Crystal structure of the cell-binding B oligomer of Verotoxin-1 from *E. coli*." Nature **355**: 748 - 750.

90. Stirpe, F. (2004). "Ribosome-inactivating proteins." Toxicon **44**(4): 371-383.

91. Stirpe, F. (2013). "Ribosome-inactivating proteins: from toxins to useful proteins." Toxicon **67**: 12-16.

92. Strockbine, N. A., M. Jackson, L. Sung, R. Holmes and A. D. O'Brien (1988). "Cloning and sequencing of the genes for Shiga toxin from *Shigella dysenteriae* type 1." Journal of bacteriology **170**(3): 1116-1122.

93. Strockbine, N. A., L. Marques, J. W. Newland, H. W. Smith, R. K. Holmes and A. D. O'brien (1986). "Two toxin-converting phages from *Escherichia coli* O157: H7 strain 933 encode antigenically distinct toxins with similar biologic activities." Infection and immunity **53**(1): 135-140.

94. Sturm, M. B. and V. L. Schramm (2009). "Detecting ricin: sensitive luminescent assay for ricin A-chain ribosome depurination kinetics." Analytical chemistry **81**(8): 2847-2853.

95. Tchórzewski, M., A. Boguszewska, P. Dukowski and N. Grankowski (2000). "Oligomerization properties of the acidic ribosomal P-proteins from *Saccharomyces cerevisiae*: effect of P1A protein phosphorylation on the formation of the P1A-P2B hetero-complex." BBA Clin. **1499**(1-2): 63.

96. Tesh, V. L., J. Burris, J. Owens, V. Gordon, E. Wadolkowski, A. O'brien and J. Samuel (1993). "Comparison of the relative toxicities of Shiga-like toxins type I and type II for mice." Infection and immunity **61**(8): 3392-3402.

97. Too, P. H.-M., M. K.-W. Ma, A. N.-S. Mak, Y.-T. Wong, C. K.-C. Tung, G. Zhu, S. W.-N. Au, K.-B. Wong and P.-C. Shaw (2009). "The C-terminal fragment of the ribosomal P protein complexed to trichosanthin reveals the interaction between the ribosome-inactivating protein and the ribosome." Nucleic acids research **37**(2): 602-610.

98. van Deurs, B. and K. Sandvig (1995). "Furin-induced cleavage and activation of Shiga toxin." Journal of Biological Chemistry **270**(18): 10817-10821.

99. Vater, C. A., L. M. Bartle, J. D. Leszyk, J. M. Lambert and V. S. Goldmacher (1995). "Ricin A chain can be chemically cross-linked to the mammalian ribosomal proteins L9 and L10e." Journal of Biological Chemistry **270**(21): 12933-12940.

100. Wadolkowski, E., L. Sung, J. Burris, J. Samuel and A. O'brien (1990). "Acute renal tubular necrosis and death of mice orally infected with *Escherichia coli* strains that produce Shiga-like toxin type II." Infection and immunity **58**(12): 3959-3965.

101. Weinstein, D. L., M. P. Jackson, L. P. Perera, R. K. Holmes and A. D. O'Brien (1989). "*In vivo* formation of hybrid toxins comprising Shiga toxin and the Shiga-like toxins and role of the B subunit in localization and cytotoxic activity." Infection and Immunity **57**(12): 3743-3750.

102. Wool, I., Y. Chan, A. Glück and K. Suzuki (1991). "The primary structure of rat ribosomal proteins P0, P1, and P2 and a proposal for a uniform nomenclature for mammalian and yeast ribosomal proteins." Biochimie **73**(7-8): 861.

103. Yamasaki, S., M. Furutani, K. Ito, K. Igarashi, M. Nishibuchi and Y. Takeda (1991). "Importance of arginine at position 170 of the A subunit of Verotoxin 1 produced by enterohemorrhagic *Escherichia coli* for toxin activity." Microbial pathogenesis **11**(1): 1.

104. Zhabokritsky, A., M. Kutky, L. Burns, R. Karran and K. Hudak (2010). "RNA toxins: mediators of stress adaptation and pathogen defense." Wiley Interdiscip. Rev. RNA **2**(6): 890-903.

105. Zumbrun, S. D., L. Hanson, J. F. Sinclair, J. Freedy, A. R. Melton-Celsa, J. Rodriguez-Canales, J. C. Hanson and A. D. O'Brien (2010). "Human intestinal tissue and cultured colonic cells contain globotriaosylceramide synthase mRNA and the alternate Shiga toxin receptor globotetraosylceramide." Infection and immunity **78**(11): 4488-4499.

CHAPTER 2: The A1 subunit of Shiga toxin 2 has higher affinity for ribosomes and higher catalytic activity than the A1 subunit Shiga toxin 1

ABSTRACT

Shiga toxin (Stx) producing *E.coli* (STEC) infections can lead to life-threatening complications, including hemorrhagic colitis (HC) and hemolytic uremic syndrome (HUS), which is the most common cause of acute renal failure in children in the US. Stx1 and Stx2 are AB_5 toxins consisting of an enzymatically active A subunit associated with a pentamer of receptor binding B subunits. Epidemiological evidence suggests that Stx2-producing *E.coli* strains are more frequently associated with HUS than Stx1-producing strains. Several studies suggest that the B subunit plays a role in mediating toxicity. However, the role of the A subunits in the increased potency of Stx2 has not been fully investigated. Here using purified A1 subunits, we show that Stx2A1 has higher affinity for yeast and mammalian ribosomes than Stx1A1. Biacore analysis indicated that Stx2A1 has a faster association and dissociation pattern with ribosomes than Stx1A1. Analysis of ribosome depurination kinetics demonstrated that Stx2A1 depurinates yeast and mammalian ribosomes and an RNA stem-loop mimic of the sarcin/ricin loop (SRL) at a higher catalytic rate and is a more efficient enzyme than Stx1A1. Stx2A1 depurinated ribosomes at a higher level *in vivo* and was more cytotoxic than Stx1A1 in yeast. Stx2A1 depurinated ribosomes and inhibited translation at a significantly higher level than Stx1A1 in human cells. These results provide the first direct evidence that the higher affinity for ribosomes in combination with higher catalytic

activity towards the SRL allows Stx2A1 to depurinate ribosomes, inhibit translation and exhibit cytotoxicity at a significantly higher level than Stx1A1.

INTRODUCTION

Shiga toxin-producing *Escherichia coli* (STEC) is an emerging food and water-borne pathogen. STEC infections can lead to life-threatening complications including hemorrhagic colitis (HC) and hemolytic uremic syndrome (HUS) with potentially lethal consequences (Boerlin, McEwen et al. 1999). Due to very low infectious dose and ease of person to person spread, STEC infection is the leading cause of death in children from foodborne bacterial infection (Siegler and Oakes 2005). Presently there are no post exposure therapeutics or vaccines available for STEC infection. Due to recent outbreaks of *E.coli* O157:H7 in the US and the emergence of highly virulent new strains, such as *E. coli* O104:H4, which caused the deadliest HUS outbreak in Germany in 2011, STEC remains a major challenge for food safety and public health (Bielaszewska, Mellmann et al. 2011, Frank, Werber et al. 2011, Karch, Denamur et al. 2012, Kaper and O'Brien 2014).

The primary virulence factors of STEC, Shiga toxin 1 (Stx1) and Shiga toxin 2 (Stx2), are AB_5 toxins consisting of an enzymatically active A subunit associated with a pentamer of receptor binding B subunits and are known as type II ribosome inactivating proteins (RIPs). The A subunits of Stx1 and Stx2 consist of the catalytically active A1 (residues 1-251 in Stx1 and 1-250 in Stx2) and A_2 chains (residues 252-293 in Stx1 and 251-297 in Stx2), which are cleaved by the protease furin and kept together by a disulfide bond (Bergan, Dyve Lingelem et al. 2012). The B subunits bind to a common receptor,

globotriaosylceramide (Gb3 or CD77) and allow the toxin to enter mammalian cells by endocytosis. Stx holotoxin traffics in a retrograde manner from the endosome to the Golgi network and reaches the ER. The A1 chain is released from the A_2-B_5 complex by cleavage of the disulfide bond in the ER (Sandvig and van Deurs 2005). The A1 chain is proposed to be recognized as a misfolded protein by the ER chaperones and targeted for retrotranslocation across the ER membrane (Yu and Haslam 2005). The A1 chain is thought to refold into an active conformation in the cytosol to exert its cytotoxic effects (Sandvig and van Deurs 2005). The A1 chain of Shiga toxin (Stx) produced by *Shigella dysenteriae* and the A1 chains of Stx1 and Stx2 produced by STEC are *N*-glycosidases that remove a specific adenine from the highly conserved α-sarcin/ricin loop (SRL) in the large rRNA (Endo, Tsurugi et al. 1988). Irreversible modification of the SRL blocks elongation factor (EF)-1- and EF-2-dependent GTPase activity and renders the ribosome unable to bind EF-2, thereby blocking translation (Clementi, Chirkova et al. 2010, Shi, Khade et al. 2012).

Stx1 and Stx2 share only 55 % and 57 % amino acid sequence identity on the A and B subunits, respectively, and are immunologically distinct (Tesh and O'Brien 1991). The X-ray structures of Shiga toxin from *Shigella*, which differs from Stx1 in only one residue and Stx2 showed structural differences (Fraser, Chernaia et al. 1994, Fraser, Fujinaga et al. 2004, Fraser, Cherney et al. 2006). The active site of the A subunit is blocked by the A_2 chain in the *Shigella* Stx holotoxin, while the active site is accessible to a small substrate in the Stx2 holotoxin (Fraser, Chernaia et al. 1994, Fraser, Fujinaga et al. 2004). The A subunit is in a different orientation with respect to the B subunit in Stx2

compared to Stx (Fraser, Fujinaga et al. 2004). The structures of the A1 subunits without the A_2 and B subunits have not been determined for *Shigella* Stx or *E. coli* Stx1 or Stx2. Although the molecular structure and function of Stx1 and Stx2 are similar, their toxicities are different (Basu and Tumer 2015). STEC strains producing Stx2 are more commonly associated with HUS than those producing Stx1 (Pickering, Obrig et al. 1994, Nataro and Kaper 1998, Manning, Motiwala et al. 2008). A strong correlation is observed between the presence of the Stx2 gene and the severity of disease for human isolates from different serotypes (Boerlin, McEwen et al. 1999). Stx2 has one prototype (Stx2a) and seven subtypes (Stx2b-Stx2h), which display high level of sequence similarity, but significantly differ in toxicity (Fuller, Pellino et al. 2011, Scheutz, Teel et al. 2012). STEC strains producing Stx2a, Stx2c or Stx2d are more commonly associated with HUS in humans than those producing Stx1 (Fuller, Pellino et al. 2011, Scheutz, Teel et al. 2012). The lethal dose of Stx2a (LD_{50}) is over 100-fold lower than that of Stx1 in a mouse model (Head, Karmali et al. 1991, Tesh, Burris et al. 1993). However, molecular basis for the higher potency of Stx2a is unknown. Although Stx2a was more toxic in animal models, Stx1 was more toxic to Vero cells (Tesh, Burris et al. 1993). Stx1 had a higher affinity for the Gb3 receptor in Vero cells (Head, Karmali et al. 1991, Tesh, Burris et al. 1993). Surface plasmon resonance (SPR) analysis showed that Stx1 bound to the Gb3 receptor analog better than Stx2a and had faster association and dissociation rates (Nakajima, Kiyokawa et al. 2001), suggesting that differences in cell binding properties of the B subunits could account for the higher toxicity of Stx1 to Vero cells (Flagler, Mahajan et al. 2010).

To understand the contribution of the A and the B subunits to the higher toxicity of Stx2a, chimeric toxins were created by interchanging the A and B subunits of the two toxins (Head, Karmali et al. 1991). However, the chimeric toxins were usually found to be less stable than the holotoxins due to incorrect folding (Head, Karmali et al. 1991). In some cases they showed equivalent cytotoxicity (Ito, Yutsudo et al. 1988) or did not produce a functional chimera (Weinstein, Jackson et al. 1989). Therefore, clear conclusions regarding the role of each subunit in toxicity could not be deduced. A recent study used the A_2 subunit along with the B subunit to increase the stability of the chimeric toxin (Russo, Melton-Celsa et al. 2014). It was concluded that the toxicity of the chimeric toxins to Vero and HCT-8 cells depended on the origin of the B subunit. However, Vero or HCT-8 cell specific activities of the chimeric toxins differed by at least 50% (Russo, Melton-Celsa et al. 2014). Lethality to mice correlated with the B subunit in one of the hybrids, but the other hybrid was not lethal potentially due to instability (Russo, Melton-Celsa et al. 2014). This study highlighted the importance of the B subunits in the differential toxicity of Stx1 and Stx2a. However, in none of the published studies the B subunit alone accounted entirely for the differential toxicity. Therefore, the role of the A1 subunit in the higher toxicity of Stx2a compared to Stx1 has not been ruled out.

Previous studies have demonstrated the importance of the ribosomal proteins and the P- protein stalk structure for the depurination activity of RIPs (Chan, Chu et al. 2007, Chiou, Li et al. 2008, McCluskey, Poon et al. 2008, Li, Chiou et al. 2009, Too, Ma et al. 2009, McCluskey, Bolewska-Pedyczak et al. 2012). The P-protein stalk is a lateral protuberance of the large subunit of the ribosome, which is responsible for recruitment of

the translation factors to the ribosome and stimulation of GTP hydrolysis (Gonzalo and Reboud 2003). The eukaryotic stalk consists of P0, which anchors two copies of P1/P2 heterodimers organized together in a pentameric structure (Tchorzewski 2002). All stalk P-proteins contain a highly conserved motif at their C-termini, which is involved in recruitment of external factors to the ribosome (Tchorzewski 2002). We showed that the P-proteins of the ribosomal stalk are essential for the cytotoxicity of ricin A chain (RTA) and that the ribosomal stalk is the docking site where RTA interacts with the ribosome (Chiou, Li et al. 2008, Li, Chiou et al. 2009, Li, Grela et al. 2010). The catalytic A1 subunit of Stx1 was shown to interact with the conserved C-terminal motif of the P-proteins (McCluskey, Bolewska-Pedyczak et al. 2012). The interaction of Stx1A1 with the conserved peptide located at the C-terminus of all three eukaryotic ribosomal stalk proteins is mediated by cationic and hydrophobic docking surfaces on the A1 subunit (McCluskey, Bolewska-Pedyczak et al. 2012).

Since the B subunit of the RIPs is required for endocytosis and retrograde trafficking, it has not been possible to study the enzymatic activity of the A subunits in the absence of the B subunits *in vivo*. Moreover, the role of the A1 subunits in the differential toxicity was not investigated further because Stx1 and Stx2a showed similar translation inhibitory activity in a cell free system (Tesh, Burris et al. 1993). We have developed the yeast, *Saccharomyces cerevisiae* as a powerful tool to examine the toxicity and the ribosome interactions of the A subunits of Stx1 and Stx2a independent of the B subunits *in vivo* and have identified amino acids critical for toxicity (Di, Kyu et al. 2011). The depurination activity of the A subunits of Stx1 and Stx2a was reduced in the yeast P-protein mutants and Stx1 and Stx2a differed in their requirements for the stalk proteins *in*

vivo (Chiou, Li et al. 2011). The interaction of the A1 subunits of Shiga toxins with ribosomes or their catalytic activity on ribosomes has not been previously examined. In this study, we examined the interaction of the A1 subunits of Stx1 and Stx2a with yeast and mammalian ribosomes and used a highly sensitive assay to measure the kinetics of ribosome depurination. We compared the activity of the A1 subunits in yeast and in human cells. Our results provide the first direct evidence that Stx2A1 has higher affinity for ribosomes and has higher catalytic activity than Stx1A1 and depurinates ribosomes and inhibits translation to a greater extent than Stx2A1 in cells.

MATERIALS AND METHODS

Yeast Strains and Plasmids. *S. cerevisiae* strain W303 (*MATa ade2-1 trp1-1 ura3-1 leu2-3,112 his-3-11, 15 can1-100*) was grown either in YPD or minimal medium supplemented with 2 % glucose. The mature Stx1A1 (K1 to R251) [NT1419] and Stx2A1 (R1 to R250) [NT1429] were first cloned into pYES2.1/V5-His-TOPO vector and then cloned into a low copy vector, pRS416, containing the *URA3* marker at the NotI-XhoI sites with the V5 and a 6xHis epitopes at their C-termini.

Yeast cell viability assay. The W303 cells carrying Stx1A1 (NT1419) and Stx2A1 (NT1429) under the *GAL1* promoter were grown overnight at 30°C in SD-glucose medium and then were transferred to SD-galactose medium. Cells were collected at 0 and 10 hour post induction and serial dilutions of 0.1 OD_{600} were plated on SD-glucose plates. The plates were then grown at 30°C for 2-3 days.

Total protein extraction and immunoblot analysis. Yeast (W303) cells carrying Stx1A1 and Stx2A1 were grown in SD-glucose medium at 30°C overnight with continuous shaking and then was transferred to SD-galactose medium for StxA1 expression. Cells were collected at 2, 4 and 6 hours post induction. Total protein was extracted from 5 OD_{600} yeast cells as described previously (Zhang, Lei et al. 2011) and cells were resuspended in 2X Laemmli Buffer. Total protein was separated on a 12 % SDS-PAGE and monoclonal antibodies against V5 (Invitrogen, Carlsbad, CA) were used to detect Stx1A1 and Stx2A1 expression. Monoclonal antibodies against 3-phosphoglycerate kinase (Pgk1p) (Life Technologies, Grand Island, NY) were used as a loading control.

Purification of 10xHis-tagged and untagged Stx1A1 and Stx2A1. His-tagged and untagged Stx1A1 and Stx2A1 proteins were purified by Dr. Karen Chave at the Northeast Biodefense Center protein expression core facility using the IMPACT™ protein expression system (New England Biolabs, Ipswich, MA). DNA encoding Stx1A1 (K1 to R251) and Stx2A1 (R1 to R250) were PCR amplified using primers to incorporate a 10xHis-tag at their N-termini using the primers, pTXB1_His_Stx1A1_F (5'- ggtggt cat atgcac cat cac cat cac cat cac cat aaggaatttaccttagac ttc-3') and pTXB1_Stx1A1_R (5'-ggt ggttgctcttccgcatctggcaactcgcga tgc-3') to generate NT1570 (Stx1A1) and primers pTXB1_His_Stx2A1_F (5'-ggt ggt cat atgcac cat cac cat cac cat cac cat cac cat cgg gag tttacgatagacttt tcg-3') and pTXB1_Stx2A1_R (5'-ggt ggttgctcttccgcagcgaacagaacgcgc cc-3') to generate NT1567 (Stx2A1). NdeI and SapI restriction sites were incorporated into the forward and reverse primers, respectively, to facilitate in-frame cloning of the PCR

fragments into the polylinker of the pTXB1 vector (New England Biolabs, Ipswich, MA) resulting in a C-terminal fusion of the *Mycobacterium xenopi* intein tag and a chitin binding domain. For the untagged protein purification, pTXB1_Stx1A1_F (5'- ggtggt cat atg aaggaatttaccttagac ttc-3') and pTXB1_Stx2A1_F (5'-ggt ggt cat atg cgg gag tttacgatagacttt tcg-3') were used. Restriction sites NdeI and SapI were introduced to clone untagged Stx1A1 [NT1576] and Stx2A1 [NT1577] in frame into the polylinker of the pTXB1 vector as previously described. Constructs were expressed in the *E. coli* strain Rosetta2 (DE3) pLysS in 2xYT media, overnight at 16°C. The fusion proteins were purified from *E. coli* lysates using chitin beads and thiol-induced cleavage of the intein was used to release the target proteins from the chitin beads.

Analysis of depurination. Yeast cells containing Stx1A1 and Stx2A1 plasmids were grown in minimal media with 2 % glucose and then switched to minimal media with 2 % galactose to induce the toxin expression. Cells were collected at 0, 1, 2 and 3 h after induction. Total RNA was extracted using the RNeasy Mini Kit (Qiagen, Valencia, CA) with on column DNase treatment and qRT-PCR assay was used to quantify depurination (Pierce, Kahn et al. 2011). RNA was converted to cDNA using the High Capacity cDNA Reverse Transcription Kit (Applied Biosystems, Grand Island, NY) and depurination was detected with a quantitative real time PCR method using the StepOnePlus™ Real-Time PCR system (Applied Biosystems, Grand Island, NY). The 25S reference rRNA was measured using (5'-AGA CCG TCG CTT GCT ACA AT-3'and 5'- ATG ACG AGG CAT TTG GCT AC- 3'). The depurinated rRNA was detected using the forward primer (5'- CTA TCG ATC CTT TAG TCC CTC-3') and the reverse primer

(5'- CCG AAT GAA CTG TTC CAC A-3'). The ΔΔCT method was used to calculate the depurination levels and data were expressed as fold change of depurination in Stx-treated RNA over depurination in control non-treated RNA as described (Pierce, Kahn et al. 2011).

Monomeric ribosomes (7 pmol) were incubated with different concentrations of Stx1A1 and Stx2A1 (0.08 nM, 0.25 nM and 0.75 nM) in a final volume of 100 µL in 1X RIP buffer [60 mM KCl, 10 mM Tris-HCl (pH 7.4), 10 mM $MgCl_2$] at 30°C for 5 min. To this mixture 100 µL of 2X Extraction Buffer [120 mM NaCl, 25 mM Tris-HCl (pH 8.8), 10 mM EDTA, 1% SDS] was added and vortexed. RNA was extracted from this mixture (Li, Kahn et al. 2013) and depurination was determined using qRT-PCR (Pierce, Kahn et al. 2011).

Total RNA was extracted from overnight cultures of yeast cells using the RNeasy Mini Kit (Qiagen, Valencia, CA). Total RNA (1µg) was incubated with different concentrations of Stx1A1 and Stx2A1 (62.5 nM, 125 nM and 250 nM) in a final volume of 20 µL in 20 mM citrate buffer (pH 5) at 37°C for 15 min. RNA was purified (Li, Kahn et al. 2013) and the depurination of rRNA was quantified using qRT-PCR assay (Pierce, Kahn et al. 2011). The ΔΔCT method was used to calculate the depurination level and data were expressed as fold change of depurination in Stx-treated RNA over depurination in non-treated RNA as described (Chiou, Li et al. 2011, Pierce, Kahn et al. 2011).

Isolation of yeast monomeric ribosomes. Monomeric ribosomes were isolated from W303 cells as described previously (Chiou, Li et al. 2011) with the following modifications. The cell free supernatant was incubated with 1 % Triton X-100 for 30 min

at 4°C with gentle shaking to increase the ribosome yield. The supernatant was loaded on the Buffer C cushion to pellet the ribosome by centrifugation at 200,000 *g* for 2 h. The following steps were as previously published (Chiou, Li et al. 2011).

Isolation of rat liver ribosomes. Livers were dissected rapidly after CO_2 knockdown and decapitation of rats, rinsed in cold buffer A (20 mM HEPES-KOH pH 7.6, 5 mM MgOAc, 50 mM KCl, 10 % glycerol) with 1 mM PMSF, 1 mM DTT, and protease inhibitor cocktail for mammalian tissue culture (Sigma-Aldrich, St. Louis, MO) and frozen in liquid N_2. Thawed livers were homogenized disrupted by 10 strokes of a Dounce homogenizer in cold Buffer A plus 1 mM PMSF, 1mM DTT, and protease inhibitor cocktail for mammalian tissue culture (Sigma-Aldrich, St. Louis, MO) and cell debris removed at 20,000 *g* centrifugation for 20 min. Sodium deoxycholate was added to 1 %. After 10 min of stirring in ice ribosomes were sedimented at 150,000 *g* for 90 min. The pellet was rinsed twice in Buffer B (20 mM HEPES-KOH, pH 7.6, 20 mM MgOAc, 0.5 M KCl, 10 % Glycerol) with 1 mM PMSF, 1 mM DTT, and stored overnight at 4°C in a small amount of the same buffer. The ribosomes were resuspended with a Dounce homogenizer in buffer B with 1 mM DTT and 1 mM PMSF and incubated 30 min at 30°C with 1 mM puromycin, 1 mM GTP. The supernatant was clarified by centrifugation at 20,000 *g* for 15 min and layered over a cushion of buffer B with glycerol raised to 25 %. Ribosomes were sedimented at 150,000 *g* for 2 h. The pellets were rinsed in Buffer C (50 mM HEPES-KOH pH 7.6, 5 mM MgOAc, 50 mM NH_4Cl, 0.1 mM DTT and 25% glycerol), resuspended in 5 ml Buffer C and stored -80 ºC. A further step of purification was performed on hydroxylapetite essentially as described by

Hoffman and Ilan (Hoffman and Ilan 1974), except that a column was used rather than batch elution.

Interaction of Stx1A1 and Stx2A1 with the ribosome and the ribosomal stalk complex. The interactions were measured using a Biacore T200 (GE Healthcare Bio-Sciences, Pittsburgh, PA) instrument using either untagged or 10xHis-tagged A1 subunits. The untagged toxins were immobilized on the CM5 chip by amine coupling and Biacore T200 monitored the amount of immobilized toxin in real time. The amount immobilized was 1692 RU for the untagged Stx1A1 and 1672 RU for the untagged Stx2A1. Flow cell one was activated and blocked as the reference channel. Single cycle kinetic method was used. Ribosomes at different concentrations were passed over the surface at 40 μL/min for 2 min. Dissociation was for 5 min. Running buffer contained 10 mM Hepes pH 7.4, 150 mM NaCl and 5 mM MgOAc, 50 μM EDTA and 0.003 % Surfactant P20. The surface was regenerated by two one-minute injections of 3 M NaCl. The 10xHis-tagged Stx1A1 and Stx2A1 captured on a NTA chip. The amount of captured toxin monitored in real time by Biacore T200 was 2300 and 2230 RU for 10xHis-Stx1A1 and 10xHis-Stx2A1, respectively. Ribosomes were passed over each surface at different concentrations. The interaction conditions were the same as for the untagged A1 subunits except the surface was fresh captured at each cycle. For the interaction of the A1 subunits with the isolated ribosomal stalk pentamer, 10xHis-tagged Stx1A1 and Stx2A1 were captured on a NTA chip at around 1000 RU and the same amount of 10xHis-tagged EGFP was captured on the reference channel. Yeast stalk

pentamer was passed over the surface at 70 μL/min for 5 min and the final dissociation was for 10 min.

Ribosome depurination kinetics assay. Yeast monomeric ribosomes were isolated as previously described (Li, Chiou et al. 2009). Prior to use, the yeast ribosomes were passed through a 0.5 mL Zeba™ spin desalting column (Life Technologies, Grand Island, NY) to reduce AMP and ATP contamination as described (Sturm and Schramm 2009). At the same step the buffer was changed to ribosome depurination buffer (20 mM Tris-HCl, pH 7.4, 25 mM KCl, 5 mM $MgCl_2$). Depurination was measured by the continuous luminescence assay as described by Sturm and Schramm (Sturm and Schramm 2009). Toxin concentrations used were 4 pM for Stx1A1 and 3 pM for Stx2A1 when yeast ribosomes were used as substrate and 4 pM for both Stx1A1 and Stx2A1 when rat ribosomes were used as a substrate. The reaction was set up in a 96-well plate in a total reaction volume of 50 μL. The reaction was started by adding toxin to the reaction mixture and the luminescence intensity was recorded continuously for 30 min using a BioTek Synergy 4 Microplate Reader (Winooski, VT, USA). The rates were determined from the linear region of the luminescence intensity. The Stx independent rate of adenine generation was subtracted. Adenine standards covering the range of depurination were measured on the same plate and at the same time. The initial rate of adenine formation was calculated by converting luminescent rate (lumens/s) to enzymatic rate (pmoles of adenine/min/pmole of enzyme) using the adenine standard curve. Kinetic parameters (k_{cat} and K_m) were calculated by fitting initial rates to the Michaelis-Menten equation using Sigma Enzyme Kinetics Module 1.3 (Systat Software, Inc., San Jose, CA 95110 USA).

SRL depurination kinetics assay. Stem-loop depurination was performed using a synthetic 10-mer SRL oligonucleotide (5′-rCrGrCrGrArGrArGrCrG-3′) purchased from Integrated DNA Technologies (San Diego, CA). The discontinuous luminescence assay developed by Sturm and Schramm (Sturm and Schramm 2009) was used with modification of both temperature and pH. Although linear depurination could be achieved with ricin at 37°C and pH 4.0 (Li, Kahn et al. 2013) , these conditions rapidly inactivated Stx1A1 and Stx2A1. Lowering the temperature to 20°C and raising the pH to 4.5 slowed both reaction and inactivation such that linearity could be achieved for at least 5 min. Dilutions of the stem loop RNA in 30 µL 10 mM potassium citrate-KOH and 1 mM EDTA were equilibrated at 20°C. Each A1 subunit was preincubated at 2x final concentration in the same buffer for 5 min at 20°C prior to the addition to RNA to start the reaction. Samples (9 µL) were withdrawn at timed intervals up to 5 min and added to 9 µL of 2x coupling buffer (Sturm and Schramm 2009) in a chilled 96 white luminescence plate. At the termination of the assay the plate was warmed to 30°C for 10 min to initiate the coupled reaction. 35 µL of ATPlite™ (PerkinElmer, Waltham, MA) reagent was added per well. Adenine standards of 0.5 to 2 pmol prepared in pH 4.5 buffer give a linear response under these conditions. Luminescence intensity was measured using a BioTek Synergy 4 Microplate Reader (Winooski, VT, USA) at high sensitivity after incubation of the plate for 10 min in the dark. Parameters were calculated for Michaelis-Menten kinetics using the Sigma Enzyme Kinetics module 1.3 (Systat Software, Inc., San Jose, CA 95110 USA).

Transfection of HEK293T cells with the A1 subunits. The mature Stx1A1 (K1 to R251) [NT1776] and Stx2A1 (R1 to R250) [NT1777] constructs with V5 and a 10xHis-tags were cloned into the mammalian expression vector pCAGGS, at the SacI-XhoI sites. HEK 293-T cells were cotransfected with these constructs and an EGFP expression plasmid, also in pCAGGS, using Lipofectamine 2000 (Invitrogen, Carlsbad, CA). Cells were plated in DMEM medium (phenol red free) and 10 % fetal calf serum at $5x10^4$ /ml in black clear-bottom 96 well plates. After 24 h, with cells at approximately 90 % confluence, the media was removed and replaced with 50 µL medium lacking calf serum which had been preincubated 10 min with 50 ng of each DNA and 0.3 µL Lipofectamine. After 2 h of incubation at 37 °C, 5 % CO_2, the transfecting solution was removed and replaced by 100 µL medium containing 10 % fetal calf serum. EGFP fluorescence was read at 22 h post DNA exposure in a Biotek plate reader from the bottom of plate with 485/20 excitation filter and 530/25 emission filter. Assays were performed in quadruplicate. Fluorescence measured in cells cotransfected with EGFP and empty vector was considered as 100 % and fluorescence in controls lacking EGFP plasmid as background (Redmann, Oresic et al. 2011).

Analysis of ribosome depurination in HEK293T cells. For the *in vivo* depurination, HEK 293-T cells containing mature Stx1A1 and Stx2A1 plasmids were first grown as described above. Cell samples were collected at 23 h after DNA exposure. Total RNA was extracted using the RNeasy Mini Kit (Qiagen, Valencia, CA) with on column DNase treatment. qRT-PCR assay was used to quantify depurination (Jetzt, Cheng et al. 2012, May, Li et al. 2012).

Statistical analysis. Statistical analyses were conducted using SAS 9.4 (SAS Institute Inc., Cary, NC). Statistical analysis of data in Figs. 2.1B, 2.6A, and 2.6B were performed using PROC GLM (general linear models). Statistical analyses of data in Figs. 2.1D, 2.2C and 2.2D were conducted using SAS 9.4 (SAS Institute Inc., Cary, NC). Data were analyzed by generalized mixed linear models using PROC GLIMMIX to test for statistical differences between treatments. PROC GLIMMIX permits the inclusion of a random effect (PCR experiment as a block) into the generalized mixed linear model. All treatments were considered fixed effects and blocks (separate qRT-PCR plates) were considered random effects (Rieu and Powers 2009). Least square means were calculated and specific preplanned contrasts (Steel and Torrie 1980) were computed to compare treatment means between Stx1A1 and Stx2A1 for each treatment.

RESULTS:

Stx2A1 is more toxic and shows higher depurination than Stx1A1 in yeast. To compare the cytotoxicity of the A1 subunits of Stx1 and Stx2 *in vivo*, the mature A1 subunits were expressed in the yeast *S. cerevisiae*, with the V5 and 10xHis epitope tags under the tightly controlled *GAL1* promoter. Previous results indicated that the V5 and 10xHis epitope tags do not affect the activity of the A subunits (Chiou, Li et al. 2011, Di, Kyu et al. 2011). Irreversible growth inhibition by Stx1A1 and Stx2A1 was determined by plating cells on media containing 2% dextrose after galactose induction for the indicated times in liquid media. Cells transformed with empty vector were used as a control. As shown in Figs. 2.1A and B, Stx1A1 and Stx2A1 reduced viability of cells by

10-fold and 100-fold, respectively comparing to vector control. Yeast cells expressing Stx2A1 grew over 10-fold less than those expressing Stx1A1, indicating that Stx2A1 is more toxic than Stx1A1.

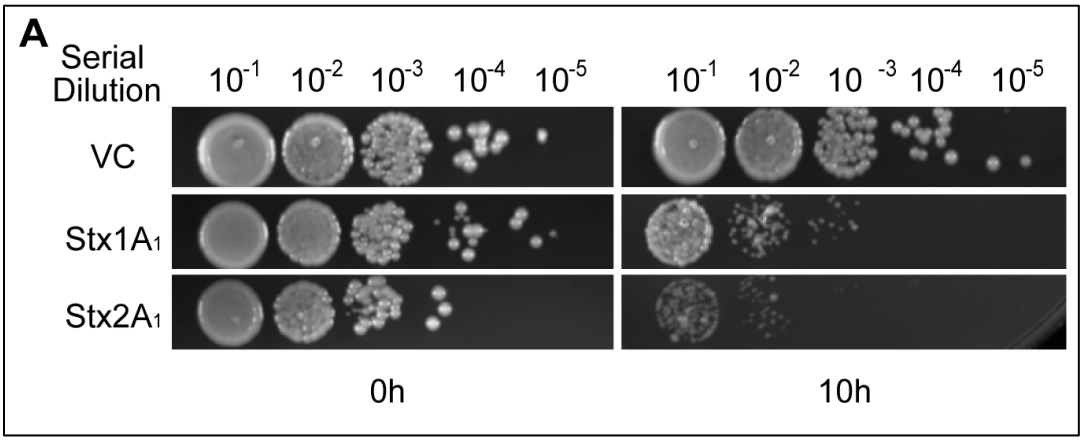

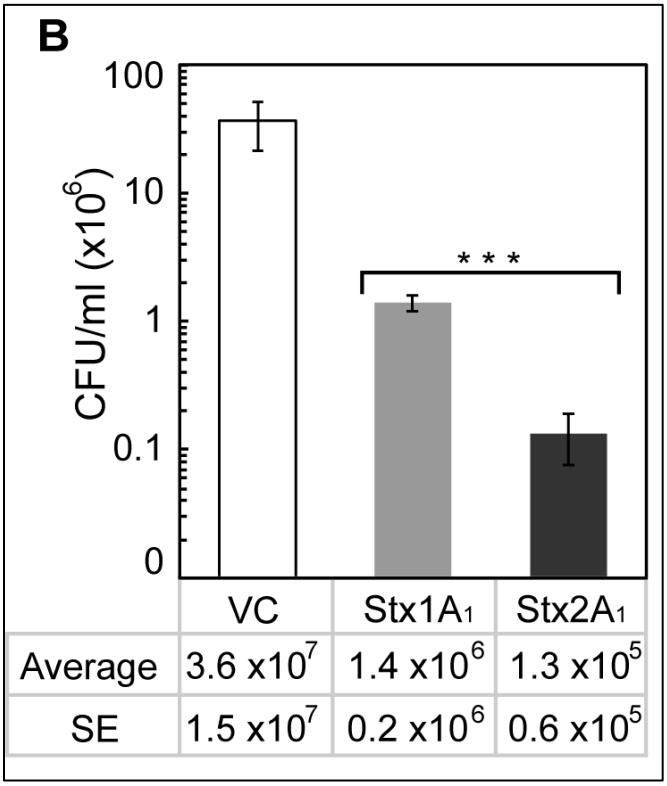

FIG 2.1 (A) Viability and ribosome depurination in yeast expressing Stx1A1 or Stx2A1. Yeast cells transformed with a plasmid carrying Stx1A1 or Stx2A1 and yeast cells carrying the empty vector (VC) were grown in SD medium supplemented with 2 % glucose and then transferred to SD medium supplemented with 2 % galactose. At 0 and 10 hours post induction (hpi), a series of 10-fold dilutions were plated on media containing 2 % glucose and grown at 30°C for 1-2 days**. (B) Colony forming units per ml (CFU/ml) were calculated at 10 hpi from at least 3 independent transformants.** Error bars represent S. E. where n=3 independent experiments. Means of Stx2A1 and Stx1A1 were significantly different using one tailed t-test ($p < 0.001$).

To examine the expression of the A1 subunits in yeast, whole cell lysates were analyzed by immunoblotting with monoclonal antibodies against the V5 epitope. Monoclonal antibodies against phosphoglycerate kinase 1 (Pgk1) were used as a loading control (Fig. 2.1C). Cells harboring Stx1A1 and Stx2A1 showed a gradual increase in expression with time. Stx1A1 was expressed at a higher level than Stx2A1. These results were consistent with previous observations, which showed that the expression level of the toxins is correlated inversely with their toxicity (Li, Kahn et al. 2013). A lower level of protein expression was detected for Stx2A1 consistent with our finding that Stx2A1 was more toxic than Stx1A1.

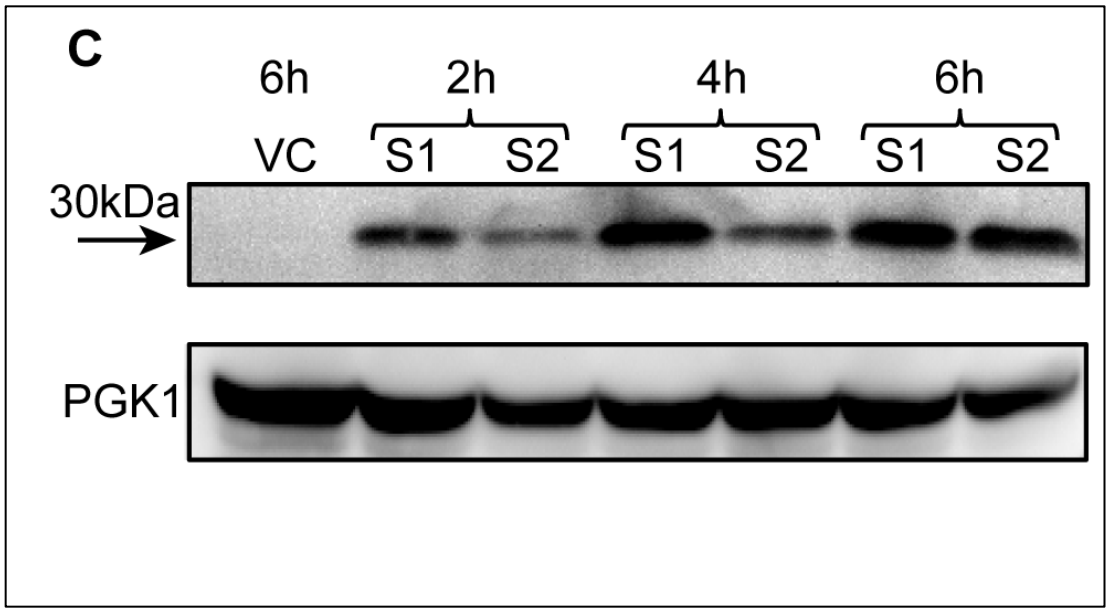

FIG 2.1 (C) Immunoblot analysis of yeast cells transformed with Stx1A1 and Stx2A1. Total protein from 5 OD_{600} cells isolated at 2, 4, 6 hpi was separated on SDS-PAGE and probed with anti-V5. Anti-Pgk1 was used as a loading control.

To determine if the higher toxicity of Stx2A1 over Stx1A1 is due to higher level of ribosome depurination in yeast, total RNA was isolated from yeast at different times after induction and relative levels of depurination over time were quantified using qRT-PCR. In this assay, two pairs of primers are used to amplify the target amplicon (depurinated SRL) and the reference amplicon (25S rRNA), and the data are analyzed by the comparative CT method (ΔΔCT) relative to yeast harboring the empty vector (Pierce, Kahn et al. 2011). Data obtained using 3 independent colonies showed that cells expressing Stx2A1 exhibited 1.7 to 2.4-fold higher levels of depurination compared to cells expressing Stx1A1 (Fig. 2.1D). This difference was statistically significant using PROC GLIMMIX (Steel and Torrie 1980), which permits the inclusion of a random effect (separate qRT-PCR plates) into the generalized mixed linear model (Table 2.S1).

Collectively these data indicate that Stx2A1 depurinates ribosomes at a higher level and is more toxic to yeast than Stx1A1.

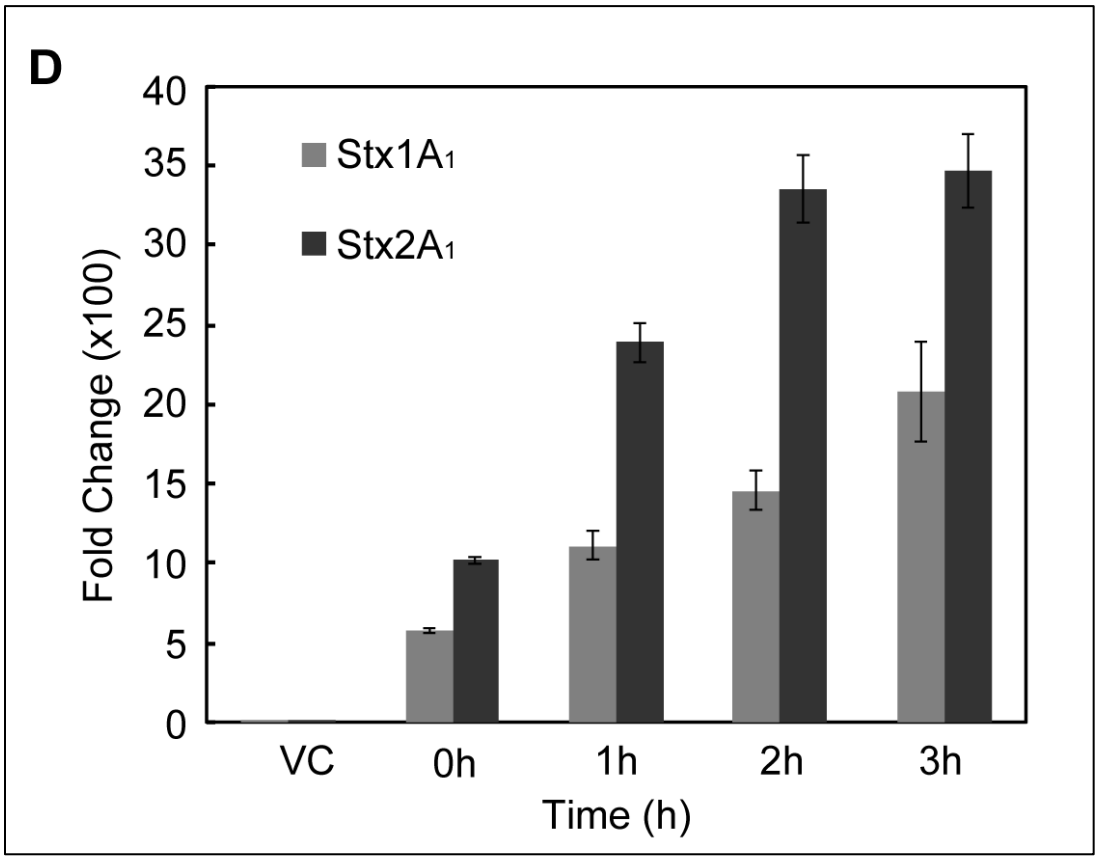

FIG 2.1 (D) Depurination of ribosomes in yeast. Total RNA (375 ng) isolated from 1 OD_{600} cells expressing Stx1A1 (grey bars) or Stx2A1 (black bars) collected at 0, 1, 2 and 3 hpi was used to quantify the relative level of depurination using qRT-PCR. The analysis was repeated three times and one representative experiment is shown. The y-axis shows the fold change in depurination of toxin-treated samples over the control samples without toxin (VC). Error bars represent S. E. where n=3 replicates. Means of Stx2A1 and Stx1A1 were significantly different using PROC GLIMMIX at 125 nM (**P< 0.01) and 250 nM (****P< 0.0001).

Stx2A1 depurinates yeast ribosomes and RNA at a higher level than Stx1A1. To examine the ribosome depurination by Stx1A1 and Stx2A1 *in vitro*, the 10xHis tagged and untagged Stx1A1 and Stx2A1 were expressed in *E. coli* and purified to homogeneity. Equal amounts of purified toxins were analyzed by SDS-PAGE (Fig. 2.2A) and by immunoblot analysis (Fig. 2.2B). Each toxin migrated on SDS-PAGE as expected for its size. The 10xHis-tagged proteins migrated slower on SDS-PAGE as expected (Fig. 2.2A) due to their larger size (28.9 kDa and 29.2 kDa for tagged Stx1A1 and Stx2A1 respectively, compared to 27.6 kDa and 27.9 kDa for untagged Stx1A1 and Stx2A1, respectively). Protein thermal shift assay was used to examine the relative stability of untagged Stx1A1 and Stx2A1 at pH 4, 5 and 7.4 and the results showed that purified Stx1A1 is more stable than Stx2A1 at the tested pH conditions (Fig. 2.S1).

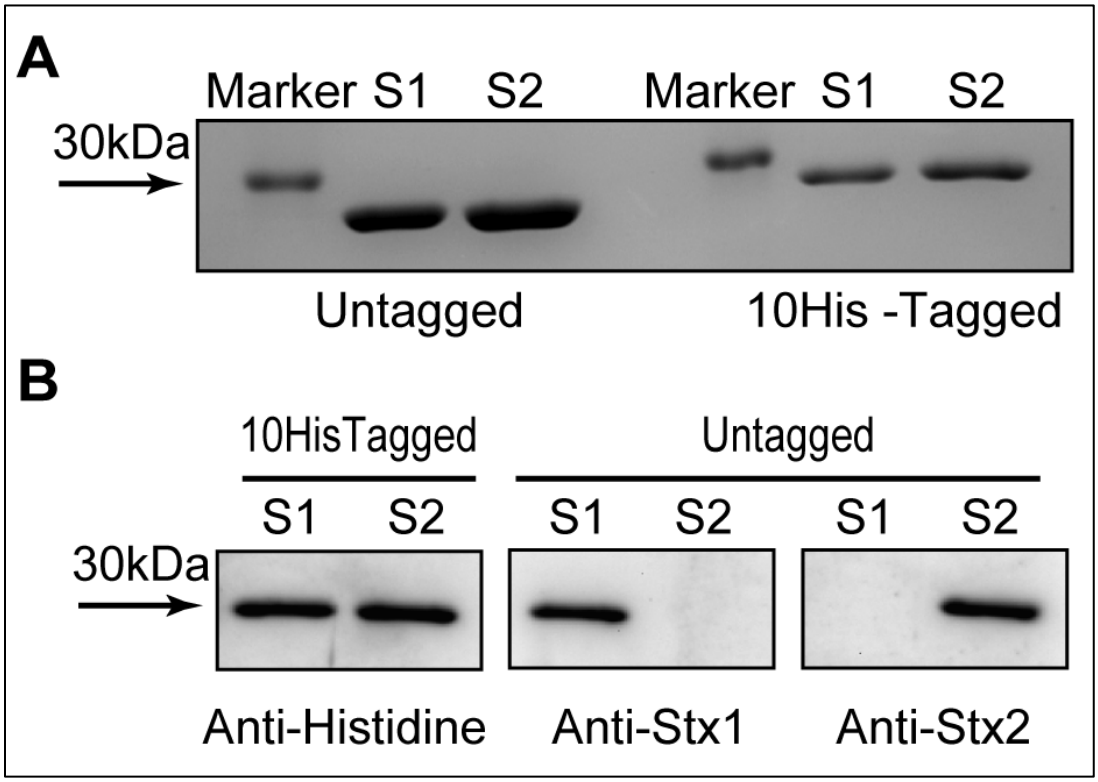

FIG 2.2 (A) Coomassie blue staining of purified 10xHis-tagged and untagged Stx1A1 and Stx2A1. Equal amount (1 μg) of purified Stx1A1 (S1) and Stx2A1 (S2) were separated on a 12 % SDS-polyacrylamide gel and stained by coomassie blue. **(B) Immunoblot analysis of purified 10xHis-tagged and untagged Stx1A1 and Stx2A1.** Equal amount (100 ng) of purified Stx1A1 (S1) and Stx2A1 (S2) were separated on a 12 % SDS-polyacrylamide gel. 10xHis-tagged Stx1A1 (S1) and Stx2A1 (S2) were detected by monoclonal anti-His. Untagged Stx1A1 (S1) and Stx2A1 (S2) were detected by polyclonal anti-Stx1 or anti-Stx2.

Depurination activity of untagged Stx2A1 and Stx1A1 on yeast ribosomes was measured by qRT-PCR (Fig. 2.2C). Yeast ribosomes were treated with 0.08 nM to 0.75 nM Stx1A1 and Stx2A1. Untreated ribosomes were used as a control. The experiment was repeated at least three times. The depurination level of Stx2A1 was 1.4 to 1.9-fold higher than the depurination level of Stx1A1 at each toxin concentration tested. This difference was statistically significant (Table 2.S2).

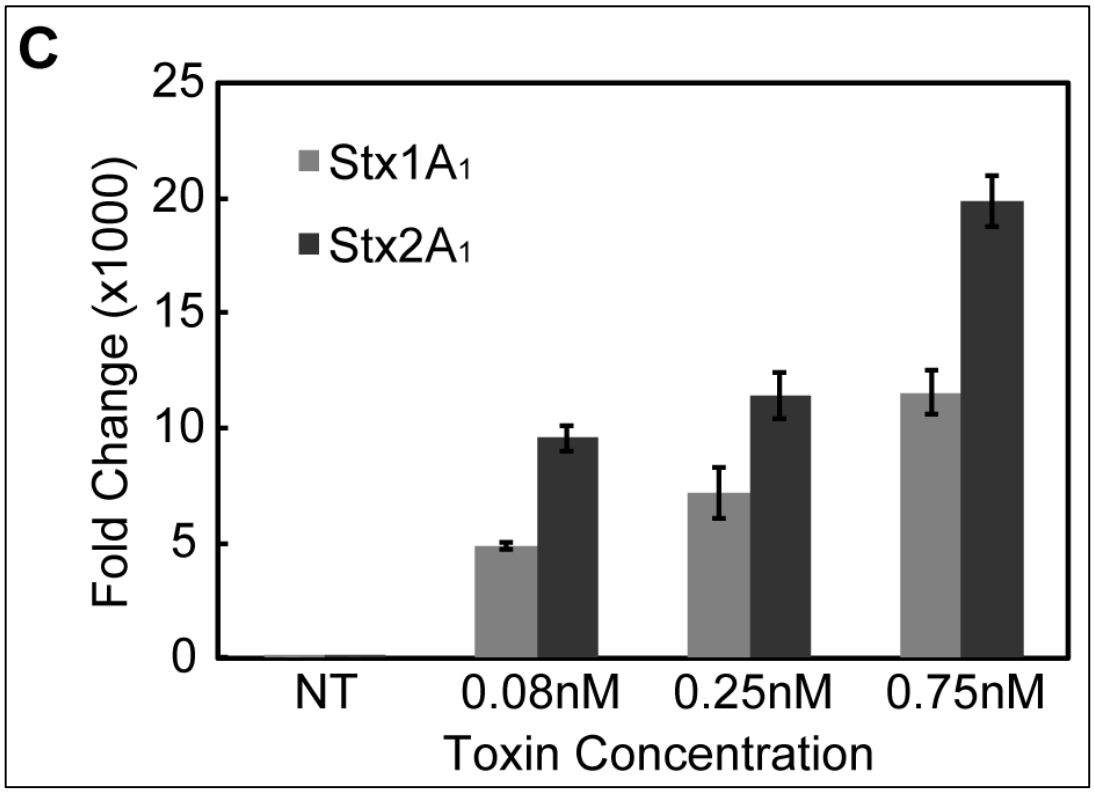

FIG 2.2 (C) Depurination of yeast ribosomes by purified Stx1A1 and Stx2A1. Yeast ribosomes (7 pmol) were incubated with different concentrations of Stx1A1 (grey bars) or Stx2A1 (black bars) at 30°C for 5 min. The rRNA (375 ng) was used to quantify the relative levels of depurination by qRT-PCR (Pierce, Kahn et al. 2011). The y-axis shows the fold change in depurination of toxin-treated samples over the control samples without toxin treatment (NT). The analysis was repeated three times and one representative experiment is shown. Error bars represent S. E. where n=3 replicates. Means of Stx1A1 and Stx2A1 were significantly different using PROC GLIMMIX at 0.08 nM (***P< 0.001), 0.25 nM (****P< 0.0001) and 0.75 nM (****P< 0.0001).

Since ribosome depurination is determined by toxin-ribosome interaction and catalytic activity once the toxin is bound, to determine whether the observed difference in

ribosome depurination is due to difference in the catalytic activity, we compared the depurination activity of Stx1A1 and Stx2A1 on free RNA. Total RNA from yeast cells was isolated and treated with different concentrations (62.5, 125 and 250 nM) of Stx1A1 and Stx2A1. The relative levels of depurination were quantified using qRT-PCR. Stx2A1 depurinated RNA at a 1.6 to 4.3-fold higher level compared to Stx1A1 (Fig. 2.2D). This difference was statistically significant (Table 2.S3). These results demonstrate that Stx2A1 depurinates yeast ribosomes and RNA at a higher level than Stx1A1 *in vitro*.

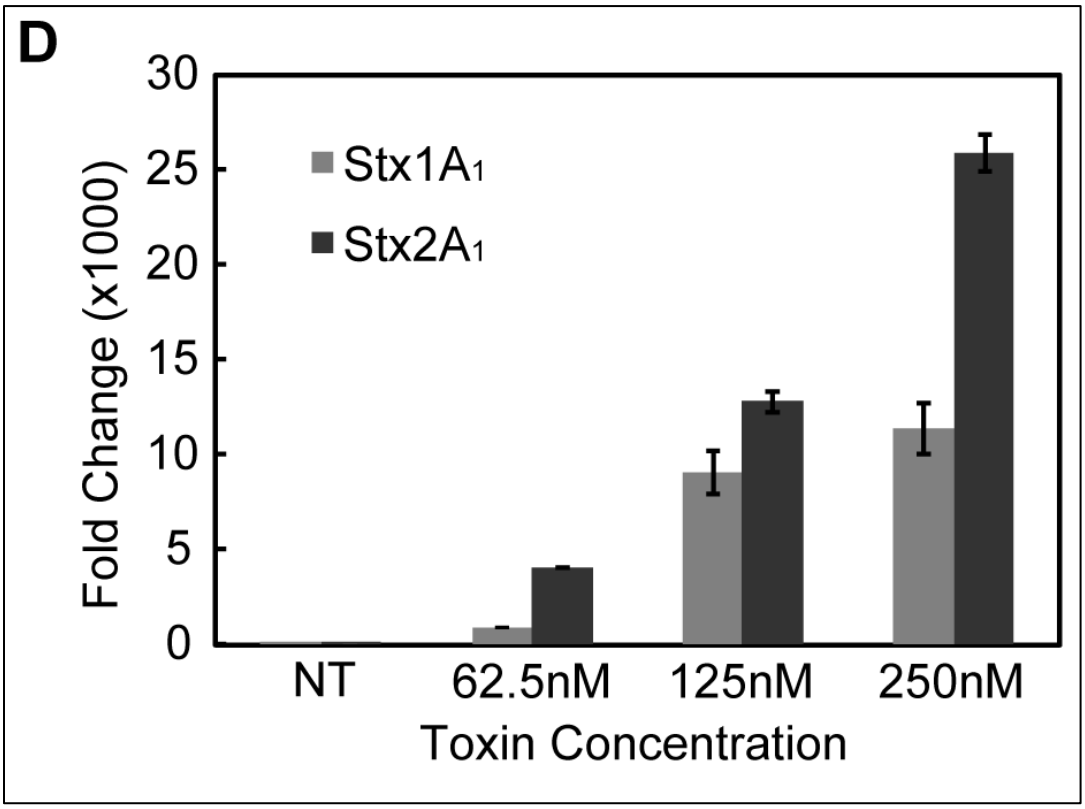

FIG 2.2 (D) Depurination of total RNA from yeast by purified Stx1A1 or Stx2A1. Total RNA (1µg) was incubated with different amounts of Stx1A1 (grey bars) or Stx2A1 (black bars) at 37°C for 15 min. The relative levels of depurination were determined using qRT-PCR (Pierce, Kahn et al. 2011). The y-axis shows the fold change in

depurination over the control samples without toxin treatment (NT). The analysis was repeated three times. Error bars represent S. E. where n=3 replicates. Means of Stx2A1 and Stx1A1 were significantly different using PROC GLIMMIX at 125 nM (**P< 0.01) and 250 nM (****P< 0.0001).

Stx2A1 has higher affinity for yeast and mammalian ribosomes than Stx1A1. Since ribosome binding is critical for ribosome depurination, we examined the direct interaction of A1 subunits with ribosomes using surface plasmon resonance with a Biacore. To compare the interaction of Stx1A1 and Stx2A1 with the ribosome, the untagged A1 subunits were immobilized on a CM5 chip of a Biacore T200 at 1692 RU and 1672 RU, respectively using amine coupling and their interaction with yeast ribosomes was measured using single cycle kinetic analysis by passing ribosomes over the surface at different concentrations. Since the surface is not regenerated between injections in the single-cycle analysis, multiple samples can be analyzed in a shorter period of time allowing comparison of binding under identical conditions (Li, Grela et al. 2010). As shown in Fig. 2.3A, the binding level of Stx2A1 was 12-fold higher than Stx1A1 when yeast ribosomes were used at 2.5 nM and was 5-fold higher than Stx1A1 when yeast ribosomes were used at 40 nM. Since binding did not reach equilibrium and did not fit the 1:1 model, resonance units (RU), which show the level of binding at the end of each ribosome concentration were used to calculate the dissociation constants (K_D) (Table 2.1). The apparent K_D for untagged Stx2A1 for yeast ribosomes was 6.5-fold lower than the apparent K_D for Stx1A1, and this difference was statistically significant. The binding level of 10xHis tagged Stx2A1 to yeast ribosomes was 2.7 to 4-fold higher than the

binding level of Stx1A1 (Fig. 2.3B). The 10xHis tagged Stx2A1 had 3-fold lower K_D for yeast ribosomes compared to 10xHis tagged Stx1A1 (Table 2.1). However, this difference did not achieve statistical significance. The major difference in the interaction of Stx1A1 and Stx2A1 with ribosomes was in their interaction patterns. The untagged and 10xHis tagged Stx2A1 had a much faster association and dissociation pattern compared to Stx1A1 (Fig. 2.3B). The K_D does not reflect this difference. The association (k_{on}) and dissociation (k_{off}) rates could not be accurately determined because the interaction did not fit a 1:1 interaction model.

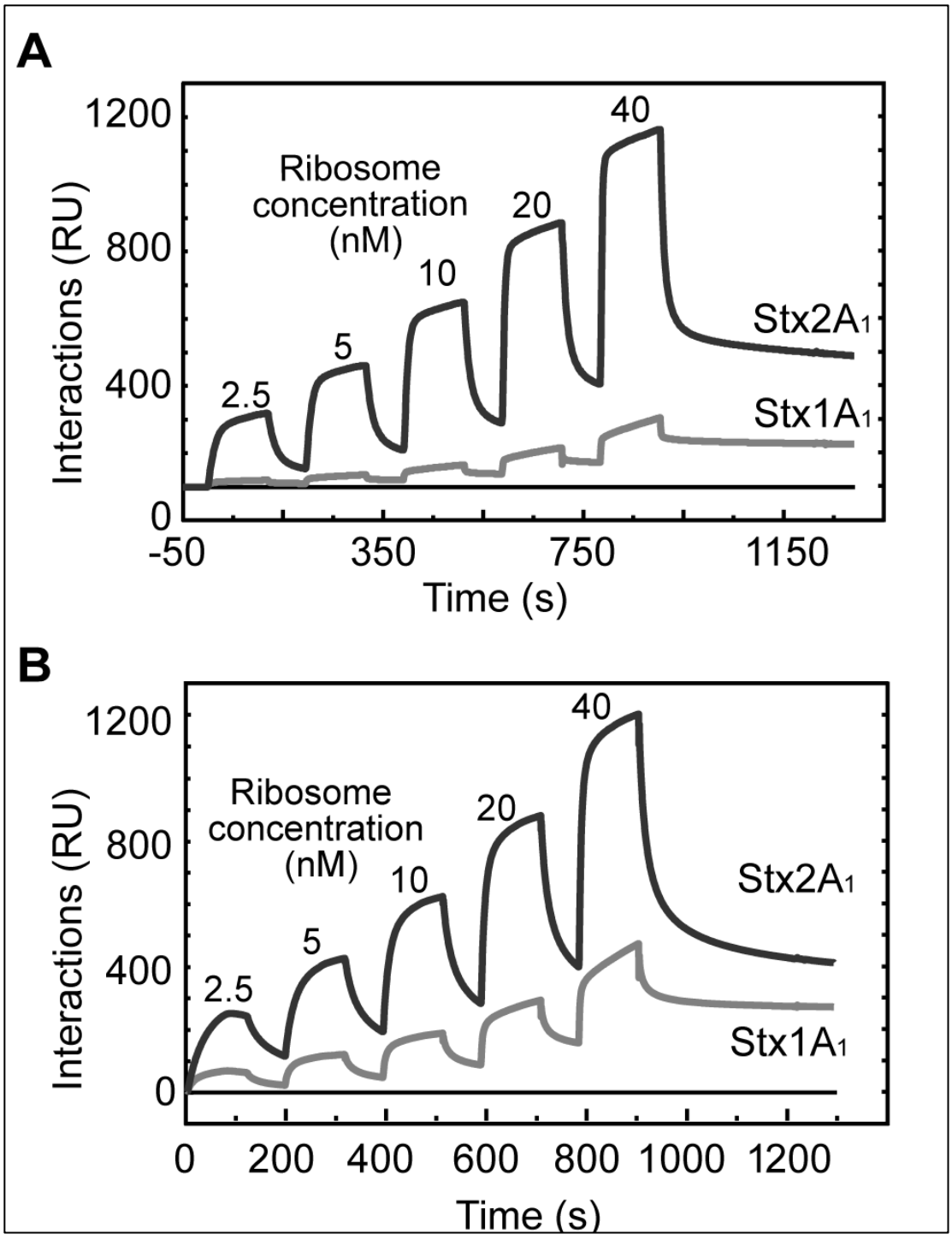

FIG 2.3 (A) Interaction of Stx1A1 and Stx2A1 with yeast ribosomes. Untagged Stx1A1 (grey) and untagged Stx2A1 (black) were captured on a CM5 chip at 1692 RU and 1672 RU respectively. Different concentrations of ribosome were passed over the

surface as analyte as shown. **(B) Interaction of 10xHis tagged Stx1A1 and Stx2A1 with yeast ribosomes.** 10xHis-Stx1A1 (grey) and 10xHis-Stx2A1 (black) were captured on an NTA chip. Different concentrations of ribosome were passed over the surface as analyte as shown.

TABLE 2.1. Apparent K_D (M) of the interaction of the A1 subunits with ribosome[A]

Toxin	Yeast Ribosome	Rat Liver Ribosome
Stx1A1	**$16.8\pm0.6 \times 10^{-8}$ a**	**$8.6\pm1.6 \times 10^{-8}$ c**
Stx2A1	**$2.3\pm0.3 \times 10^{-8}$ b**	**$2.8\pm0.4 \times 10^{-8}$ d**
10xHis-Stx1A1	**$4.6\pm2.2 \times 10^{-8}$ e**	**$3.0\pm1.1 \times 10^{-8}$ e**
10xHis-Stx2A1	**$2.2\pm0.4 \times 10^{-8}$ f**	**$3.6\pm1.0 \times 10^{-8}$ f**

[A] Letters indicate statistical comparisons, where means were significantly different between a and b (P 0.01) and between c and d (P 0.05) and means were not significantly between e and f, as determined by using a one-tailed t test.

Previous studies showed that the P-proteins of the ribosomal stalk are important for ribosome depurination by Stx1 and Stx2 (Chiou, Li et al. 2011). The A1 chain of Stx1 interacts with the conserved C-termini of P-proteins (McCluskey, Poon et al. 2008, McCluskey, Bolewska-Pedyczak et al. 2012). To determine if the higher level of binding

of Stx2A1 to the ribosome is due to a higher level of binding to the ribosomal P-protein stalk complex, we examined the interaction of the A1 subunits with the pentameric stalk complex from yeast (Li, Grela et al. 2010). We captured the 10xHis-tagged Stx1A1 and Stx2A1 on an NTA chip at the same level and passed the purified stalk pentamer complex over the surface. As shown in Fig. 2.3C, the binding level of Stx2A1 was slightly higher than Stx1A1. The interaction of the A1 subunits with the stalk pentamer fit into a 1:1 interaction model (Table 2.2). 10xHis-tagged Stx2A1 showed slightly slower dissociation and had slightly higher affinity for the stalk compared to 10xHis-tagged Stx1A1 (Table 2.2). However the differences in the affinity (K_D) and the association (k_{on}) and dissociation (k_{off}) rates of Stx1A1 and Stx2A1 for the stalk complex were not significant. Therefore, the differences observed in the binding affinities of Stx1A1 and Stx2A1 for yeast ribosomes and the differences in ribosome depurination are not due to differences in their binding to the P-protein stalk.

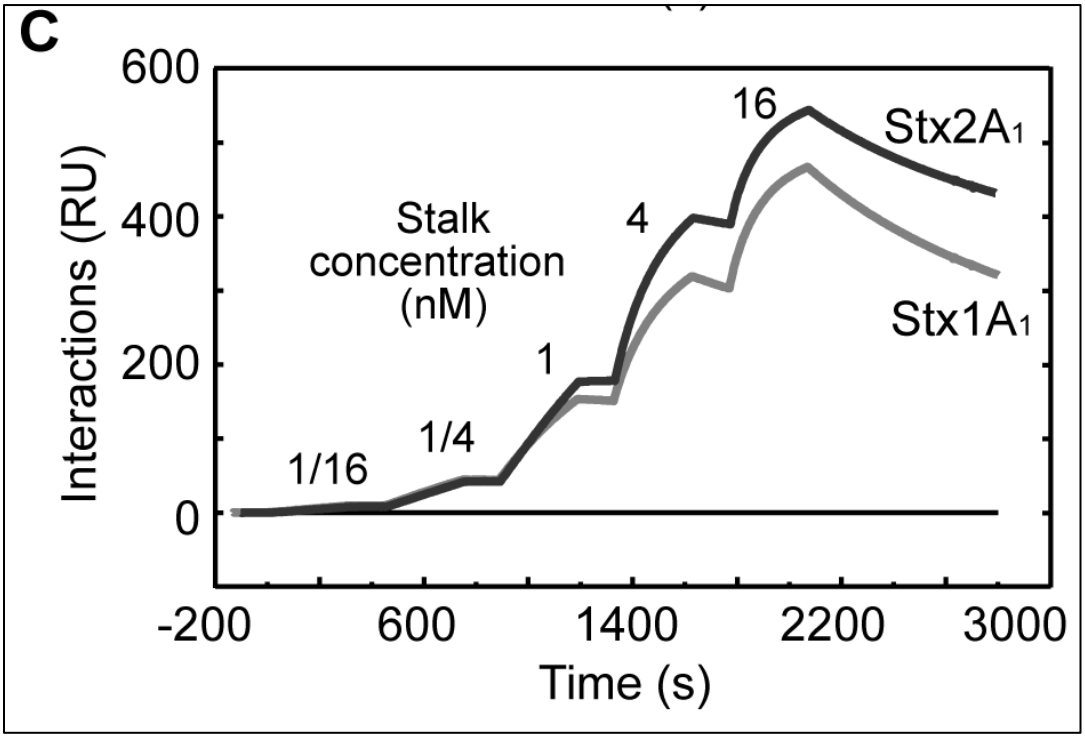

FIG 2.3 (C) Interaction of Stx1A1 and Stx2A1 with the isolated yeast ribosomal stalk pentamer. 10xHis-Stx1A1 (grey) or 10xHis- Stx2A1 (black) was captured on an NTA chip at 1000 RU and the same amount of EGFP was captured on the reference channel. Different concentrations of stalk pentamer were passed over the surface as analyte as shown.

TABLE 2.2. Stalk interaction Parameters [A]

Toxin	K_{on} ($M^{-1}s^{-1}$)	K_{off} (s^{-1})	K_D (M)
Stx1A1	$1.6\pm0.6 \times 10^{6}$ a	$4.1\pm1.7 \times 10^{-4}$ c	$3.0\pm2.2 \times 10^{-10}$ e
Stx2A1	$1.8\pm0.9 \times 10^{6}$ b	$2.2\pm1.0 \times 10^{-4}$ d	$1.6\pm1.4 \times 10^{-10}$ f

[A] Letters indicate statistical comparisons, where means were not significantly different between a and b, between c and d, and between e and f, as determined by using a one-tailed t test.

To examine the relative affinity of Stx2A1 and Stx1A1 for mammalian ribosomes, the interaction of untagged Stx1A1 and Stx2A1 with rat liver ribosomes was analyzed with a Biacore. The untagged A1 chains were immobilized on a CM5 chip using amine coupling at the same ligand level and rat liver ribosomes were passed over the surface at different concentrations using single cycle kinetics. As shown in Fig. 2.4A, rat ribosomes bound Stx2A1 at a considerably higher level than Stx1A1. The binding level of Stx2A1

was about 14-fold higher than Stx1A1 at 80 nM ribosome concentration. We calculated the apparent K_D using the RU values at the end of the injection of each ribosome concentration. The apparent K_D of Stx2A1 for rat liver ribosomes was significantly (3-fold) lower than the apparent K_D of Stx1A1 for rat liver ribosomes (Table 2.1). Differences in binding level were observed when 10xHis tagged Stx1A1 and Stx2A1 were used (Fig. 2.4B). The apparent K_D of 10xHis tagged Stx2A1 for rat liver ribosome was about 1.7-fold lower than the apparent K_D of 10xHis tagged Stx1A1 for rat liver ribosomes (Table 2.1), which was not statistically significant. These data indicate that Stx2A1 has higher affinity for mammalian ribosomes than Stx1A1.

Stx2A1 has higher catalytic activity on yeast and mammalian ribosomes. To examine the correlation between ribosome interaction and depurination, we measured the depurination kinetics of Stx1A1 and Stx2A1 towards monomeric yeast and rat liver ribosomes using a continuous enzymatically coupled luminescence assay with sufficient sensitivity to continuously measure single adenine release from nanomolar concentrations of intact eukaryotic ribosomes (Sturm and Schramm 2009). This assay can detect femtomoles of ricin in minutes using APRTase to convert adenine to AMP and then to ATP with PPDK. ATP generates light via luciferase and the AMP regenerated is converted to ATP by PPDK (Sturm and Schramm 2009).

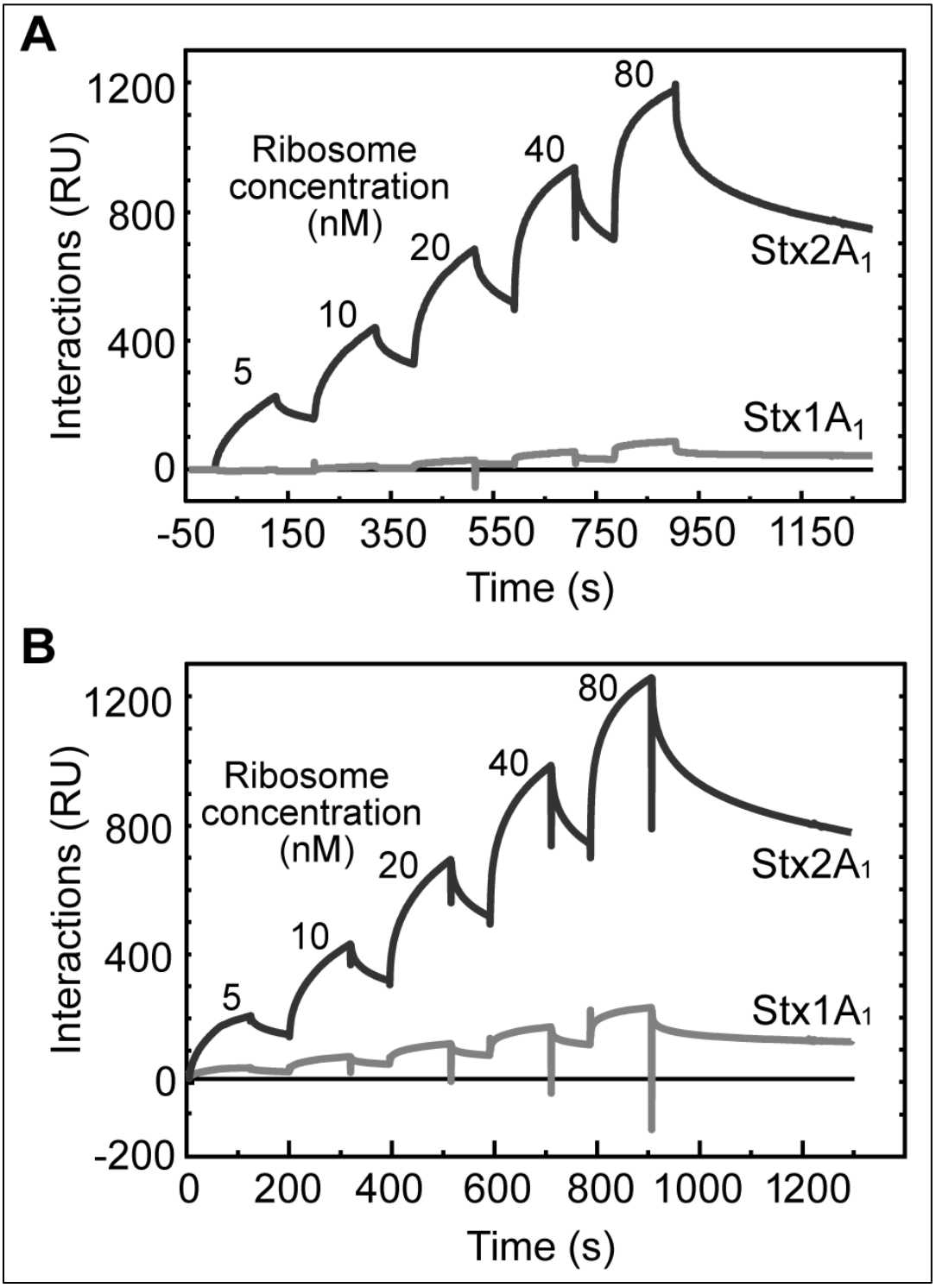

FIG 2.4 (A) Interaction of Stx1A1 and Stx2A1 with ribosomes from rat liver. The same conditions as the interaction with yeast ribosomes were used. Different concentrations of ribosome were passed over the surface as analyte as shown. **(B)**

Interaction of 10xHis- Stx1A1 and 10xHis-Stx2A1 with ribosomes from rat liver. 10xHis- Stx1A1 (grey) and 10xHis-Stx2A1 (black) were captured on a NTA chip. The same conditions as the interaction with yeast ribosomes were used**.** Different concentrations of ribosome were passed over the surface as analyte as shown.

TABLE 2.3. Kinetic parameters of A1 subunits with ribosomes and stem-loop RNA

Substrate		Toxin	K_m (μM)	k_{cat} (min^{-1})	k_{cat}/K_m ($M^{-1}s^{-1}$)
Ribosome [B]	Yeast	Stx1A1	1.04 ± 0.11 [a]	2257 ± 202 [c]	3.6 ± 0.1 X 10^7 [e]
		Stx2A1	1.10 ± 0.14 [b]	3406 ± 133 [d]	5.2± 0.5 X 10^7 [f]
	Rat	Stx1A1	0.31 ± 0.03 [g]	401 ± 13.1 [i]	2.2 ± 0.1 X 10^7 [k]
		Stx2A1	0.36 ± 0.03 [h]	1098 ± 85.0 [j]	5.1 ± 0.7 X 10^7 [l]
Synthetic SRL [C]		Stx1A1	0.93 ± 0.22 [m]	21.5 ± 0.6 [o]	4.0 ± 0.9 X 10^5 [q]
		Stx2A1	2.46 ± 0.55 [n]	62.6 ± 22.3 [p]	4.4 ± 1.6 X 10^5 [r]

[A] Letters indicate statistical comparisons, where means were not significantly different between a and b, between g and h, and between q and r; means were significantly different between c and d, between i and j, and between m and n with a P value of 0.01; and means were significantly different between e and f, between k and l, and between o and p with a P value of 0.05, as determined by using a one-tailed t test. [B] The ribosome substrate was assayed in a continuous format. [C] The synthetic SRL was assayed in a discontinuous format.

As shown in Fig. 2.5A, the initial rates of Stx2A1 and Stx1A1 were dependent on the concentration of yeast ribosomes and were fitted to the Michaelis Menten equation. Stx2A1 showed a k_{cat} of 3406 min^{-1} and catalytic efficiency (k_{cat}/K_m) of 5.2 x 10^7 $M^{-1}s^{-1}$, while Stx1A1 showed a k_{cat} of 2257 min^{-1} and k_{cat}/K_m of 3.6 x 10^7 $M^{-1}s^{-1}$ towards yeast ribosomes. The differences in k_{cat} and k_{cat}/K_m between Stx1A1 and Stx2A1 towards yeast ribosomes were statistically significant. However, Stx1A1 and Stx2A1 showed a similar K_m (about 1 μM) (Fig. 2.5A and Table 2.3). These results indicate that Stx2A1 depurinates yeast ribosomes at a significantly (1.5-fold) higher rate and significantly (1.4-fold) more efficiently than Stx1A1.

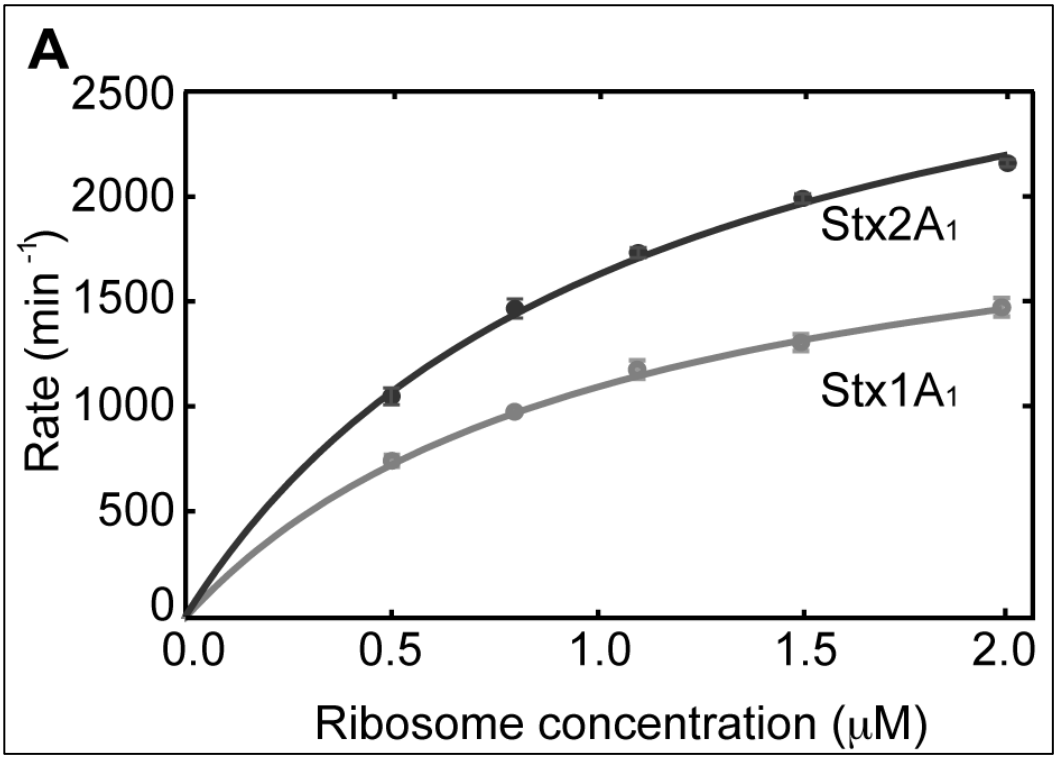

FIG 2.5 (A) Michaelis-Menten fits of yeast ribosome depurination performed with the continuous luminescence assay. The Stx-independent rate of adenine generation

was subtracted. Stx1A1 was used at 4 pM (grey) and Stx2A1 was used at 3 pM (black). Adenine standards covering the range of depurination were measured for each toxin. Error bars represent S. E. where n=3 replicates.

To determine if Stx2A1 has higher catalytic activity towards mammalian ribosomes, the enzymatically coupled assay was used to examine the depurination kinetics of Stx1A1 and Stx2A1 using rat liver ribosomes. The purification of rat liver ribosomes required an additional purification step compared to yeast ribosomes to reduce the background in the enzymatically coupled assay. As shown in Fig. 2.5B, greater differences were observed in the initial rate and catalytic efficiency compared to yeast ribosomes. Stx2A1 had a k_{cat} of 1098 compared to a k_{cat} of 404 min^{-1} for Stx1A1 towards rat liver ribosomes. Stx2A1 depurinated rat liver ribosomes with a k_{cat}/K_m of 5.1 x 10^7 $M^{-1}s^{-1}$ compared to 2.2 x 10^7 $M^{-1}s^{-1}$ for Stx1A1 (Fig. 2.5B and Table 2.3). The differences in k_{cat} and k_{cat}/K_m between Stx1A1 and Stx2A1 towards rat liver ribosomes were statistically significant. There was no difference in the K_m for rat ribosomes (about 0.3 μM). These results demonstrated that Stx2A1 depurinated rat liver ribosomes at a significantly (2.7-fold) higher rate and significantly (2.3-fold) more efficiently than Stx1A1.

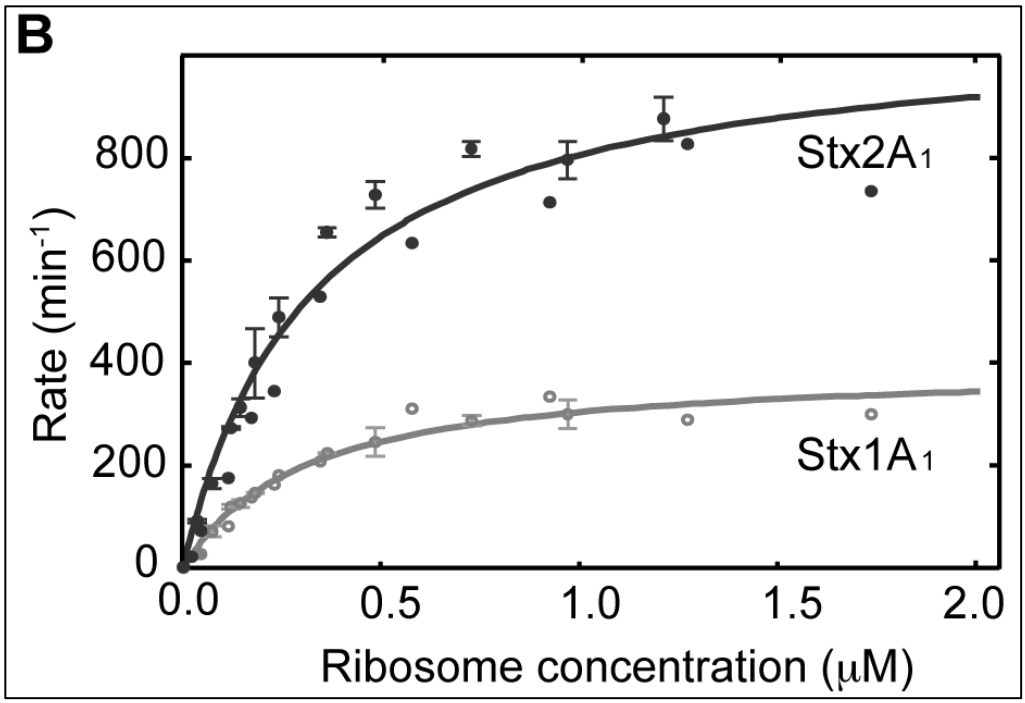

FIG 2.5 (B) Michaelis-Menten fits of rat liver ribosome depurination performed with the continuous assay. The Stx-independent rate of adenine generation was subtracted. Stx1A1 (grey) and Stx2A1 (black) were used at 4 pM for depurination. Adenine standards covering the range of depurination were measured for each toxin. Error bars represent S. E. where n=3 replicates.

Since ribosome depurination requires interaction of toxin with the P-protein stalk to reach the SRL, we measured the depurination kinetics towards a 10-mer stem-loop RNA mimic of the SRL using a discontinuous luminescence assay (Sturm and Schramm 2009). Previous results indicated that RTA depurinates stem-loop RNA substrates at pH 4.0, but not pH 7.0 (Sturm and Schramm 2009). Similarly, the A1 subunits of Shiga toxins could not depurinate the stem-loop RNA at neutral pH, but depurinated it at pH 4.5. Since adenine to ATP conversion requires a neutral pH, the assay was done using

the discontinuous format by quenching to neutral pH at timed intervals. The amount of adenine released was determined by the luminescence assay. The results (Fig. 2.5C and Table 2.3) showed that Stx2A1 depurinated the stem-loop RNA at a significantly higher (3-fold) initial rate (k_{cat} of 62.6 nM) compared to Stx1A1 (k_{cat} of 21.5). However, Stx1A1 had a significantly lower K_m (0.93 μM) for the stem loop RNA than Stx2A1 (2.46 μM). Consequently, there was no difference in the depurination efficiency of Stx1A1 and Stx2A1 towards the stem loop RNA.

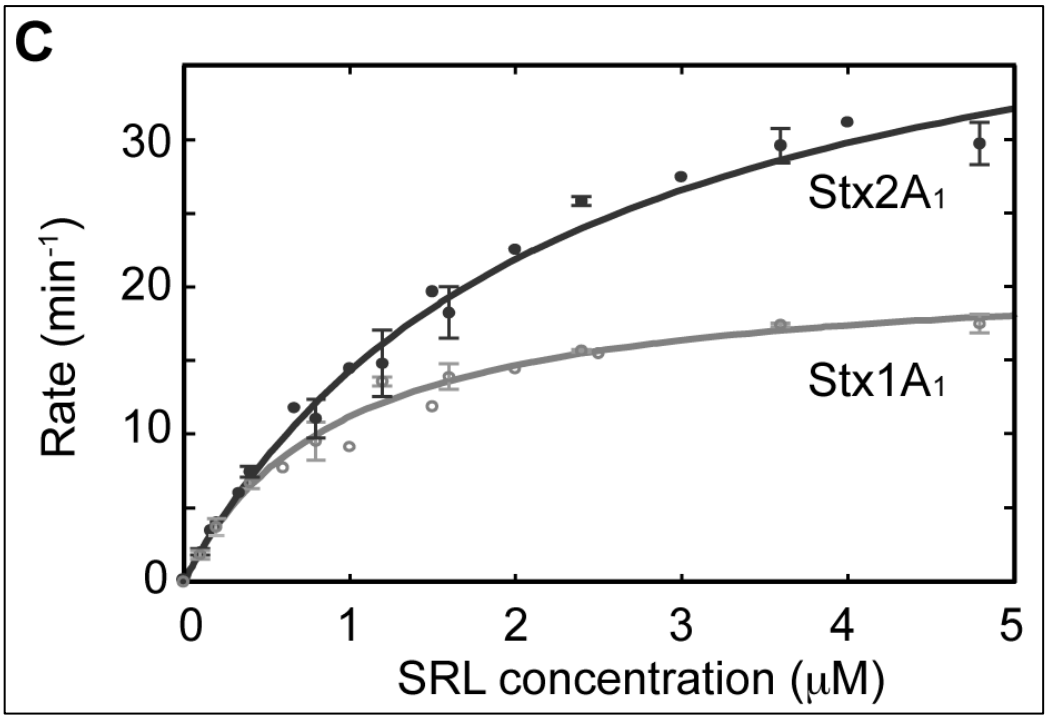

FIG 2.5 (C) Michaelis-Menten fits of stem-loop RNA depurination performed with the discontinuous luminescence assay. Stx1A1 (grey) was used at 3 nM and Stx2A1 (black) was used at 2 nM. The Stx-independent rate of adenine generation was subtracted for each. Adenine standards covering the range of depurination were measured for each toxin. Error bars represent S. E. where n=3 replicates.

Stx2A1 inhibits protein expression to a greater extent in human cells than Stx1A1. In order to examine the relative activity of Stx1A1 and Stx2A1 in mammalian cells, independent of B chain influence, an EGFP transfection assay was used (Redmann, Oresic et al. 2011, Jetzt, Cheng et al. 2012). Changes in ribosome depurination correlate with the extent of inhibition of EGFP expression in this assay (Redmann, Oresic et al. 2011, Jetzt, Cheng et al. 2012). Human embryonic kidney cells (HEK293T) were cotransfected with equal amounts of an EGFP reporter plasmid and Stx1A1 or Stx2A1 expression plasmid and EGFP signal was measured 22 h after transfection as readout of translation activity. The base fluorescence in cells transfected with Stx1A1 and Stx2A1 without EGFP was about the same as the cells transfected with the empty vector. Stx2A1 showed significantly higher (40-fold) inhibition of EGFP expression in comparison with Stx1A1 (Fig. 2.6A).

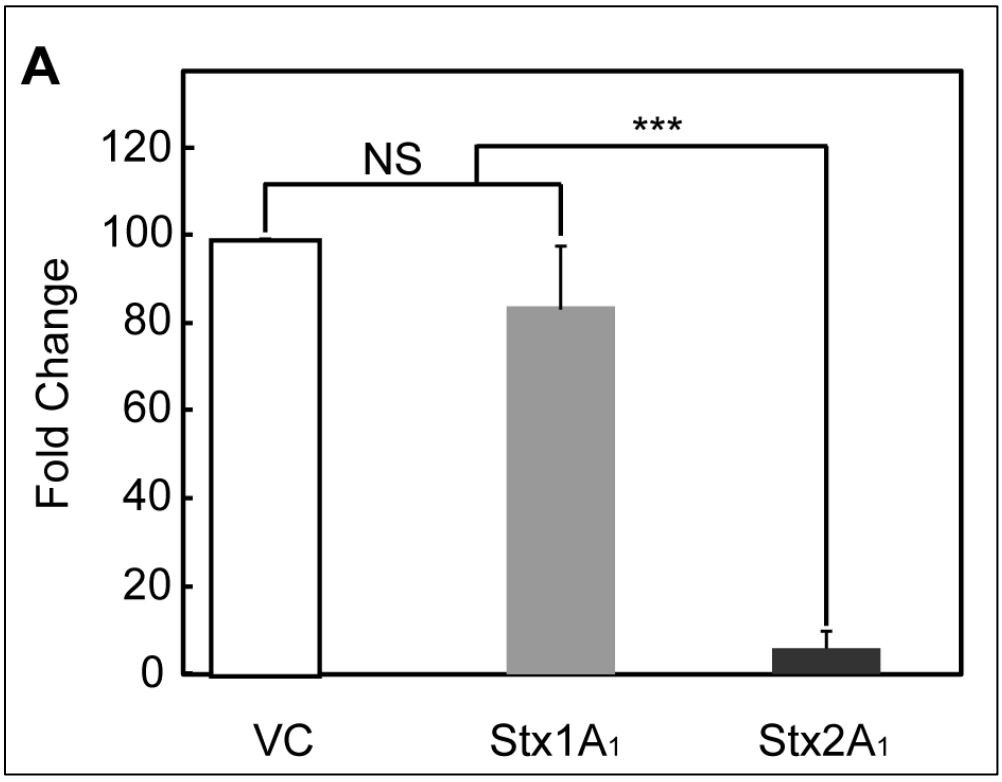

FIG 2.6 (A) Translation inhibition and ribosome depurination in mammalian cells expressing Stx1A1 or Stx2A1. HEK293T cells were cotransfected with Stx1A1 (grey bars) or Stx2A1 (black bars) and EGFP. Cells carrying the empty vector (VC) were used as controls. EGFP fluorescence was read at 22 h post transfection. Fluorescence measured in cells cotransfected with EGFP and empty vector was considered as 100 % and fluorescence in controls lacking EGFP plasmid as background. Statistical analyses were conducted using SAS 9.4 (SAS Institute Inc). Data were analyzed by general linear models using PROC GLM to test for statistical differences between treatments and Tukey's test was used to perform pairwise comparisons (***P<0.001, NS= Not significant). Error bars represent S. E. where n=3 replicates.

Since the expression of the A1 subunits was below detection by immunoblot analysis, mRNA levels were measured by qRT-PCR. Expression levels of Stx1A1 and Stx2A1 were comparable after transfection (Fig. 2.S2). To determine if translation inhibition by endogenously expressed Stx2A1 correlated with depurination, total RNA from HEK293T cells was analyzed by qRT-PCR (Jetzt, Cheng et al. 2012, May, Li et al. 2012). As shown in Fig. 2.6B, ribosomes were depurinated in cells transfected with Stx1A1 and Stx2A1 relative to cells transfected with the empty vector (Fig. 2.6B), indicating that both proteins were expressed. Stx2A1 depurinated ribosomes at a significantly higher (10-fold) level than Stx1A1 in HEK293T cells. These results demonstrate that Stx2A1 is significantly more active in depurinating ribosomes and inhibiting translation than Stx1A1 in human cells.

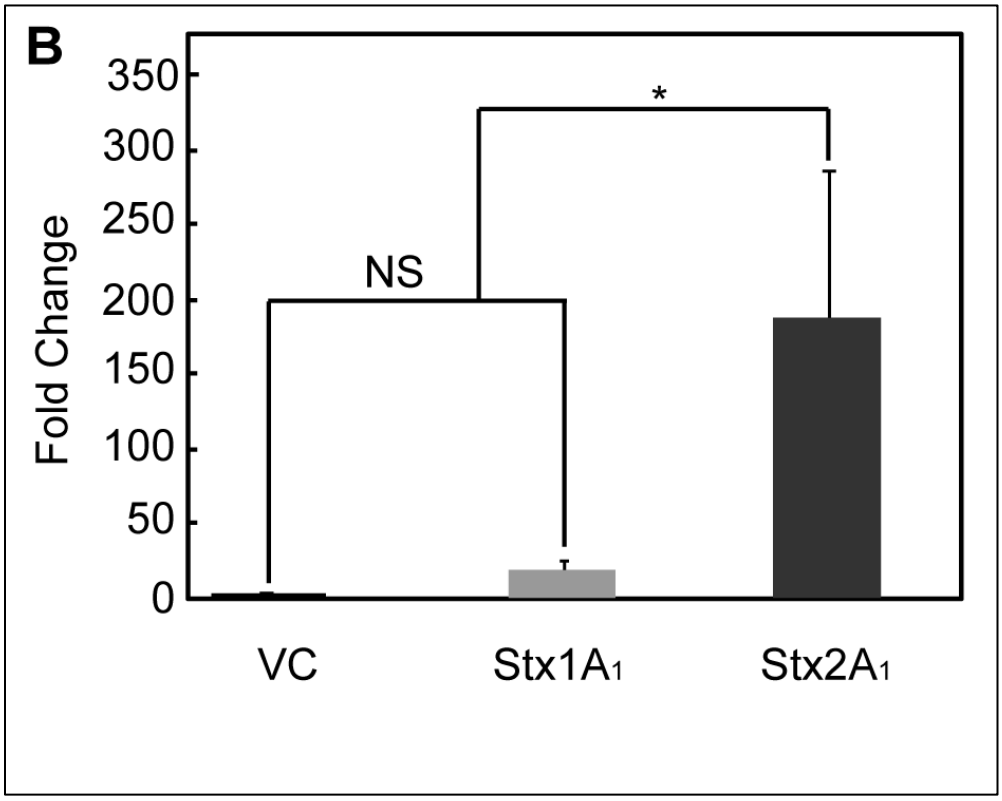

FIG 2.6 (B) Depurination of ribosomes from mammalian by Stx1A1 and Stx2A1. Total RNA (375 ng) from mammalian cells expressing Stx1A1 (grey bars) or Stx2A1 (black bars) collected at 23 hour post DNA exposure were used to quantify the relative levels of depurination using qRT-PCR (Pierce, Kahn et al. 2011). The y-axis shows the fold change in depurination over the control samples (VC). The table shows the fold change in depurination levels in cells transfected with Stx1A1 and Stx2A1 relative to cells transfected with the empty vector. Data were analyzed with PROC GLM to test for statistical differences between treatments and Tukey's test was used to perform pairwise comparisons (*P<0.05). Error bars represent S. E. where n=3 independent experiments.

DISCUSSION

The A1 subunit of Stx2 is more toxic and has higher activity in yeast and in mammalian cells. We expressed the mature A1 subunit of Stx1A1 and Stx2A1 in yeast and in mammalian cells to compare their cytotoxicity and activity directly without the B subunits. Our results showed that Stx2A1 is 10-fold more toxic to yeast than Stx1A1 (Figs. 2.1A and B). The expression level of Stx1A1 was higher than Stx2A1 at all-time points (Fig 2.1C), consistent with our previous results, which showed that RTA mutants with reduced toxicity are expressed at higher levels (Li, Kahn et al. 2013, Yan, Li et al. 2014). Using a highly sensitive qRT-PCR assay we showed that Stx2A1 depurinates yeast ribosomes at a significantly higher level than Stx1A1 during the first 3 h of toxin induction (Fig 2.1D). To confirm the *in vivo* results, we purified mature Stx1A1 and Stx2A1 from *E. coli* and showed that Stx2A1 depurinated yeast ribosomes (Fig. 2.2C) and yeast RNA (Fig 2.2D) at a significantly higher level than Stx1A1 *in vitro*. Although

the difference in the depurination level of Stx1A1 and Stx2A1 was 2 to 3-fold, it gave rise to a 10-fold difference in toxicity, indicating that small changes in depurination activity could have much larger consequences for toxicity in cells.

We demonstrated that Stx2A1 is significantly more active in depurinating ribosomes and inhibiting protein synthesis than Stx1A1 in human cells. Larger differences were observed in the activity of Stx1A1 and Stx2A1 in human cells than in yeast. A 10-fold increase in depurination gave rise to 40-fold higher translation inhibition by Stx2A1 compared to Stx1A1 in human cells. It is unlikely that the observed differences were due to lower stability of Stx1A1 since the purified Stx1A1 was more stable than Stx2A1 by protein thermal shift analysis (Fig. 2.S1) and since each endogenously expressed A1 subunit would be folded in the cytosol as the holotoxin derived A1 subunit after retrotranslocation from the ER to the cytosol. Although A1 subunits were expressed in human cells below detectable levels by immunoblot analysis, Stx1A1 depurinated ribosomes in human cells at a 16-fold higher level relative to cells transfected with the empty vector (Fig. 2.6B), indicating that it was expressed in the cell.

In previous studies differences were not observed in the protein synthesis inhibition ability of Stx1 and Stx2 using cell free translation assays (Head, Karmali et al. 1991, Tesh, Burris et al. 1993, Brigotti, Carnicelli et al. 1997). While in some of these studies, the holotoxin was used (Tesh, Burris et al. 1993) in others the holotoxin was activated by digestion with trypsin to release the A1 chain from A_2-B_5 complex or by chemical treatment with urea or DTT to break the disulfide bond between the A1 and the A_2 chains (Head, Karmali et al. 1991, Kozlov, Chernaia et al. 1993, Tesh, Burris et al. 1993, Siegler, Obrig et al. 2003). The amount of activated protein may vary after these

treatments, precluding accurate comparison of the enzymatic activity of the trypsin and DTT-activated toxins (Chiou, Li et al. 2011). Moreover, since translation inhibition is a downstream effect of depurination, cell free translation assays measure toxin activity indirectly and do not quantify the catalytic activity of Stx1A1 and Stx2A1 on the ribosome. Consistent with previous reports, we did not see any difference between the translation inhibitory activity of recombinant Stx1A1 and Stx2A1 in the reticulocyte lysate cell-free translation system. To understand the basis for the higher activity of Stx2A1 over Stx1A1, we measured their depurination kinetics with an enzymatically coupled luminescence assay using yeast, rat liver ribosomes, and RNA as substrates. The results showed that Stx2A1 has a higher k_{cat} than Stx1A1 when either yeast or rat liver ribosomes were used as a substrate. Similarly, Stx2A1 has a higher k_{cat} than Stx1A1 when RNA was used as a substrate. These results indicated that Stx2A1 has higher catalytic activity than Stx1A1 and were consistent with the *in vivo* data.

Ribosomes were better substrates than the stem-loop RNA and were depurinated optimally at physiological pH. However, Stx1A1 and Stx2A1 could not depurinate the stem-loop RNA at neutral pH. Even at acidic pH RNA was depurinated at a very low rate. Stx1A1 and Stx2A1 depurinated the stem-loop RNA at pH 4.5 with a catalytic efficiency (k_{cat}/K_m), which was 55-fold and 110-fold slower, respectively than the SRL on rat liver ribosomes at pH 7.4 (Table 2.3). The increase in catalytic efficiency was due to an improvement in k_{cat}. Previous results indicated that Shiga toxins bind to the P-protein stalk to depurinate the SRL (McCluskey, Poon et al. 2008, Chiou, Li et al. 2011, McCluskey, Bolewska-Pedyczak et al. 2012). Therefore interaction of the A1 subunits

with the stalk proteins and with other binding sites on the ribosome appears to have a profound effect on the catalytic efficiency of Shiga toxins towards the SRL.

Structural differences result in the higher affinity of Stx2A1 towards the ribosome. Previous results indicated that Stx1A1 interacts with peptides corresponding to the conserved C-termini of the ribosomal P- protein stalk (McCluskey, Poon et al. 2008, McCluskey, Bolewska-Pedyczak et al. 2012). However, the interaction of Stx1 and Stx2 with either the ribosome or the ribosomal stalk complex has not been investigated. To investigate the basis for the higher activity of Stx2A1, we compared the interaction of the A1 subunits with yeast ribosomes and with the isolated ribosomal P-protein stalk pentamer from yeast (Li, Grela et al. 2010). Our previous results indicated that the interaction of RTA with ribosomes did not fit a simple 1:1 interaction model (Li, Chiou et al. 2009). We showed that the ribosomal P-protein stalk binding surface of RTA is on the opposite face of the active site and proposed a model to explain how RTA depurinates ribosomes (38). According to this model, electrostatic interactions between RTA and the ribosome concentrate RTA molecules around the ribosome and allow their diffusion towards the P-protein stalk. Specific electrostatic interactions with the P-protein stalk stimulate the catalysis of ribosome depurination by orienting the active site of RTA towards the SRL and deliver the properly oriented RTA to the SRL through a conformational change of the hinge region of the P-proteins (38). As observed with RTA, the interaction of Stx1A1 and Stx2A1 with either yeast or rat ribosomes did not fit a simple 1:1 interaction model. The interaction had an initial fast association and dissociation phase followed by a slow association and dissociation phase similar to the

interaction of RTA with ribosomes (Li, Kahn et al. 2013). This biphasic interaction curve was more obvious for the interaction of Stx2A1 with yeast and mammalian ribosomes (Figs. 2.3 and 2.4). Due to the structural similarity between RTA and Shiga toxins, the ribosome interaction model proposed for RTA may be applicable to Stx1A1 and Stx2A1.

Because of the size of the ribosome relative to the A1 subunits, not every interaction between Stx1A1 and Stx2A1 and the ribosome will result in depurination of the SRL. Therefore, the on and off rates (k_{on} and k_{off}) are more important than the affinity (K_D) since they determine how fast the depurination reaction will take place. Although we could not determine the on and off rates of the interaction between the A1 subunits and ribosomes, Stx2A1 had a much faster association and dissociation pattern compared to Stx1A1 (Figs. 2.3 and 2.4). We have previously shown that the fast on and off rates reflect the interaction of RTA with the ribosomal P-protein stalk on yeast (Li, Chiou et al. 2009) and human (May, Li et al. 2012) ribosomes. The interaction of RTA with the ribosomal stalk is determined by the local concentration of RTA around the ribosome (Li, Kahn et al. 2013). Since we did not observe a significant difference in the interaction of the A1 subunits with the P-protein complex (Fig. 2.3C), but observed large differences in their interaction with ribosomes, the differences in the interaction of Stx1A1 and Stx2A1 with ribosomes might be due to the differences in the toxin concentration around the ribosome. The higher local concentration around the ribosome should stimulate the interaction of Stx2A1 with the stalk complex on the ribosome, as reflected by the initial fast association and dissociation phase of the interaction between Stx2A1 and ribosomes (Figs. 2.3 and 2.4).

Our results indicate that there is over 40-fold difference in the apparent K_D between the interaction of the untagged and His-tagged Stx1A1 with the ribosome. This difference may be due to the differences in the way the two proteins are immobilized on the sensor chip surface in the Biacore T200. The untagged toxins are immobilized on the CM5 chip by amine coupling and thus are orientated randomly, while the His-tagged toxins are captured through the N-terminal His-tag on the NTA chip and thus are in the same orientation. When toxins are immobilized on the CM5 chip in random orientation, the ability of each toxin to access the ribosome would be different. In contrast, when they are immobilized on the NTA chip in the same orientation, their interaction with the ribosome would be more even. Differences were observed in the Biacore interaction patterns of RTA with yeast (Li, Chiou et al. 2009) or human (May, Li et al. 2012) ribosomes. The results reported here indicate differences in the interaction pattern of Stx1A1 and Stx2A1 with yeast or rat ribosomes. Further studies will address the basis for these differences.

The Stx1A and Stx2A have 55% amino acid sequence identity. Although the structures of Stx and Stx2 are similar, the sequence divergence between Stx2A1 and Stx1A1 has some influence on the structure. In the published structure of holotoxins some of the loops in the A1 subunits were missing. We have reconstructed the missing loops in the A1 subunits of Stx and Stx2 in the holotoxins as previously described (Di, Kyu et al. 2011) and calculated the electrostatic surfaces with the Adaptive Poisson-Boltzmann Solver (APBS) (Holst and Saied 1995, Baker, Sept et al. 2001).

The electrostatic surfaces of Stx1A1 and Stx2A1 show a number of differences, and the molecular surfaces, on which the electrostatic charges are shown, also have

somewhat different shapes (Fig. 2.7). Stx1A1 has a negatively charged crease running diagonally across the front (Fig. 2.7A), which is missing in Stx2A1 (Fig. 2.7B). The active site is masked by the left end of the crease in Stx1A1 and by the positive area that extends up to this region in both proteins. The negatively charged crease in Stx1A1 would decrease the ability of the protein to interact initially with the negatively charged surface of the ribosome.

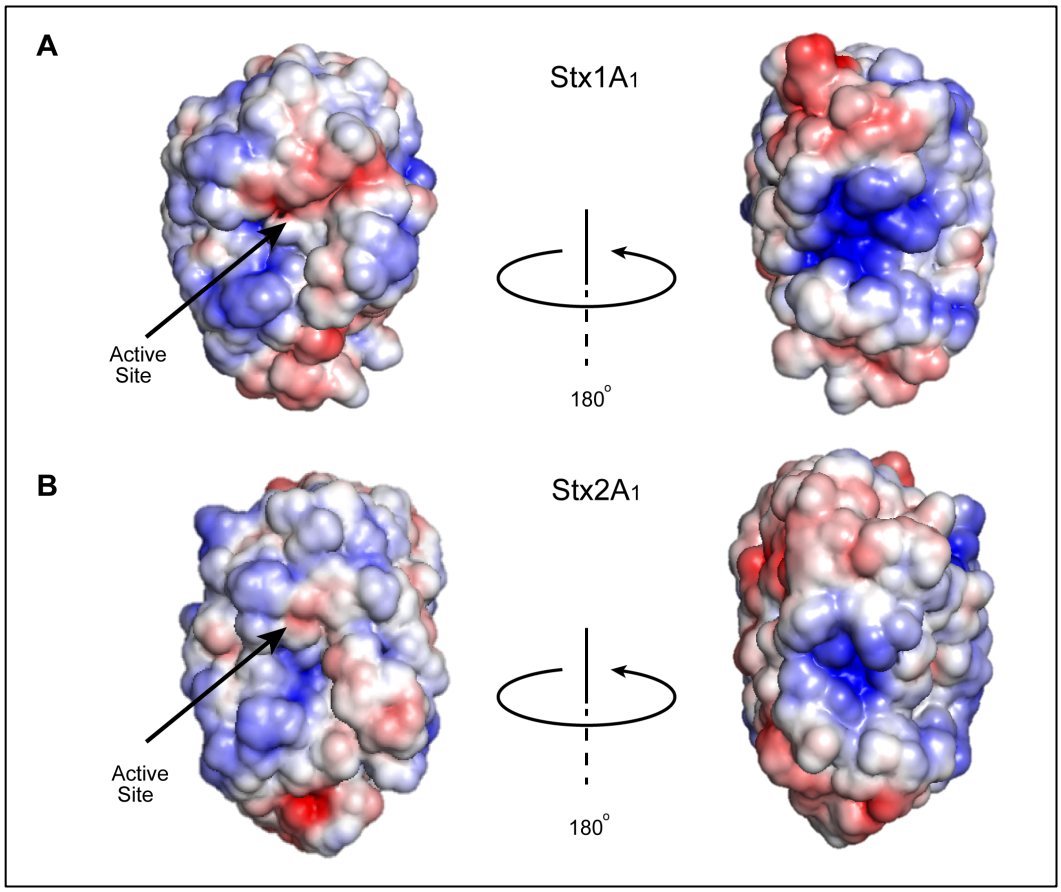

FIG 2.7 Crystallographic structure of Stx1A1 and Stx2A1 showing electrostatic charge distribution. The A1 subunits of Shiga toxin and Shiga toxin 2 were modeled from the Protein Data Bank ID: 1DM0 [Shiga toxin] and 1R4P [Shiga toxin 2]) as described earlier (Di, Kyu et al. 2011). The solvent accessible molecular surfaces are

colored according to electrostatic charge, with blue indicating positive, red negative and white neutral. (A) Stx1A1 has a negatively charged (red) crease running diagonally across the front of the active site. A rotation about the y-axis by approximately 180˚ reveals a positive zone (blue) in Stx1A1 has which is considerably larger and more open to the outside than Stx2A1. (B) The active site in Stx2A1 has little negative charge, most of the surface being neutral. A rotation about the y-axis by approximately 180˚ reveals a smaller positive (blue) zone at the center.

Rotation of the molecules by approximately 180 degrees along the y-axis (Figs. 2.7A and 2.7B) brings a large, intense positively charged zone into view. The Stx1A1 zone (Fig. 2.7A) is considerably larger and more open to the outside than in Stx2A1 (Fig. 2.7B). This positively charged region is on the opposite side of the molecule from the active site. Its interaction with the negatively charged RNA may reduce the availability of the active site residues to perform catalysis. Previous results showed that mutation of residues at the active site of Stx1A and Stx2A affect the cytotoxicity and catalytic activity differently (Di, Kyu et al. 2011). The residues previously shown to be involved in the depurination reaction in Stx1 and Stx2 (E167 and R170) are more exposed in Stx2A1 than in Stx1A1 (Di, Kyu et al. 2011). Further studies are needed to understand if these differences are responsible for the affinity of the Shiga toxins towards the RNA and their catalytic activity.

Stx2A1 is catalytically more efficient than Stx1A1 due to higher catalytic activity towards the SRL and higher affinity for the ribosome. Although Stx2A1 has higher

apparent affinity for both yeast and rat ribosomes compared to Stx1A1, Stx1A1 and Stx2A1 have similar K_m towards yeast (1μM) and rat ribosomes (0.3 μM) (Table 2.3). The similar K_m values for Stx1A1 and Stx2A1 indicate that while ribosome interaction is a necessary step, it is not the only step in depurination. The K_m values were higher than the apparent K_D for both Stx1A1 and Stx2A1. The high K_m value reflects multiple interactions that occur between the A1 subunits and the ribosome and suggests that ribosome binds multiple A1 subunits to trigger depurination.

Since depurination of the stem-loop RNA measures the catalytic activity in the absence of the ribosomal proteins, we examined the activity of Stx1A1 and Stx2A1 on the stem-loop RNA. Stx2A1 had 3-fold higher catalytic activity (k_{cat}) towards the stem-loop RNA than Stx1A1. But Stx1A1 had a lower K_m towards the stem-loop RNA than Stx2A1, resulting in similar catalytic efficiency for depurination of the SRL (Table 2.3). The higher K_m reflects the lower affinity of Stx2A1 for the stem-loop RNA at lower pH. However, Stx2A1 has higher affinity for the ribosome due to its interaction with the ribosomal proteins at physiological pH. Therefore the higher affinity of Stx2A1 for the ribosome, in combination with its higher catalytic activity towards the SRL allows Stx2A1 to depurinate the ribosome more efficiently than Stx1A1.

We examine here the differences in the interaction of the A1 subunits of Stx1 and Stx2 with ribosomes, depurination of the SRL and the resulting translational arrest and show for the first time that in the absence of the B subunits the catalytic subunits of Shiga toxins interact differently with ribosomes, they depurinate the ribosome and the SRL with different catalytic rates and cause different level of inhibition of translation in mammalian cells. Our results indicate that small differences in depurination activity lead

to much larger differences in translation inhibition and toxicity in cells and are likely to lead to even larger differences in animals. The A subunit influences potency in animal models (Sauter, Melton-Celsa et al. 2008, Stone, Thorpe et al. 2012, Russo, Melton-Celsa et al. 2014). We conclude that differences in the A1 subunits together with the previously defined differences in the B subunits (Russo, Melton-Celsa et al. 2014) contribute to the differential toxicity of Stx1 and Stx2. Further investigations on the importance of the A1 subunit for the higher toxicity of Stx2 will identify mechanistic differences in the action of Stxs on ribosomes and will provide a major step towards understanding the mechanism of catalysis and how to block their activity.

REFERENCES:

1. Baker, N. A., D. Sept, S. Joseph, M. J. Holst and J. A. McCammon (2001). "Electrostatics of nanosystems: application to microtubules and the ribosome." Proceedings of the National Academy of Sciences **98**(18): 10037-10041.

2. Basu, D. and N. E. Tumer (2015). "Do the A Subunits Contribute to the Differences in the Toxicity of Shiga Toxin 1 and Shiga Toxin 2?" Toxins (Basel) **7**(5): 1467-1485.

3. Bergan, J., A. B. Dyve Lingelem, R. Simm, T. Skotland and K. Sandvig (2012). "Shiga toxins." Toxicon **60**(6): 1085-1107.

4. Bielaszewska, M., A. Mellmann, W. Zhang, R. Köck, A. Fruth, A. Bauwens, G. Peters and H. Karch (2011). "Characterisation of the *Escherichia coli* strain associated with an outbreak of haemolytic uraemic syndrome in Germany, 2011: a microbiological study." The Lancet Infectious Diseases **11**(9): 671-676.

5. Boerlin, P., S. McEwen, F. Boerlin-Petzold, J. Wilson, R. Johnson and C. Gyles (1999). "Associations between virulence factors of Shiga toxin-producing *Escherichia coli* and disease in humans." Journal of Clinical Microbiology **37**(3): 497-503.

6. Boerlin, P., S. A. McEwen, F. Boerlin-Petzold, J. B. Wilson, R. P. Johnson and C. L. Gyles (1999). "Associations between virulence factors of Shiga toxin-producing

Escherichia coli and disease in humans." Journal of Clinical Microbiology **37**(3): 497-503.

7. Brigotti, M., D. Carnicelli, P. Alvergna, R. Mazzaracchio, S. Sperti and L. Montanaro (1997). "The RNA-N-glycosidase activity of Shiga-like toxin I: Kinetic parameters of the native and activated toxin." Toxicon **35**(9): 1431-1437.

8. Chan, D. S., L.-O. Chu, K.-M. Lee, P. H. Too, K.-W. Ma, K.-H. Sze, G. Zhu, P.-C. Shaw and K.-B. Wong (2007). "Interaction between trichosanthin, a ribosome-inactivating protein, and the ribosomal stalk protein P2 by chemical shift perturbation and mutagenesis analyses." Nucleic acids research **35**(5): 1660-1672.

9. Chiou, J.-C., X.-P. Li, M. Remacha, J. P. Ballesta and N. E. Tumer (2011). "Shiga toxin 1 is more dependent on the P proteins of the ribosomal stalk for depurination activity than Shiga toxin 2." The international journal of biochemistry & cell biology **43**(12): 1792-1801.

10. Chiou, J. C., X. P. Li, M. Remacha, J. P. Ballesta and N. E. Tumer (2008). "The ribosomal stalk is required for ribosome binding, depurination of the rRNA and cytotoxicity of ricin A chain in *Saccharomyces cerevisiae*." Molecular microbiology **70**(6): 1441-1452.

11. Clementi, N., A. Chirkova, B. Puffer, R. Micura and N. Polacek (2010). "Atomic mutagenesis reveals A2660 of 23S ribosomal RNA as key to EF-G GTPase activation." Nat Chem Biol **6**(5): 344-351.

12. Di, R., E. Kyu, V. Shete, H. Saidasan, P. Kahn and N. Tumer (2011). "Identification of amino acids critical for the cytotoxicity of Shiga toxin 1 and 2 in *Saccharomyces cerevisiae*." Toxicon **57**(4): 525-539.

13. Endo, Y., K. Tsurugi, T. Yutsudo, Y. Takeda, T. Ogasawara and K. Igarashi (1988). "Site of action of a Vero toxin (VT2) from Escherichia coli O157:H7 and of Shiga toxin on eukaryotic ribosomes. RNA N-glycosidase activity of the toxins." Eur J Biochem **171**(1-2): 45-50.

14. Flagler, M. J., S. S. Mahajan, A. A. Kulkarni, S. S. Iyer and A. A. Weiss (2010). "Comparison of binding platforms yields insights into receptor binding differences between shiga toxins 1 and 2." Biochemistry **49**(8): 1649-1657.

15. Frank, C., D. Werber, J. P. Cramer, M. Askar, M. Faber, M. an der Heiden, H. Bernard, A. Fruth, R. Prager and A. Spode (2011). "Epidemic profile of Shiga-toxin–producing *Escherichia coli* O104: H4 outbreak in Germany." New England Journal of Medicine **365**(19): 1771-1780.

16. Fraser, M., M. Chernaia, Y. Kozlov and M. James (1994). "Crystal structure of the holotoxin from *Shigella dysenteriae* at 2.5 A resolution." Nature structural biology **1**(1): 59.

17. Fraser, M. E., M. M. Cherney, P. Marcato, G. L. Mulvey, G. D. Armstrong and M. N. James (2006). "Binding of adenine to Stx2, the protein toxin from *Escherichia coli* O157: H7." Acta Crystallographica Section F: Structural Biology and Crystallization Communications **62**(7): 627-630.

18. Fraser, M. E., M. Fujinaga, M. M. Cherney, A. R. Melton-Celsa, E. M. Twiddy, A. D. O'Brien and M. N. James (2004). "Structure of Shiga toxin type 2 (Stx2) from *Escherichia coli* O157: H7." Journal of Biological Chemistry **279**(26): 27511-27517.

19. Fuller, C. A., C. A. Pellino, M. J. Flagler, J. E. Strasser and A. A. Weiss (2011). "Shiga toxin subtypes display dramatic differences in potency." Infect Immun **79**(3): 1329-1337.

20. Gonzalo, P. and J. P. Reboud (2003). "The puzzling lateral flexible stalk of the ribosome." Biol Cell **95**(3-4): 179-193.

21. Head, S., M. Karmali and C. Lingwood (1991). "Preparation of VT1 and VT2 hybrid toxins from their purified dissociated subunits. Evidence for B subunit modulation of a subunit function." Journal of Biological Chemistry **266**(6): 3617-3621.

22. Hoffman, W. L. and J. Ilan (1974). "Purification on hydroxyapatite of liver ribosomes and polysomes from unfasted mice." Biochimica et Biophysica Acta (BBA)-Nucleic Acids and Protein Synthesis **366**(2): 199-214.

23. Holst, M. J. and F. Saied (1995). "Numerical solution of the nonlinear Poisson–Boltzmann equation: developing more robust and efficient methods." Journal of computational chemistry **16**(3): 337-364.

24. Ito, H., T. Yutsudo, T. Hirayama and Y. Takeda (1988). "Isolation and some properties of A and B subunits of Vero toxin 2 and in vitro formation of hybrid toxins between subunits of Vero toxin 1 and Vero toxin 2 from Escherichia coli O157:H7." Microb Pathog **5**(3): 189-195.

25. Jetzt, A. E., J. S. Cheng, X. P. Li, N. E. Tumer and W. S. Cohick (2012). "A relatively low level of ribosome depurination by mutant forms of ricin toxin A chain can trigger protein synthesis inhibition, cell signaling and apoptosis in mammalian cells." Int J Biochem Cell Biol **44**(12): 2204-2211.

26. Kaper, J. and A. O'Brien (2014). "Overview and historical perspectives." Microbiol. Spectr. **2**(2).

27. Karch, H., E. Denamur, U. Dobrindt, B. B. Finlay, R. Hengge, L. Johannes, E. Z. Ron, T. Tønjum, P. J. Sansonetti and M. Vicente (2012). "The enemy within us:

lessons from the 2011 European *Escherichia coli* O104: H4 outbreak." EMBO Mol. Med. **4**(9): 841-848.

28. Kozlov, Y. V., M. M. Chernaia, M. E. Fraser and M. N. James (1993). "Purification and Crystallization of Shiga Toxin from Shigella dysenteriae." Journal of molecular biology **232**(2): 704-706.

29. Li, X.-P., J.-C. Chiou, M. Remacha, J. P. Ballesta and N. E. Tumer (2009). "A two-step binding model proposed for the electrostatic interactions of ricin a chain with ribosomes." Biochemistry **48**(18): 3853-3863.

30. Li, X.-P., P. Grela, D. Krokowski, M. Tchórzewski and N. E. Tumer (2010). "Pentameric organization of the ribosomal stalk accelerates recruitment of ricin a chain to the ribosome for depurination." Journal of Biological Chemistry **285**(53): 41463-41471.

31. Li, X.-P., P. C. Kahn, J. N. Kahn, P. Grela and N. E. Tumer (2013). "Arginine residues on the opposite side of the active site stimulate the catalysis of ribosome depurination by ricin A chain by interacting with the P-protein stalk." Journal of Biological Chemistry **288**(42): 30270-30284.

32. Manning, S. D., A. S. Motiwala, A. C. Springman, W. Qi, D. W. Lacher, L. M. Ouellette, J. M. Mladonicky, P. Somsel, J. T. Rudrik and S. E. Dietrich (2008).

"Variation in virulence among clades of *Escherichia coli* O157: H7 associated with disease outbreaks." Proc. Natl. Acad. Sci. USA. **105**(12): 4868-4873.

33. May, K. L., X. P. Li, F. Martinez-Azorin, J. P. Ballesta, P. Grela, M. Tchorzewski and N. E. Tumer (2012). "The P1/P2 proteins of the human ribosomal stalk are required for ribosome binding and depurination by ricin in human cells." FEBS J **279**(20): 3925-3936.

34. McCluskey, A. J., E. Bolewska-Pedyczak, N. Jarvik, G. Chen, S. S. Sidhu and J. Gariépy (2012). "Charged and Hydrophobic Surfaces on the A chain of Shiga-like toxin 1 Recognize the C-terminal Domain of Ribosomal Stalk Proteins." PLoS One **7**(2): e31191.

35. McCluskey, A. J., G. M. Poon, E. Bolewska-Pedyczak, T. Srikumar, S. M. Jeram, B. Raught and J. Gariépy (2008). "The catalytic subunit of Shiga-like toxin 1 interacts with ribosomal stalk proteins and is inhibited by their conserved C-terminal domain." Journal of molecular biology **378**(2): 375-386.

36. Nakajima, H., N. Kiyokawa, Y. U. Katagiri, T. Taguchi, T. Suzuki, T. Sekino, K. Mimori, T. Ebata, M. Saito and H. Nakao (2001). "Kinetic analysis of binding between Shiga toxin and receptor glycolipid Gb3Cer by surface plasmon resonance." Journal of Biological Chemistry **276**(46): 42915-42922.

37. Nataro, J. P. and J. B. Kaper (1998). "Diarrheagenic *Escherichia coli*." Clinical microbiology reviews **11**(1): 142-201.

38. Pickering, L., T. Obrig and F. Stapleton (1994). "Hemolytic-uremic syndrome and enterohemorrhagic *Escherichia coli*." The Pediatric Infectious Disease Journal **13**(6): 459.

39. Pierce, M., J. N. Kahn, J. Chiou and N. E. Tumer (2011). "Development of a quantitative RT-PCR assay to examine the kinetics of ribosome depurination by ribosome inactivating proteins using *Saccharomyces cerevisiae* as a model." RNA **17**(1): 201-210.

40. Redmann, V., K. Oresic, L. L. Tortorella, J. P. Cook, M. Lord and D. Tortorella (2011). "Dislocation of ricin toxin A chains in human cells utilizes selective cellular factors." The Journal of biological chemistry **286**(24): 21231-21238.

41. Rieu, I. and S. J. Powers (2009). "Real-time quantitative RT-PCR: design, calculations, and statistics." Plant Cell **21**(4): 1031-1033.

42. Russo, L. M., A. R. Melton-Celsa, M. A. Smith, M. J. Smith and A. D. O'Brien (2014). "Oral intoxication of mice with Shiga toxin type 2a (Stx2a) and protection by anti-Stx2a monoclonal antibody 11E10." Infect Immun **82**(3): 1213-1221.

43. Russo, L. M., A. R. Melton-Celsa, M. J. Smith and A. D. O'Brien (2014). "Comparisons of native Shiga Toxins (Stxs) Type 1 and 2 with chimeric toxins indicate that the source of the binding subunit dictates degree of toxicity." PloS one **9**(3): e93463.

44. Sandvig, K. and B. van Deurs (2005). "Delivery into cells: lessons learned from plant and bacterial toxins." Gene therapy **12**(11): 865-872.

45. Sauter, K. A., A. R. Melton-Celsa, K. Larkin, M. L. Troxell, A. D. O'Brien and B. E. Magun (2008). "Mouse model of hemolytic-uremic syndrome caused by endotoxin-free Shiga toxin 2 (Stx2) and protection from lethal outcome by anti-Stx2 antibody." Infect Immun **76**(10): 4469-4478.

46. Scheutz, F., L. D. Teel, L. Beutin, D. Pierard, G. Buvens, H. Karch, A. Mellmann, A. Caprioli, R. Tozzoli, S. Morabito, N. A. Strockbine, A. R. Melton-Celsa, M. Sanchez, S. Persson and A. D. O'Brien (2012). "Multicenter evaluation of a sequence-based protocol for subtyping Shiga toxins and standardizing Stx nomenclature." J Clin Microbiol **50**(9): 2951-2963.

47. Shi, X., P. K. Khade, K. Y. Sanbonmatsu and S. Joseph (2012). "Functional role of the sarcin-ricin loop of the 23S rRNA in the elongation cycle of protein synthesis." J Mol Biol **419**(3-4): 125-138.

48. Siegler, R. and R. Oakes (2005). "Hemolytic uremic syndrome; pathogenesis, treatment, and outcome." Current opinion in pediatrics **17**(2): 200-204.

49. Siegler, R. L., T. G. Obrig, T. J. Pysher, V. L. Tesh, N. D. Denkers and F. B. Taylor (2003). "Response to Shiga toxin 1 and 2 in a baboon model of hemolytic uremic syndrome." Pediatric Nephrology **18**(2): 92-96.

50. Steel, R. G. D. and J. H. Torrie (1980). Principles and procedures of statistics : a biometrical approach. New York, McGraw-Hill.

51. Stone, S. M., C. M. Thorpe, A. Ahluwalia, A. B. Rogers, F. Obata, A. Vozenilek, G. L. Kolling, A. V. Kane, B. E. Magun and D. M. Jandhyala (2012). "Shiga toxin 2-induced intestinal pathology in infant rabbits is A-subunit dependent and responsive to the tyrosine kinase and potential ZAK inhibitor imatinib." Front Cell Infect Microbiol **2**: 135.

52. Sturm, M. B. and V. L. Schramm (2009). "Detecting ricin: sensitive luminescent assay for ricin A-chain ribosome depurination kinetics." Analytical chemistry **81**(8): 2847-2853.

53. Tchorzewski, M. (2002). "The acidic ribosomal P proteins." Int J Biochem Cell Biol **34**(8): 911-915.

54. Tesh, V. L., J. Burris, J. Owens, V. Gordon, E. Wadolkowski, A. O'brien and J. Samuel (1993). "Comparison of the relative toxicities of Shiga-like toxins type I and type II for mice." Infection and immunity **61**(8): 3392-3402.

55. Tesh, V. L. and A. D. O'Brien (1991). "The pathogenic mechanisms of Shiga toxin and the Shiga-like toxins." Mol Microbiol **5**(8): 1817-1822.

56. Too, P. H.-M., M. K.-W. Ma, A. N.-S. Mak, Y.-T. Wong, C. K.-C. Tung, G. Zhu, S. W.-N. Au, K.-B. Wong and P.-C. Shaw (2009). "The C-terminal fragment of the ribosomal P protein complexed to trichosanthin reveals the interaction between the ribosome-inactivating protein and the ribosome." Nucleic acids research **37**(2): 602-610.

57. Weinstein, D. L., M. P. Jackson, L. P. Perera, R. K. Holmes and A. D. O'Brien (1989). "*In vivo* formation of hybrid toxins comprising Shiga toxin and the Shiga-like toxins and role of the B subunit in localization and cytotoxic activity." Infection and Immunity **57**(12): 3743-3750.

58. Yan, Q., X.-P. Li and N. E. Tumer (2014). "Wild Type RTA and Less Toxic Variants Have Distinct Requirements for Png1 for Their Depurination Activity and Toxicity in Saccharomyces cerevisiae." PLoS ONE **9**(12): e113719.

59. Yu, M. and D. B. Haslam (2005). "Shiga toxin is transported from the endoplasmic reticulum following interaction with the luminal chaperone HEDJ/ERdj3." Infect Immun **73**(4): 2524-2532.

60. Zhang, T., J. Lei, H. Yang, K. Xu, R. Wang and Z. Zhang (2011). "An improved method for whole protein extraction from yeast Saccharomyces cerevisiae." Yeast **28**(11): 795-798.

SUPPLEMENT

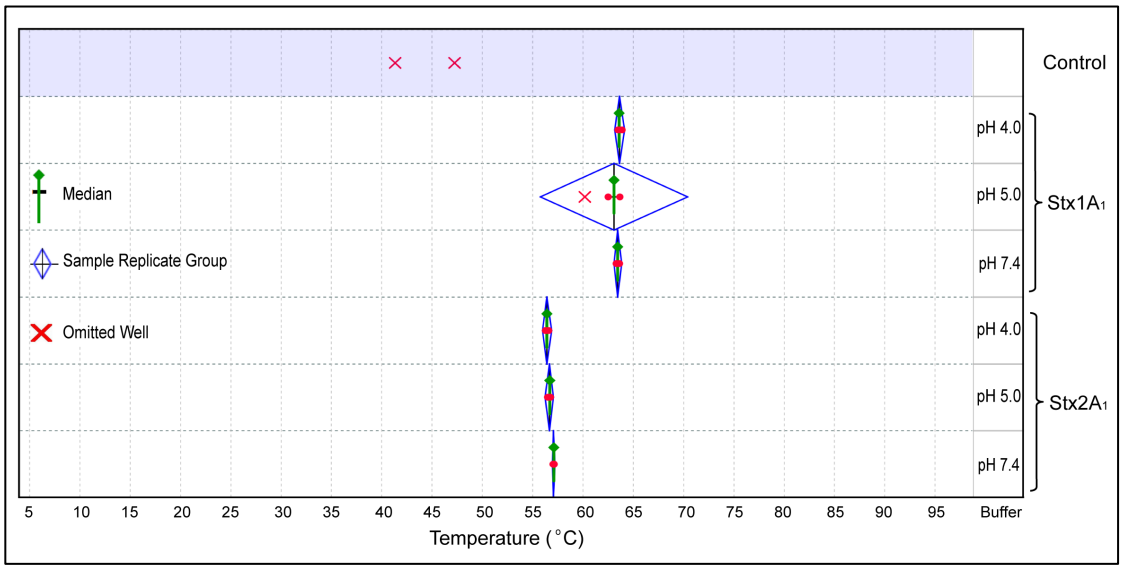

FIG 2. S1. Shiga toxin stability by protein thermal shift assay. To monitor protein unfolding due to systematic increase in temperature, the Protein Thermal Shift™ Dye Kit (Applied Biosystems, Grand Island, NY) was used. The unfolding process resulted in exposure of the hydrophobic region of proteins leading to a large increase in fluorescence, which was used to monitor the protein-unfolding transition using StepOnePlus™ Real-Time PCR system (Applied Biosystems,Grand Island, NY).1 µM of purified untagged Stx1A1 or Stx2A1, 2.5 µl of 8X Protein Thermal Shift™ Dye, 2 µl of 200 µM (10X) phosphate buffer (pH 4,5 or 7.4), and 10 µl of 2X Protein Thermal Shift™ Buffer to a final volume of 20 µl each were added to the wells of the 96-well PCR plate. The plate was heated from 25 to 99 °C with a heating rate of 1 °C/min. The data was analyzed using Protein Thermal Shift™ Software (version).

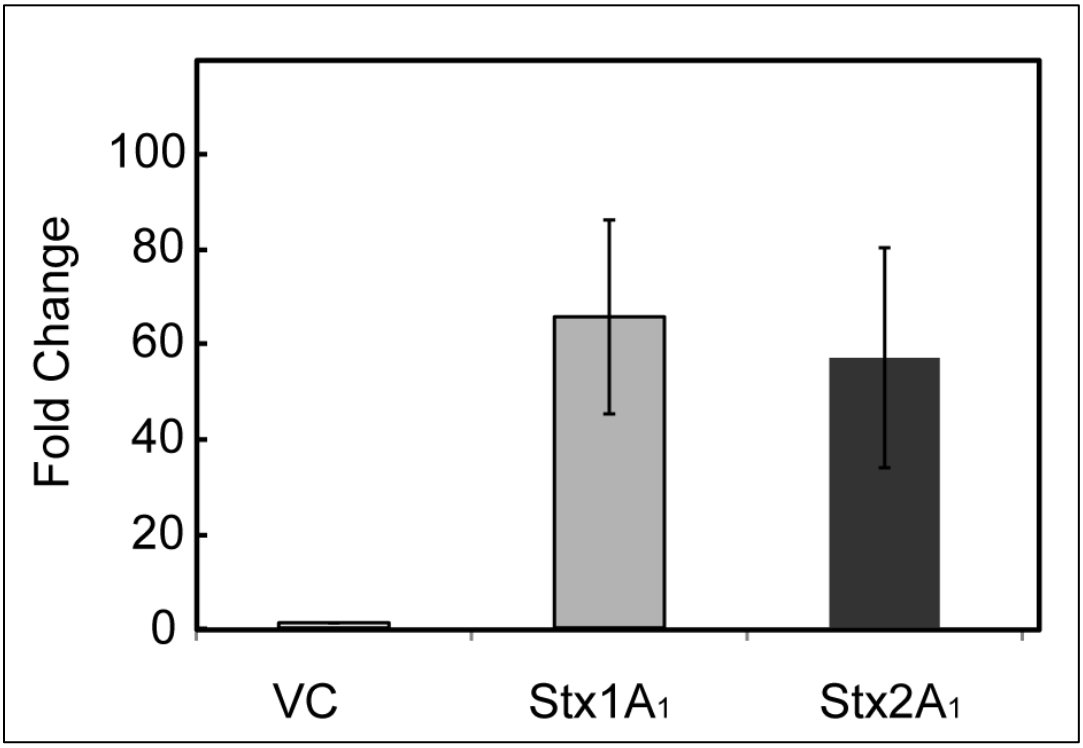

FIG 2. S2. Shiga toxin gene expression in mammalian by qPCR. Total RNA (375 ng) isolated from mammalian cells expressing Stx1A1 (grey bars) or Stx2A1 (black bars) collected at 23 hour post DNA exposure were used to quantify the relative levels of Shiga gene expression using qRT-PCR by the comparative CT method (CT). The Stx1A1 primers were Stx1_qPCR_F5' aatgtcgcatagtggaacctca 3' and Stx1_qPCR_R 5' aacatcgctcttgccacagac3', while the Stx2 primers were Stx2_qPCR_F5' gtatacgatgacgccgggag 3' and Stx2_qPCR_R 5' attcgcccccagttcagagt 3'. β-actin was used as internal control. The y-axis shows the fold change of toxin-gene carrying samples over the control samples without toxin gene (VC). Results (means ± standard errors of the means [SEM]) represent 3 independent biological replicates.

TABLE 2. S1. *In vivo* Depurination Statistical Significance of the Contrasts

Least Square Mean Estimates						
Effect	Label	Estimate	SE	DF	t Value	Pr > [t]
Treatment	Compare $Stx1A_1$-0h with $Stx2A_1$-0h	-408	295.1	16	-1.4	0.1858
Treatment	Compare $Stx1A_1$-1h with $Stx2A_1$-1h	-877.8	295.1	16	-2.9	0.0089
Treatment	Compare $Stx1A_1$-2h with $Stx2A_1$-2h	-1182.4	295.1	16	-4	0.001
Treatment	Compare $Stx1A_1$-3h with $Stx2A_1$-3h	-1044.4	295.1	16	-3.5	0.0027

*To estimate and test the differences of treatment means, ProcGlimmix in SAS was used to compute least square mean estimates for the pairwise comparisons between Stx1A1 and Stx2A1 (for trait depurination, *in vivo*) at four time points (0, 1, 2 and 3 hpi). The estimate term (for the given trait such as depurination, etc.) represents the least squared mean difference between Stx1A1 and Stx2A1at a particular time point. Because the data are balanced, the estimated standard errors for each pairwise comparison are identical. The degrees of freedom (DF) are derived from the denominator degrees of freedom calculated from the Type III Tests of Fixed Effects. The LSMESTIMATE statement in PROC GLIMMIX produces a t test and corresponding p value for each LS-mean difference comparison computed. Reported P values and standard errors were adjusted using Tukey's honestly significant difference to correct for multiple comparisons. There are highly significant differences between Stx1A1 and Stx2A1at most time points.

TABLE 2. S2. Ribosome Depurination Statistical Significance of the Contrasts

Least Square Mean Estimates						
Effect	Label	Estimate	SE	DF	t Value	Pr > [t]
Treatment	Compare $Stx1A_1$-0.08nM with $Stx2A_1$-0.08nM	-3398.6	863.3	54	-3.9	0.0002
Treatment	Compare $Stx1A_1$-0.25nM with $Stx2A_1$-0.25nM	-4491.2	863.3	54	-5.2	< 0.0001
Treatment	Compare $Stx1A_1$-0.75nM with $Stx2A_1$-0.75nM	-7763.2	863.3	54	-8.9	< 0.0001

*To estimate and test the differences of treatment means, ProcGlimmix in SAS was used to compute least square mean estimates for the pairwise comparisons between Stx1A1 and Stx2A1 (for trait depurination, *in vitro*) at three different concentrations of toxin (0.08, 0.25 and 0.75 nM) as previously described. There are highly significant differences between Stx1A1 and Stx2A1 at all three toxin concentrations tested. At 0.08 nM the difference between Stx1A1 and Stx2A1 is significant ($p=0.0002$) and at 0.25 and 0.75nM, the mean differences between the two toxins are significant ($p<0.0001$).

TABLE 2. S3. RNA Depurination Statistical Significance of the Contrasts

Least Square Mean Estimates						
Effect	Label	Estimate	SE	DF	t Value	Pr > [t]
Treatment	Compare $Stx1A_1$-62.5nM with $Stx2A_1$-62.5nM	-2221.4	1148.2	54	-1.9	0.0583
Treatment	Compare $Stx1A_1$-125nM with $Stx2A_1$-125nM	-3829.7	1148.2	54	-3.3	0.0015
Treatment	Compare $Stx1A_1$-250nM with $Stx2A_1$-250nM	-12237	1148.2	54	-10.7	< 0.0001

*To estimate and test the differences of treatment means, ProcGlimmix in SAS was used to compute least square mean estimates for the pairwise comparisons between Stx1A1 and Stx2A1 (for trait depurination, *in vitro*) at three different concentrations of toxin (62.5, 125 and 250 nM) as previously described. There are highly significant differences between Stx1A1 and Stx2A1 at all three toxin concentrations tested. At 250 nM, the mean differences between the two toxins are significant ($p<0.0001$).

CHAPTER 3: The higher affinity of the A1 subunit of Shiga toxin 2 toward the ribosome compared to Shiga toxin 1 is not due to conserved arginines at the P-protein stalk binding site or at the active site.

ABSTRACT

The A1 subunit of Shiga toxin 1 (Stx1A1) and Shiga toxin 2 (Stx2A1) interact with the conserved C-terminal peptide of ribosomal stalk P-proteins to remove a specific adenine from the sarcin/ricin loop. We previously showed that Stx2A1 has higher affinity for the ribosome and higher catalytic activity than Stx1A1. To determine if conserved arginines at the distal face of the active site contribute to the higher affinity of Stx2A1 for the ribosome, we mutated Arg172, Arg176 and Arg179 in Stx1A1 and Stx2A1. We show that Arg172 and Arg176 are more important than Arg179 for depurination activity and toxicity of Stx1A1 and Stx2A1. Mutation of at least two of the three arginines is required to significantly reduce depurination by Stx2A1 *in vitro* and in cells. R176A and R172A/R176A mutations eliminated interaction of StxA1 and Stx2A1 with ribosomes and with the stalk, indicating that toxicity can be reduced by inhibiting ribosome interactions of Stx1A1 and Stx2A1. Mutation of Arg170 at the active site reduced binding affinity of Stx1A1 and Stx2A1 for the ribosome, but not for the stalk. These results demonstrate that conserved arginines at the distal face of the active site are critical for interactions of Stx1A1 and Stx2A1 with the stalk, while a conserved arginine at the active site is critical for non-stalk specific interactions with the ribosome. Mutations at conserved arginines at either site reduced ribosome interactions of Stx1A1 and Stx2A1

similarly, indicating that they do not contribute to the higher affinity of Stx2A1 for the ribosome.

INTRODUCTION

Shiga toxin (Stx) producing *E. coli* (STEC) is an emerging foodborne and waterborne pathogen responsible for hemolytic uremic syndrome (HUS) and hemorrhagic colitis (HC), which are the leading cause of acute renal failure and mortality in children in the US (Siegler and Oakes (2005). STEC serotypes, such as *E.coli* O157:H7 are associated with severe disease (Boerlin, McEwen et al. 1999). Antibiotics are known to exacerbate the disease symptoms, and at the present there are no FDA approved vaccines or therapeutics against STEC infection (Kimmitt, Harwood et al. 2000, Tarr, Gordon et al. 2005, McGannon, Fuller et al. 2010). STEC produces a family of structurally and functionally related virulence factors called Shiga toxins, the most predominant ones being Shiga toxin 1 (Stx1) and Shiga toxin 2 (Stx2) (Bergan, Lingelem et al. 2012). Stx2 and Stx1 have one prototype (Stx1a and Stx2a) and several subtypes. Stxs are type II ribosome-inactivating proteins (RIPs) with a catalytically active A subunit, attached to a pentamer of B subunits. The B subunits facilitate the endocytosis of the toxins into the cell by binding to a common receptor globotriasylceramide (GB3 or CD77). The toxin travels in a retrograde manner from the endosome to the endoplasmic reticulum (ER) via the Golgi network (Sandvig and van Deurs 2005). In order to intoxicate the cell the A subunit is cleaved into the A1 fragment and A2 fragment, which remain together by a disulfide bond. After reduction of the disulfide bond, the A1 fragment is translocated into the cytosol from the endoplasmic reticulum (ER), where it refolds into an active

conformation, binds to the ribosome and removes a specific adenine (A_{4324}) from the highly conserved sarcin/ricin loop (SRL) of the 28S rRNA (Endo, Tsurugi et al. 1988). Depurination of the SRL prevents binding of elongation factor 1 (EF-1)-dependent amino-acyl tRNA and EF-2, resulting in arrest of protein synthesis at the elongation step (Clementi, Chirkova et al. 2010, Shi, Khade et al. 2012).

Stx1 as well as other structurally and functionally related RIPs, such as ricin and trichosanthin (TCS) interact with the ribosomal P-protein stalk to depurinate the SRL (Chan, Chu et al. 2007, Chiou, Li et al. 2008, McCluskey, Poon et al. 2008, Too, Ma et al. 2009). The ribosomal stalk and the SRL are part of the GTPase Associated Center (GAC) of the ribosome, which is involved in binding of elongation factors and stimulation of translation factor-dependent GTP hydrolysis (Spahn, Jan et al. 2004, Diaconu, Kothe et al. 2005). In eukaryotes, the stalk is organized as pentamer with ribosomal uL10 protein (former name P0 (Ban, Beckmann et al. 2014)) which constitutes the base of the stalk and anchors two eukaryotic unique P1/P2 heterodimers (Gonzalo and Reboud 2003). Lower eukaryotes, such as *Saccharomyces cerevisiae*, possess two P1/P2 protein forms, P1A, P1B, P2A and P2B, which form two dimers, P1A/P2B and P1B/P2A, bound to two specific contiguous sites on the uL10 protein (Krokowski, Boguszewska et al. 2006). The most prominent feature of the eukaryotic stalk proteins is the highly conserved motif present at the C-terminal part in the uL10 and P1/P2 proteins, consisting of a stretch of highly acidic and hydrophobic amino acids, involved in interaction with trGTPases and RIPs (Choi, Wong et al. 2015). We established that the ribosomal stalk is the primary docking site for ricin A chain (RTA) on the ribosome (Chiou, Li et al. 2008) and showed that multiplication of P-proteins is a critical factor accelerating the

recruitment of RTA to the ribosome (Li, Grela et al. 2010). Using the yeast model we showed that the two P1A/P2B and P1B/P2A stalk dimers on the ribosome do not contribute equally to the interaction of ribosomes with RTA (Grela, Li et al. 2014).

The crystal structure of the P11 peptide [SDDDMGFGLFD] corresponding to the conserved last 11 residues of P-proteins (P11) in a complex with TCS, a single chain RIP showed that the acidic amino acids at the amino end of P11 [DDD] forms electrostatic interactions with the positively charged Lys173, Arg174 and Lys177 of TCS, while the LF motif in the hydrophobic carboxyl end of P11 [FGLF] is inserted into a hydrophobic pocket at the C-terminal domain of TCS (Too, Ma et al. 2009). Stx1A1 has been shown to interact with the P11 peptide using Arg172, Arg176 and Arg179 located on the distal face of the active site (McCluskey, Poon et al. 2008, McCluskey, Bolewska-Pedyczak et al. 2012). Since P-proteins exist as a pentameric complex on the ribosome, these studies provided a valuable view, but did not address the interactions with P11 in the context of the intact ribosome or the pentameric stalk complex. The interactions of Stx2A1 with P11 or with the ribosome were not investigated.

We previously showed that ribosomal P-protein stalk is required for ribosome depurination and toxicity of the A subunits of Stx1 and Stx2 (Chiou, Li et al. 2011). The depurination activity of Stx1A on the ribosome was greatly reduced if P1/P2 binding sites on P0 were deleted, while the depurination activity of Stx2A was not affected as much, indicating that although stalk P-proteins were important for ribosome depurination by both toxins, Stx2A was less dependent on the stalk proteins for depurination of the SRL than Stx1A (Chiou, Li et al. 2011). We recently showed that Stx2A1 has a higher affinity for the ribosome, higher catalytic activity and toxicity than Stx1A1 in both yeast and

mammalian cells (Basu, Li et al. 2016). The interaction of RTA with the ribosome depended on electrostatic interactions and followed a two-step binding model, where the slower non-stalk dependent electrostatic interactions concentrated RTA molecules on the ribosome and allowed the faster electrostatic interactions with the stalk P-proteins (Li, Chiou et al. 2009, Li, Kahn et al. 2013). Analysis of the electrostatic surface of the A1 subunits revealed differences in charge distribution around the conserved active site and on the distal face of the active site, in a region shown to be important for the interaction of Stx1A1 with the P11 peptide (Basu, Li et al. 2016). In the present study, we mutated the conserved arginines on the distal face of the active site and at the active site in both Stx1A1 and Stx2A1 to determine if they arginines contribute to the higher affinity of Stx2A1 for the ribosome. Our results demonstrate for the first time that conserved arginines at the distal face of the active site are critical for the interaction of Shiga toxins with the ribosome and with the ribosomal stalk, their depurination activity and toxicity, while a conserved arginine at the active site affects non-stalk specific interactions with the ribosome. We show that conserved arginines in neither site contribute to the higher affinity of Stx2A1 for the ribosome.

MATERIALS AND METHODS

Yeast Strains and Plasmids. Point mutations of arginines to alanines were introduced into mature Stx1A1 (NT1643) and Stx2A1 (NT1644) in pBluescript by site-directed mutagenesis using the Q5® High-Fidelity DNA Polymerase kit (New England Biolabs, Ipswich, MA). All mutations were confirmed by DNA sequencing. The wild type (WT) Stx1A1 (K1 to R251) (NT1651) and Stx2A1 (R1 to R250) (NT1652) and the mutated

genes for Stx1A1 E167K (NT1660), R170A (NT1661), R172A (NT1704), R176A (NT1706), R172A/R176A (NT1730) and for Stx2A1, E167K (NT1664), R170A (NT1663), R172A (NT1696), R176A (NT1699), R172A/R176A (NT1731), were sub-cloned into a yeast expression vector NT1617 carrying a *URA3* marker and *GAL1* promoter with V5 and 10xHis epitope at their C-termini. *S. cerevisiae* strain W303 (*MATa ade2-1 trp1-1 ura3-1 leu2-3,112 his-3-11, 15 can1-100*) was transformed with each of the constructs or the empty vector.

Yeast cell viability assay. The W303 cells containing Stx constructs were grown at 30°C in synthetic dropout (SD) medium supplemented with 2% glucose overnight and toxin expression was induced by transferring them to SD medium with 2% galactose. Cells were collected at 0 and 4 hours post induction and serial dilutions of 0.1 OD_{600} were plated on SD-URA plates containing 2% glucose. The plates were then grown at 30°C for 2-3 days.

Total protein extraction and immunoblot analysis. The W303 expressing WT and mutant forms of Stxs were collected at 6 hours post induction and total protein was extracted from 5 OD_{600} yeast cells as described previously (Zhang, Lei et al. 2011). Stx1A1 and Stx2A1 expression were detected using monoclonal antibodies against V5 (Invitrogen, Carlsbad, CA). Monoclonal antibodies against 3-phosphoglycerate kinase (Pgk1p) (Life Technologies, Grand Island, NY) were used as a loading control.

Purification of 10xHis-tagged and untagged Stx1A1 and Stx2A1. 10xHis-tagged WT (NT1570) and mutants R172A (NT1761), R176A (NT1741) and R172A/R176A

(NT1765) in Stx1A1 and WT (NT1567) and mutants R172A (NT1762), R176A (NT1742) and R172A/R176A (NT1766) in Stx2A1 were purified by Dr. Karen Chave at the Northeast Biodefense Center protein expression core facility using the IMPACT™ protein expression system (New England Biolabs, Ipswich, MA) as described previously (Basu, Li et al. 2016). Briefly, forward and reverse primers with NdeI and SapI restriction sites were synthesized to enable in-frame cloning of the PCR fragments into the polylinker of the pTXB1 vector (New England Biolabs, Ipswich, MA) resulting in a C-terminal fusion of the *Mycobacterium xenopi* intein tag and a chitin binding domain. *E. coli* strain Rosetta2 (DE3) pLysS, transformed with the constructs were grown in 2xYT media, overnight at 16°C. The fusion proteins were purified from *E. coli* lysates using chitin beads and the proteins were eluted by thiol-induced cleavage.

Analysis of depurination. W303 cells expressing WT and mutant forms of Stx1A1 and Stx2A1 were collected at 1 hour post induction. RNeasy Mini Kit (Qiagen, Valencia, CA) with on column DNase treatment was used to extract the total RNA. cDNA was obtained from the RNA using the High Capacity cDNA Reverse Transcription Kit (Applied Biosystems, Grand Island, NY) and depurination was detected with a quantitative real time PCR method using the StepOnePlus™ Real-Time PCR system (Applied Biosystems, Grand Island, NY). The 25S reference primers were 5'-AGA CCG TCG CTT GCT ACA AT-3'and 5'- ATG ACG AGG CAT TTG GCT AC- 3' and the depurination primers were 5'- CTA TCG ATC CTT TAG TCC CTC-3' and 5'- CCG AAT GAA CTG TTC CAC A-3' respectively. The ΔΔCT method was used to calculate the depurination levels and data were expressed as fold change of depurination in Stx-

treated RNA over depurination in control non-treated RNA as described (Pierce, Kahn et al. 2011).

Monomeric ribosomes were isolated as previously published (Basu, Li et al. 2016). 1nM of WT Stx1A1 and Stx2A1 and 3-fold dilutions of mutant proteins (R170A, R176A, and R172A/R176A) (9 nM, 3 nM and 1 nM) were added to 1X RIP buffer (60 mM KCl, 10 mM Tris-HCl (pH 7.4), 10 mM MgCl2) in a final volume of 100 µL. The reaction was started by adding 7 pmol of monomeric ribosomes and incubated at 30°C for 10 min. 100 µL of 2X Extraction Buffer (120 mM NaCl, 25 mM Tris-HCl (pH 8.8), 10 mM EDTA, 1 % SDS) was added to stop the reaction. RNA was extracted with phenol and then phenol/chloroform, and precipitated overnight with ethanol. Depurination was determined using qRT-PCR (Pierce, Kahn et al. 2011).

Total RNA (1µg) from yeast cells (RNeasy Mini Kit (Qiagen, Valencia, CA)) was incubated with 250 nM of WT and mutant Stx1A1 and Stx2A1 (R170A, R176A, R172A/R176A) in a final volume of 20 µL in 20 mM citrate buffer (pH 5) at 37°C for 15 min. RNA was purified with phenol and then phenol/chloroform and the depurination of rRNA was quantified using qRT-PCR assay. The ΔΔCT method was used to calculate the depurination level and data were expressed as fold change of depurination in Stx-treated RNA over depurination in non-treated RNA as described (Pierce, Kahn et al. 2011).

Interaction of Stx1A1 and Stx2A1 with yeast ribosomes and with the ribosomal stalk pentamer. Biacore T200 (GE Healthcare Bio-Sciences, Pittsburgh, PA) was used to study the interaction of 10xHis-tagged A1 subunits with the ribosome using an NTA chip. The amount of captured toxin monitored in real time by Biacore T200 was 800 ± 20 RU. Ribosomes at different concentrations were passed over the surface at 30 µL/min for

2 min using the single injection kinetic method. Dissociation was for 5 min. Running buffer contained 10 mM Hepes pH 7.4, 150 mM NaCl and 5 mM $Mgcl_2$, 50 μM EDTA and 0.003 % Surfactant P20. The surface was freshly captured at each cycle. Interaction of the A1 subunits with the isolated ribosomal stalk pentamer was analyzed by capturing 1000 RU of 10xHis-tagged toxins on a NTA chip and the same amount of 10xHis-tagged EGFP on the reference channel. Running buffer is the same as the ribosome interaction buffer except it contained 10 mM $MgCl_2$. Yeast stalk pentamer was passed over the surface at different concentrations at 30 μL/min for 3 min and the final dissociation was for 5 min.

Transfection of Vero cells with the A1 subunits. WT Stx1A1 (K1 to R251) (NT1776) and Stx2A1 (R1 to R250) (NT1777) and Stx1A1 variants, E167K (NT1796), R170A (NT1784), R172A (NT1804), R176A (NT1774), R172A/R176A (NT1806) and Stx2A1 variants, E167K (NT1797), R170A (NT1785), R172A (NT1805), R176A (NT1775), R172A/R176A (NT1807) with V5 and 10xHis-tags were cloned into the mammalian expression vector pCAGGs at the SacI-XhoI sites and cotransfected into Vero cells with an EGFP expression plasmid in pCAGGs using Lipofectamine 2000 (Invitrogen, Carlsbad, CA) as previously described (Basu, Li et al. 2016). Biotek plate reader was used to measure the EGFP fluorescence at 22 h post DNA exposure from the bottom of the plate with 485/20 excitation filter and 530/25 emission filter. Assays were performed in quadruplicate. Fluorescence measured in cells cotransfected with EGFP and empty vector was considered as 100 % and fluorescence in controls lacking the EGFP plasmid as background.

Analysis of ribosome depurination in Vero cells. Vero cells containing WT Stx1A1 (K1 to R251) (NT1776) and Stx2A1 (R1 to R250) (NT1777) and Stx1A1 variants, E167K (NT1796), R170A (NT1784), R172A (NT1804), R176A (NT1774), R172A/R176A (NT1806) or Stx2A1 variants, E167K (NT1797), R170A (NT1785), R172A (NT1805), R176A (NT1775), R172A/R176A (NT1807) were grown as described above. Cells were collected at 23 h after DNA exposure. Total RNA was extracted using the RNeasy Mini Kit (Qiagen, Valencia, CA) with on column DNase treatment. qRT-PCR assay was used to quantify depurination (Pierce, Kahn et al. 2011).

Isolation of rat liver ribosomes. Monomeric ribosomes were isolated from rat livers were as previously described (Basu, Li et al. 2016). Briefly livers were dissected from rats, rinsed in cold buffer A (20 mM HEPES-KOH pH 7.6, 5 mM MgOAc, 50 mM KCl, 10 % glycerol) with 1 mM PMSF, 1 mM DTT, and protease inhibitor cocktail for mammalian tissue culture (Sigma-Aldrich, St. Louis, MO) and frozen in liquid N_2. Thawed livers were homogenized in cold Buffer A plus 1 mM PMSF, 1mM DTT, and protease inhibitor cocktail for mammalian tissue culture (Sigma-Aldrich, St. Louis, MO) and centrifuged at 20,000 *g* for 20 min. The supernatant was treated with 1% sodium deoxycholate for 10 min with constant stirring on ice and sedimented at 150,000 *g* for 90 min. The pellet was rinsed twice in Buffer B (20 mM HEPES-KOH, pH 7.6, 20 mM MgOAc, 0.5 M KCl, 10% Glycerol) with 1 mM PMSF, 1 mM DTT, and stored overnight at 4°C in a small amount of the same buffer. The ribosomes were resuspended with a Dounce homogenizer in buffer B with 1 mM DTT and 1 mM PMSF and incubated 30 min at 30°C with 1 mM puromycin, 1 mM GTP. The supernatant was clarified by centrifugation at 20,000 *g* for 15 min and layered over a cushion of buffer B with

glycerol raised to 25 %. Ribosomes were sedimented at 150,000 *g* for 2 h. The pellets were rinsed in Buffer C (50 mM HEPES-KOH pH 7.6, 5 mM MgOAc, 50 mM NH_4Cl, 0.1 mM DTT and 25% glycerol), resuspended in 5 ml Buffer C and stored -80 ºC.

Depurination of rat liver ribosomes. Depurination analysis of rat liver ribosomes was performed as described for yeast. 1nM of WT Stx1A1 and Stx2A1 and 3-fold dilutions of mutant proteins (R170A, R176A, R172A/R176A) (9 nM, 3 nM and 1 nM) were used in the treatment of 7 pmol of rat ribosomes. Depurination was analyzed by qRT-PCR (Pierce, Kahn et al. 2011).

Interaction of Stx1A1 and Stx2A1 with rat liver ribosomes. The interaction of 10xHis-tagged WT and variant Stx1A1 and Stx2A1 with rat liver ribosomes was examined using Biacore T200 (GE Healthcare Bio-Sciences, Pittsburgh, PA). The amount of toxin captured on an NTA chip was monitored in real time was 1800 ± 50 RU. Ribosomes at different concentrations were passed over the surface at 30 μL/min for 2 min using the single injection kinetic method. Dissociation was for 5 min. Running buffer contained 10 mM Hepes pH 7.4, 150 mM NaCl and 5 mM $Mgcl_2$, 50 μM EDTA and 0.01 % Surfactant P20. The surface was freshly captured at each cycle.

Statistical analysis. Data for Fig. 1-5, 7 and 8 were analyzed by student's two sample t-test using Origin software (OriginLab v.8.0, Northampton, MA). Statistical analyses of data in Fig. 6A and B were conducted by using SAS 9.4 (SAS Institute, Inc., Cary, NC). Data were analyzed by generalized mixed linear models using PROC GLM (Procedure for Generalized Linear Models) to test for statistical differences between treatments.

Least square means were calculated, and specific preplanned contrasts (Steel, James et al. 1997) were computed to compare treatment means between Stx1A1 and Stx2A1 for each treatment.

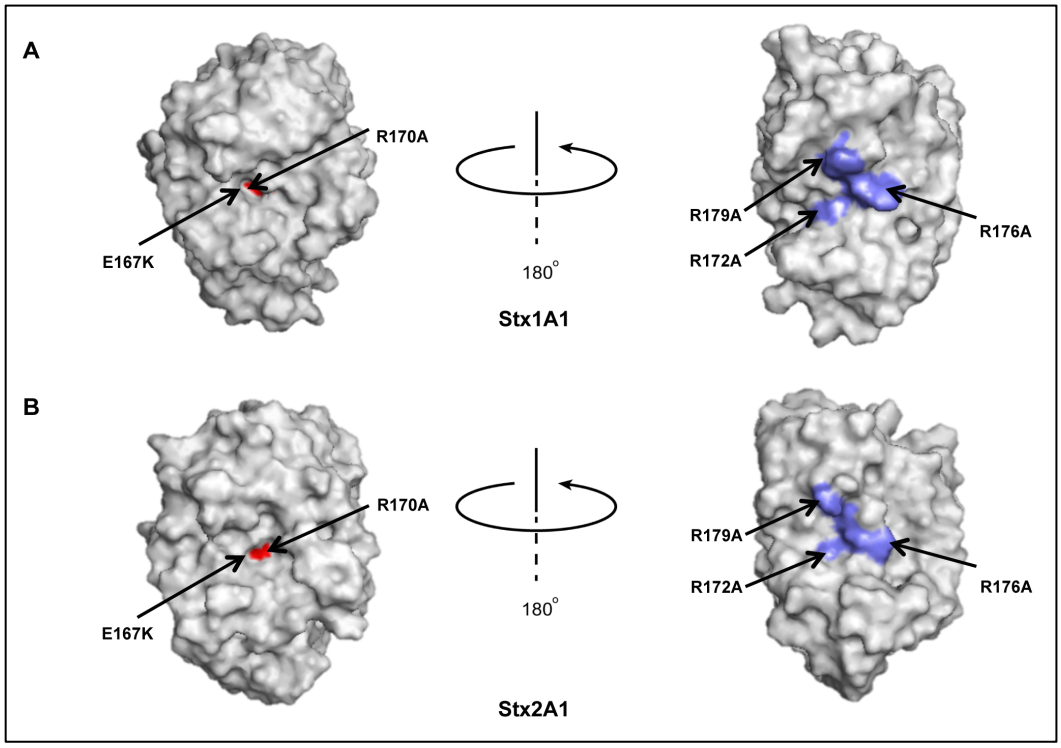

FIG 3.1 Crystallographic structures have Stx1A1 and Stx2A1 showing the active site and ribosome stalk binding mutants. Crystallographic structures of Stx1A1 and Stx2A1 showing the active site and the distal face of the active site. The A1 subunits of Shiga toxin and Shiga toxin 2 were modeled from the Protein Data Bank ID: 1DM0 (Shiga toxin) and 1R4P (Shiga toxin 2). Active site of Stx1A1 (red) is more embedded (A) than the active site of Stx2A1 (B). A rotation about the y-axis by approximately 180˚ reveals the conserved arginines (blue) in Stx1A1 (A) and in Stx2A1 (B).

RESULTS

Arginine R172 and R176 are more important than R179 in the cytotoxicity and depurination activity of Stx1A1 and Stx2A1 in yeast. Comparison of the crystallographic structures of Stx1A1 and Stx2A1 (Fig. 1A and B) show that R172, R176 and R179, previously shown to be involved in the interaction of Stx1A1 with p11 (McCluskey, Bolewska-Pedyczak et al. 2012), are more exposed in Stx1A1 than Stx2A1, suggesting that R172, R176 and R179 might play a differential role in ribosome binding in Stx1A1 and Stx2A1. We therefore mutated R172, R176 and R179 to alanine in Stx1A1 and Stx2A1. We included mutations in the active site residues Glu167 (E167K) and Arg170 (R170A) (Fig 1A and B) as controls. The wild type (WT) and mutant forms of Stx1A1 and Stx2A1 were expressed in yeast under the control of the *GAL1* promoter, and viability was determined by induction on galactose for 4 hours followed by plating serial dilutions on media containing glucose. The colony forming units calculated based on the viability assay are shown in Fig. 2A and Fig. S1A. WT Stx2A1 grew 2-fold slower than WT Stx1A1 (Fig. 2A and S1A). While there was a significant increase in the viability of R172A and R176A, R179A did not show a significant increase in viability compared to WT and was not analyzed further (Fig. S1A).

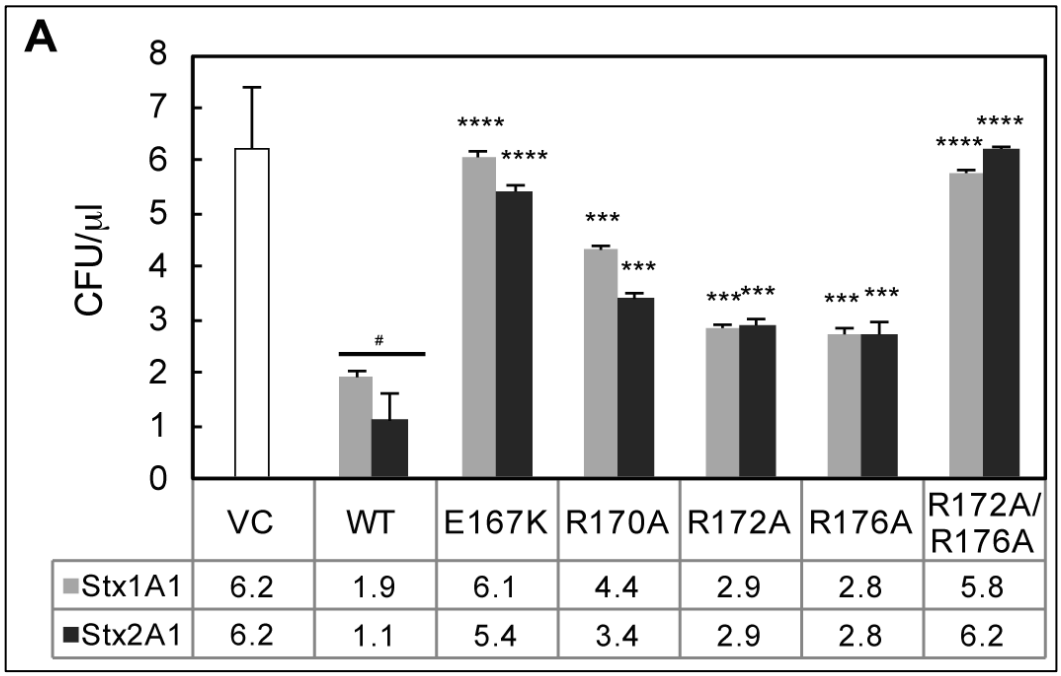

FIG 3.2 (A) Viability and ribosome depurination in yeast expressing wild type (WT) or mutant Stx1A1 or Stx2A1. Yeast cells transformed with plasmid carrying WT or mutant Stx1A1 or Stx2A1 or the empty vector (VC) were grown in SD medium supplemented with 2% glucose and then transferred to SD medium supplemented with 2% galactose. At 0 and 4 hours post induction (hpi), a series of 10-fold dilutions were plated on media containing 2% glucose and grown at 30°C for 1-2 days. Colony forming units per ml (CFU/ml) at 4 hpi were calculated from at least 3 independent transformants. Error bars represent S. E. where n=3 independent experiments. Means of Stx1A1, Stx2A1 and their variants were significantly different using two-sample t-test (*means compared to respective WT; #means compared between Stx1A1 and Stx2A1. ***$P< 0.001$, ****$P< 0.0001$, $^{\#}P< 0.05$).

To determine if mutation of more than one arginine would lead to a further reduction in toxicity, we mutated two or three different arginines at the distal face of the

active site to alanine simultaneously and compared their viability relative to WT (Fig. S1A). The growth of double (R172A/R176A and R172A/R179A) and triple (R172A/R176A/R179A) arginine mutants was similar to the empty vector (Fig. S1A), indicating that simultaneous mutation of two arginines reduced toxicity to a minimal level in both toxins. These results showed that Arg179 is not as important as Arg172 and Arg176, but has an effect in reducing the toxicity when combined with mutations at nearby arginines (Fig. S1A). Since there were not discernible differences among the growth of the double and the triple mutants (Fig. S1), R172A/R176A was selected for further analysis. The E167K mutation led to a total loss of cytotoxicity, while R170A mutation reduced toxicity of both Stx1A1 and Stx2A1 (Fig. 2A). Although Glu167 and Arg170 play a critical role in the catalytic activity of Shiga toxins, the complete loss of toxicity of E167K might be due to the drastic change from a negatively charged residue to a positively charged residue. In contrast, R170A retains some toxicity, possibly because the positive charge is replaced by a smaller neutral alanine (Fig. 2A).

The expression of arginine variants in yeast was analyzed by immunoblot analysis at 6 hpi with monoclonal antibodies against the V5 epitope (Fig. 2B). Monoclonal antibodies against phosphoglycerate kinase 1 (PGK1) were used as a loading control. As observed previously (Basu, Li et al. 2016), the expression level of the arginine variants correlated inversely with their toxicity. All mutants were expressed at higher levels than WT, consistent with their lower toxicity (Fig. 2B).

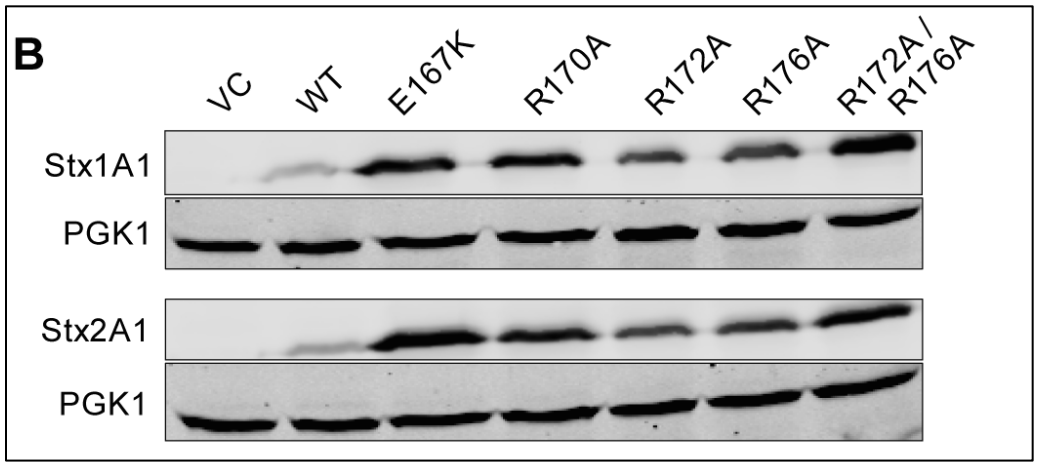

FIG 3.2 (B) Immunoblot analysis of yeast cells transformed with wild type (WT) or mutant Stx1A1 or Stx2A1 Stx1A1 and Stx2A1. Total protein from 5 OD_{600} cells isolated at 6 hpi was separated on a 12% SDS-PAGE and probed with anti-V5. Anti-phosphoglycerate kinase 1 (PGK1) was used as a loading control.

In order to determine if there is a correlation between the reduced cytotoxicity and depurination activity in yeast, the depurination activity of the arginine variants was examined using a previously described quantitative reverse transcriptase polymerase chain reaction (qRT-PCR) assay (Pierce, Kahn et al. 2011). Total RNA was collected from yeast cells at 1 hpi and depurination was determined relative to yeast harboring the empty vector using the comparative CT method (ΔΔCT). All mutants showed a significant reduction in the depurination level when compared to WT Stx1A1 and Stx2A1 except R179A (Fig. S1B). The E167K single mutation eliminated depurination consistent with the viability assay (Fig. 2C). Stx2A1 containing the single R170A, R172A or R176A mutations depurinated ribosomes at a significantly higher level than Stx1A1 containing the same mutations, while simultaneous mutations at Arg172 and Arg176 caused a similar reduction in depurination level of Stx1A1 and Stx2A1 (Fig. 2C and Fig.

S1B). These results showed that conserved arginines play a critical role in the toxicity and depurination activity of Stx1A1 and Stx2A1 in yeast. However, Arg170, Arg172 and Arg176 are more critical for the depurination activity and toxicity of Stx1A1 than Stx2A1.

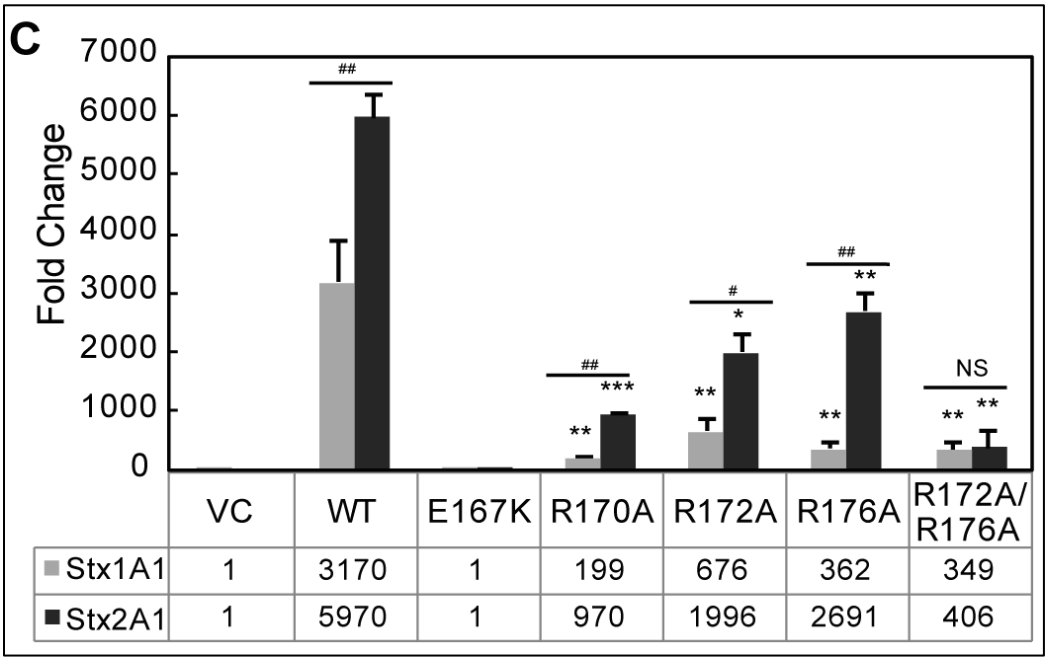

	VC	WT	E167K	R170A	R172A	R176A	R172A/ R176A
Stx1A1	1	3170	1	199	676	362	349
Stx2A1	1	5970	1	970	1996	2691	406

FIG 3.2 (C) Depurination of ribosomes in yeast. Total RNA (375 ng) isolated from 1 OD_{600} cells expressing WT or mutant $Stx1A_1$ (grey bars) or Stx2A1 (black bars) collected at 1 hpi was used to quantify the relative level of depurination using qRT-PCR. The y-axis shows the fold change in depurination of toxin-treated samples over the control samples without toxin (VC). Error bars represent S. E. where n=3 replicates. Means of WT Stx1A1, Stx2A1 and Stx1A1 and Stx2A1 variants were significantly different using two-sample t-test (*means compared to respective WT; #means compared between Stx1A1 and Stx2A1. *P< 0.05, **P< 0.01, ***P< 0.001, $^{\#}$P< 0.05, $^{\#\#}$P< 0.01, NS= Not significant).

Arginine variants depurinate yeast ribosomes at a reduced level, but depurinate yeast RNA at a similar level as WT Stx1A1 and Stx2A1. To examine the depurination activity of the arginine mutants, 10xHis-tagged WT and mutant forms of $Stx1A_1$ and $Stx2A_1$ were expressed in *E. coli* and purified. The dramatic change from glutamic acid to lysine likely affected folding and prevented purification of Stx1A1 and Stx2A1 containing E167K mutation. This mutant and Stx2A1 containing R172A mutation could not be purified. Recombinant R170A, R176, R172A/R176A mutants and WT Stx1A1 and Stx2A1 were analyzed by immunoblot analysis using monoclonal antibodies against histidine (Qiagen, Valencia, CA). Each toxin migrated on SDS-PAGE as expected for its size (Fig. 3A).

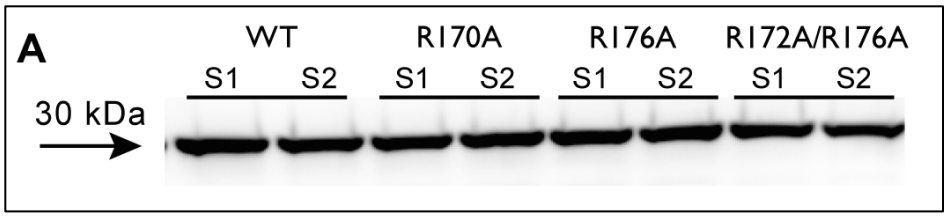

FIG 3.3 (A) Immunoblot analysis of purified 10xHis-tagged wild type (WT) or mutant Stx1A1 and Stx2A1. Equal amount (1ug) of purified Stx1A1 (S1) and Stx2A1 (S2) were separated on a 12 % SDS-polyacrylamide gel. 10xHis-tagged Stx1A1 (S1) and Stx2A1 (S2) were detected by monoclonal anti-His.

Depurination activity of recombinant Stx variants was examined using monomeric yeast ribosomes (Fig. 3B and C). The ribosomes were treated with 3-fold higher doses of the mutant toxins in order to ascertain the linear range of increase in depurination relative

to toxin concentration. Depurination by R170A variant was significantly reduced compared to WT Stx1A1 or Stx2A1 at all doses tested (Fig. 3B). Stx1A1 R176A and R172A/R176A had significantly lower depurination levels in comparison to WT even at 9 nM toxin concentration (Fig. 3C). In contrast, only Stx2A1 R172A/R176A had significantly lower depurination levels in comparison to WT at 9 nM toxin concentration (Fig. 3C). There was a highly significant reduction in depurination at the lower concentrations of Stx2A1 R176A, but the reduction in depurination was not observed when it was used at 9 nM (Fig. 3C). Stx2A1 variants containing single mutations depurinated ribosomes at a significantly higher level than Stx1A1 variants (Fig. 3B and C). The R172A/R176A double mutation resulted in a comparable level of depurination in Stx1A1 and Stx2A1 (Fig. 3C), indicating that mutation of both arginines is necessary to reduce the depurination activity of Stx2A1 to the same level as Stx1A1 (Fig. 3C).

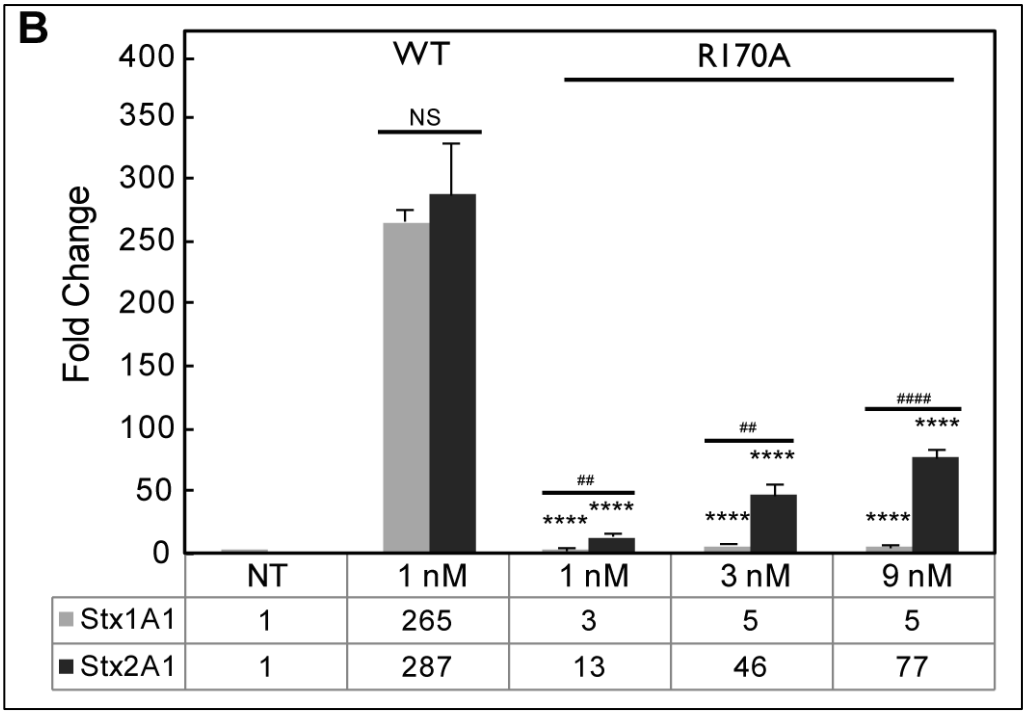

	NT	1 nM	1 nM	3 nM	9 nM
Stx1A1	1	265	3	5	5
Stx2A1	1	287	13	46	77

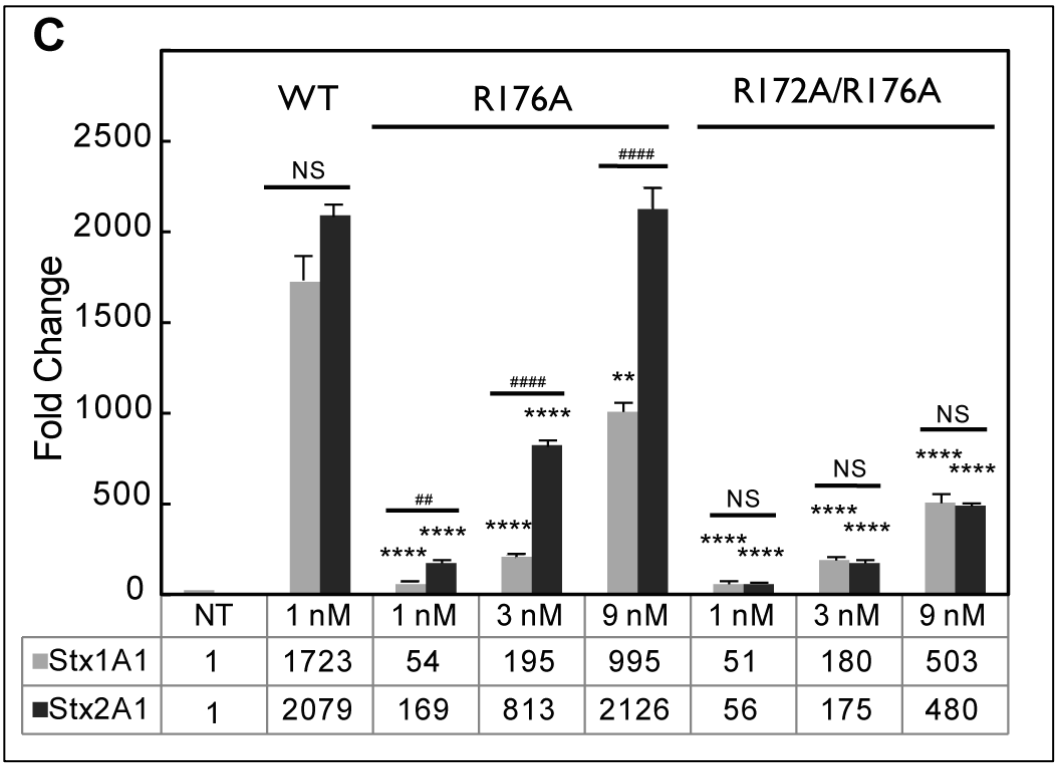

	NT	1 nM	1 nM	3 nM	9 nM	1 nM	3 nM	9 nM
Stx1A1	1	1723	54	195	995	51	180	503
Stx2A1	1	2079	169	813	2126	56	175	480

FIG 3.3 (B & C) Depurination of yeast ribosomes by purified wild type (WT), R170A and R176A 10xHis-tagged Stx1A1 and Stx2A1. Yeast ribosomes (7 pmol) were incubated with different amounts of wild type (WT), R170A, R176A, R172A/R176A 10xHis-tagged Stx1A1 (grey bars) or Stx2A1 (black bars) at 30°C for 10 min. The rRNA (375 ng) was used to quantify the relative levels of depurination by qRT-PCR. The y-axis shows the fold change in depurination of toxin-treated samples over the control samples without toxin treatment (NT). Error bars represent S. E. where n=3 replicates. Means of WT Stx1A1, Stx2A1 and their variants were significantly different using two-sample t-test (*means compared to respective WT; #means compared between Stx1A1 and Stx2A1. **P< 0.01, ****P< 0.0001, $^{\#\#}$P< 0.01, $^{\#\#\#\#}$P< 0.0001 NS= Not significant).

When total yeast RNA was used as a substrate for depurination with purified toxins, Stx1A1 and Stx2A1 containing R176A and R172A/R176A mutations showed similar

depurination activity as WT Stx1A1 and Stx2A1 (Fig. 3D and E). In contrast, R170A showed no activity on RNA, since this mutation was at the active site (Fig. 3D). WT Stx2A1 and Stx2A1 R176A and R172A/R176A depurinated RNA at a significantly higher level than WT Stx1A1 and Stx1A1 R176A and R172A/R176A, respectively, indicating that WT Stx2A1 and Stx2A1 R176A and R172A/R176A were more active. Therefore R176A and R172A/R176A mutations do not affect RNA binding or catalytic activity, providing evidence that the reduction in ribosome depurination is not due to a reduction in catalytic activity. In contrast, reduced catalytic activity is responsible for the reduction in ribosome depurination by R170A (Fig. 3D).

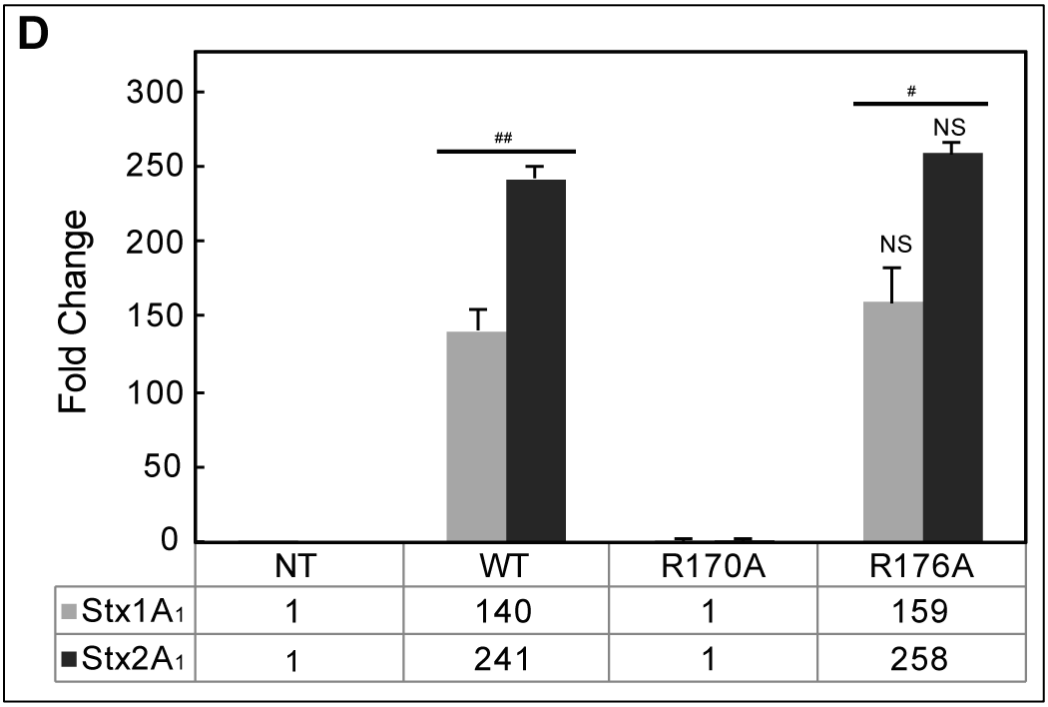

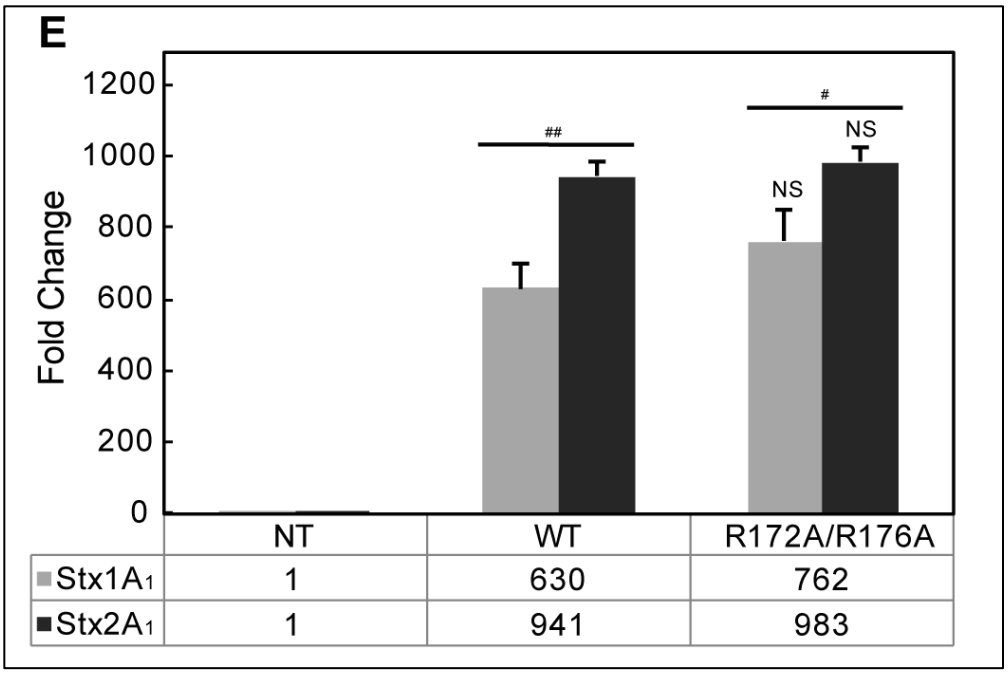

	NT	WT	R172A/R176A
Stx1A1	1	630	762
Stx2A1	1	941	983

FIG 3.3 (D & E) Depurination of total RNA from yeast by purified Stx1A1 or Stx2A1. Total RNA (1µg) was incubated with different amounts of wild type (WT), R170A, R176A, R172A/R176A 10xHis-tagged Stx1A1 (grey bars) or Stx2A1 (black bars) at 37°C for 15 min. The relative levels of depurination were determined using qRT-PCR [38]. The y-axis shows the fold change in depurination over the control samples without toxin treatment (NT). The analysis was repeated three times. Error bars represent S. E. where n=3 replicates. Means of Stx1A1, Stx2A1 and their variants were significantly different using two-sample t-test (# means compared between Stx1A1 and Stx2A1. $^{\#}P<0.05$, $^{\#\#}P< 0.01$, NS= Not significant).

Arginine mutations affect the interaction of the A1 subunits with the ribosome and with the stalk pentamer in yeast. To determine if reduced depurination is due to reduced interaction with the ribosome we examined the interaction of Stx variants with intact yeast ribosomes and with the purified stalk pentamer from yeast by surface

plasmon resonance (SPR) using Biacore. In order to detect binding, 10xHis-tagged WT Stx1A1, 10xHis-tagged WT Stx2A1 and 10xHis-tagged R176A and R172A/R176A variants were captured on a NTA chip at 800 RU. The same amount of 10xHis-tagged EGFP was captured on the reference channel as a control (Fig. 4A and B). We could not detect binding of Stx1A1 and Stx2A1 containing R176A or R172A/R176A mutations to the ribosome at concentrations up to 40 nM (Fig. 4A and B). Binding was not detected even when R176A or R172A/R176A were captured at 2500 RU. These results highlighted the importance of these residues in the interaction with the ribosome. They also showed that Stx2A1 bound ribosomes at a higher level than Stx1A1, consistent with previous results (Basu, Li et al. 2016).

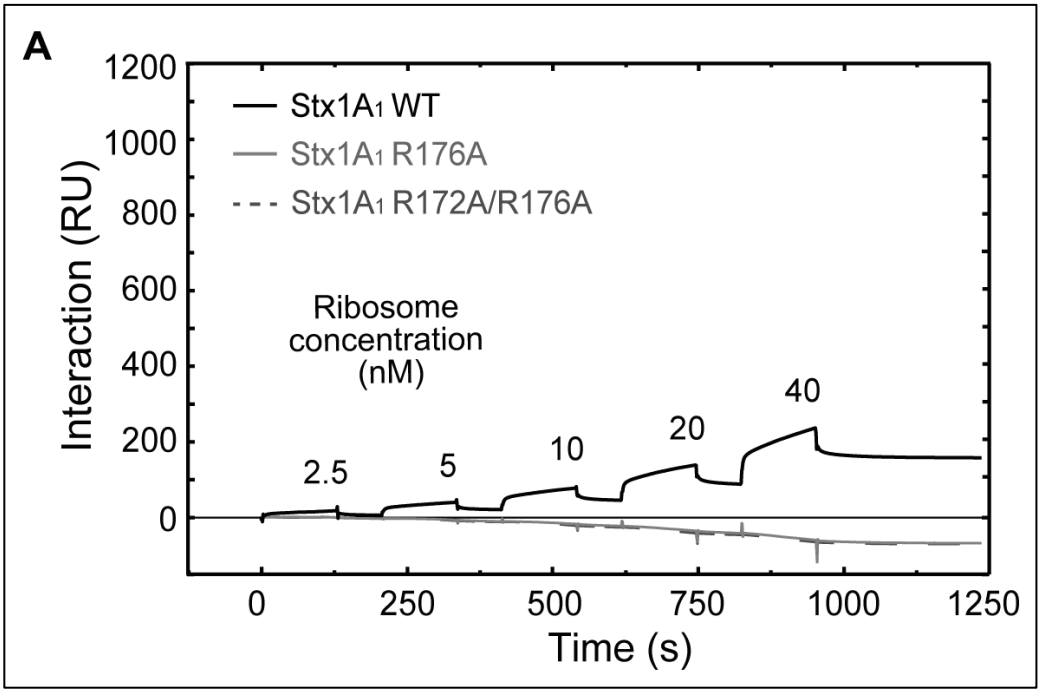

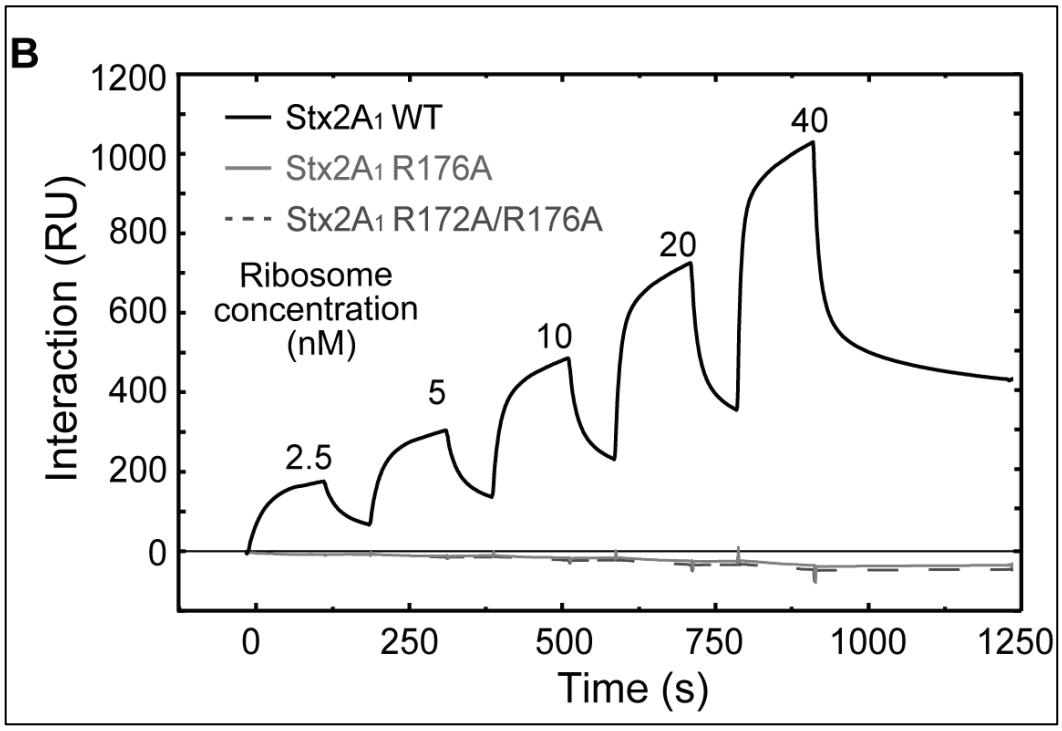

FIG 3.4 (A & B) Interaction of wild type (WT), R176A and R172A/R176A 10xHis tagged Stx1A1 and Stx2A1 with yeast ribosomes. Wild type (WT) R176A and R172A/R176A 10xHis-Stx1A1 (A) and 10xHis-Stx2A1 (B) were captured on an NTA chip. Different concentrations of ribosome were passed over the surface as analyte as shown.

TABLE 3.1. Apparent K_D (M) of the interaction of A_1 subunits with ribosomes [A]

Toxin		Mean Apparent KD (M)	
		Yeast Ribosomes	Rat Ribosomes
Stx1A1	WT	8.47±0.15 X 10^{-8} [a]	9.39±2.03 X 10^{-8} [e]
	R170A	9.37±0.23 X 10^{-8} [b]	11.71±1.91 X 10^{-8} [f]
Stx2A1	WT	2.89±0.08 X 10^{-8} [c]	4.39±0.15 X 10^{-8} [g]
	R170A	3.45±0.22 X 10^{-8} [d]	5.06±0.83 X 10^{-8} [h]

[A] Letters indicate statistical comparisons, where means were significantly different between a and b ($P<0.01$), between c and d ($P<0.05$), between b and d ($P<0.001$), between e and f ($P<0.05$), g and h ($P<0.05$) and f and h ($P<0.001$) as determined using two-sample t-test.

In order to examine the interaction of the Stx variants with the stalk pentamer, 10xHis-tagged WT Stx1A1 and Stx2A1 and 10xHis-tagged R176A and R172A/R176A variants were captured on different channels of an NTA chip at 1000 RU and the purified stalk pentamer from yeast was passed over the surface (Fig. 4C and D). The same amount of 10xHis-tagged EGFP was captured on the reference channel as a control. R176 or R172/R176 mutations eliminated the interaction of Stx1A1 and Stx2A1 with the stalk pentamer, even at 16.2 nM stalk pentamer concentration (Fig. 4C and D).

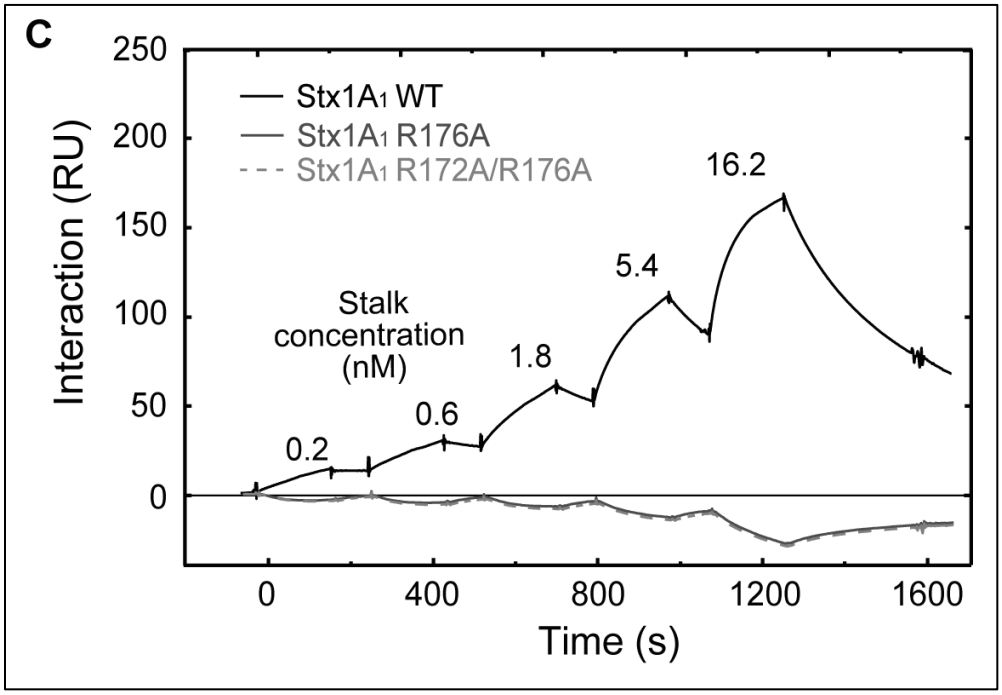

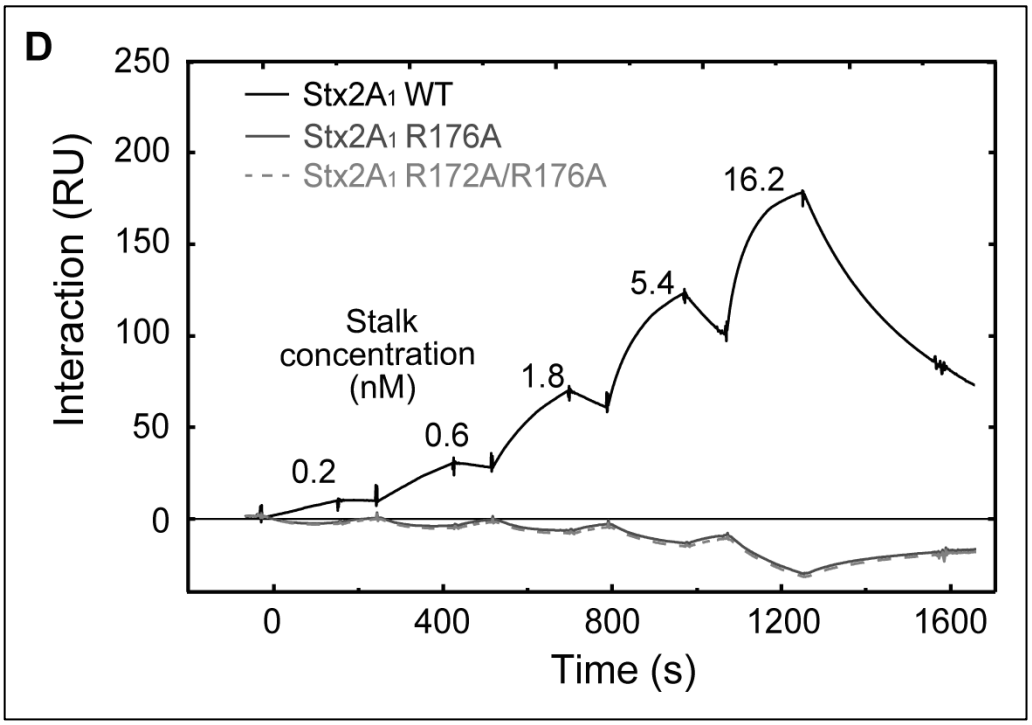

FIG 3.4 (C & D) Interaction of wild type (WT), R176A and R172A/R176A 10xHis-tagged Stx1A1 and Stx2A1 with the isolated yeast ribosomal stalk pentamer. Wild type (WT), R176A and R172A/R176A 10xHis-Stx1A1 (C) or 10xHis- Stx2A1 (D) were captured on an NTA chip at 1000 RU and the same amount of EGFP was captured on the reference channel. Different concentrations of stalk pentamer were passed over the surface as analyte as shown.

To determine if arginine to alanine conversion at the active site affected the interaction of Stx1A1 and Stx2A1 with the ribosome, we examined the interaction of R170A with ribosomes and with the purified stalk pentamer. As shown in Fig. 5A and B, Stx1A1 R170A interacted with ribosomes at a 1.7-fold lower level than WT, while Stx2A1 R170A bound ribosomes at a 1.3-fold lower level than WT when 40 nM yeast ribosomes were used. Since the interaction did not fit a 1:1 model, the association (k_{on})

and dissociation (k_{off}) rates could not be accurately determined. Instead binding level was used to calculate the equilibrium dissociation constant (K_D) (Table 1). The apparent K_D values of R170A variants were 1.2-fold higher than WT for Stx1A1 and Stx2A1 and this difference was significant. These results indicate that a slight change in the overall charge of the toxin molecule due to a mutation at the active site affects its interaction with the ribosome (Fig. 5A and B). The apparent K_D values for WT Stx1A1 and Stx1A1 R170A were 3-fold higher than the apparent K_D values for WT Stx2A1 and Stx2A1 R170A, respectively, indicating that WT Stx2A1 and Stx2A1 R170A have higher affinity for the ribosome than WT Stx1A1 and Stx1A1 R170A, respectively.

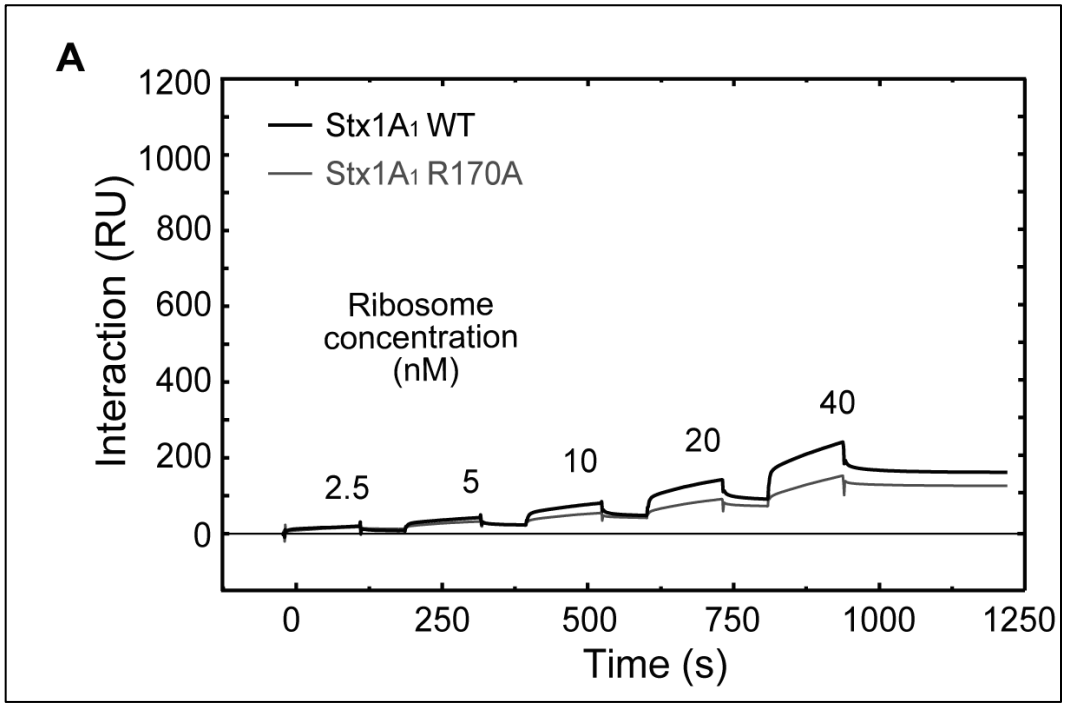

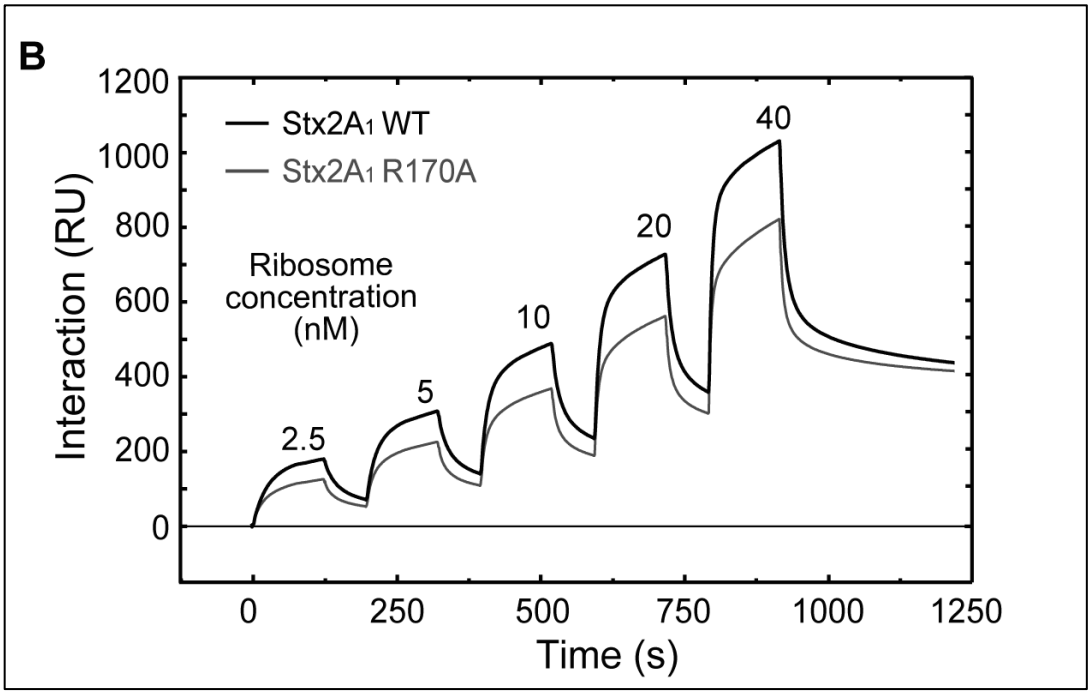

FIG 3.5 (A & B) Interaction of wild type (WT) and R170A 10xHis-tagged Stx1A1 and Stx2A1 with yeast ribosomes. Wild type (WT) and R170A 10xHis-tagged Stx1A1 (A) and Stx2A1 (B) were captured on a NTA chip at 800 RU. Different concentrations of ribosome were passed over the surface as analyte as shown.

When the interaction of R170A variants was examined with the stalk pentamer, the interaction fit into a 1:1 interaction model (Fig. 5C and D). Stx1A1 R170A showed slightly slower k_{on} and k_{off} compared to WT Stx1A1, which led to a slightly higher K_D in comparison to WT. Stx2A1 R170A, had slightly faster k_{on} and k_{off}, but K_D was almost identical to that of WT Stx2A1 (Fig. 5C and D). The affinity and association and dissociation rates of R170A variants for the stalk complex were not significantly different than WT Stx1A1 and Stx2A1 (Table 2). These results indicate that the lower affinity of the R170A variants for the ribosome compared to WT Stx1A1 and Stx2A1 is not due to their interaction with the stalk pentamer.

TABLE 3.2. Stalk interaction Parameters [A]

Toxin		k_a ($M^{-1}s^{-1}$)	k_d (s^{-1})	K_D (M)
Stx1A1	WT	1.53±0.76 X 10^6	2.29±0.56 X 10^{-3}	1.50±0.59 X 10^{-9}
	R170A	1.05±0.55 X 10^6	2.04±0.23 X 10^{-3}	1.89±0.52 X 10^{-9}
Stx2A1	WT	1.28±0.23 X 10^6	2.34±0.45 X 10^{-3}	1.84±0.21 X 10^{-9}
	R170A	1.39±0.08 X 10^6	2.55±0.28 X 10^{-3}	1.83±0.31 X 10^{-9}

[A] Letters indicate statistical comparisons, where means were not significantly different between a and b, between c and d, between e and f, between g and h, between i and j and between k and l, as determined by using a two sample t test.

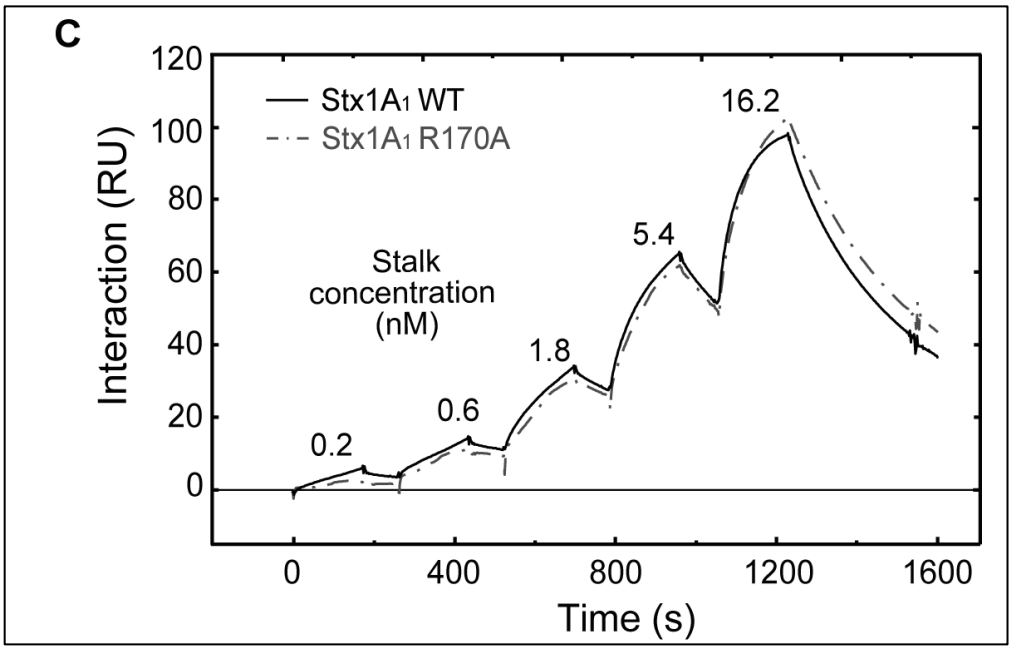

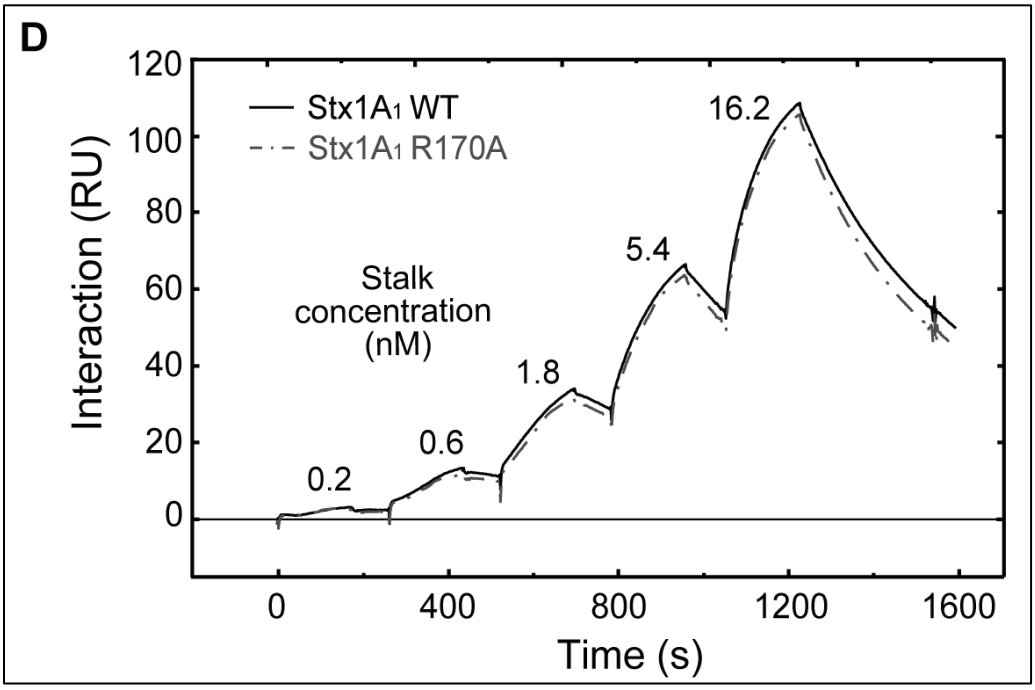

FIG 3.5 (C & D) Interaction of wild type (WT) and R170A 10xHis-tagged Stx1A1 and Stx2A1 with the isolated yeast ribosomal stalk pentamer. Wild type (WT) and R170A 10xHis-Stx1A1 (C) or 10xHis- Stx2A1 (D) were captured on an NTA chip at 1000 RU and the same amount of EGFP was captured on the reference channel. Different concentrations of stalk pentamer were passed over the surface as analyte as shown.

Stx ribosome binding mutants affect protein expression and depurination in mammalian cells. In order to determine the relative effect of the mutations in conserved arginines in mammalian cells, an EGFP transfection assay (Fig. 6A) was used to measure translation as previously described (Basu, Li et al. 2016). Vero cells were co-transfected with plasmids carrying WT Stx1A1 and Stx2A1 or their variants (E167K, R170A, R172A, R176A, R172A/R176A) and EGFP on a separate plasmid. Cells transfected with EGFP plasmid alone were used as control (Fig. 6A). Since protein levels of Stx1A1 and

Stx2A1 were too low to detect by immunoblotting, RNA expression was measured by qRT-PCR (Basu, Li et al. 2016). The RNA expression levels of WT Stx1A1 and Stx2A1 and variants were not different in Vero cells (Fig. S2). E167K and R172A/R176A variants showed significantly higher levels of EGFP fluorescence than WT Stx1A1 and Stx2A1 (Fig. 6A and Table S2). The difference in EGFP fluorescence levels in R170A, R172A and R176A variants relative to their respective WT did not achieve significance, indicating that mammalian cells are more sensitive to the toxins in comparison to yeast (Fig.6A).

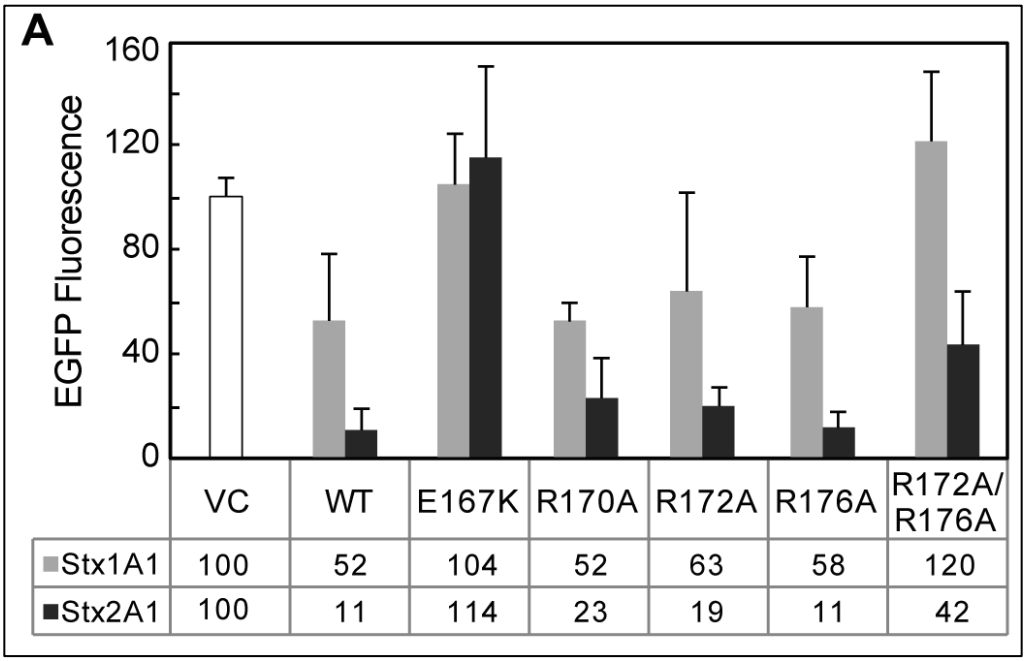

	VC	WT	E167K	R170A	R172A	R176A	R172A/ R176A
Stx1A1	100	52	104	52	63	58	120
Stx2A1	100	11	114	23	19	11	42

FIG 3.6 (A) Translation inhibition and ribosome depurination in mammalian cells expressing wild type (WT) or mutant Stx1A1 or Stx2A1. Vero cells were cotransfected with WT or mutant forms of Stx1A1 (gray bars) or Stx2A1 (black bars) and EGFP. Cells carrying the empty vector (VC) were used as controls. EGFP fluorescence was measured at 22 h post transfection. Fluorescence measured in cells cotransfected

with EGFP and empty vector was considered as 100 % and fluorescence in controls lacking EGFP plasmid as background. Experiment was repeated at least three times. A representative experiment is shown. Error bars represent S. E. where n=3 technical replicates. Statistical significance of means for WT Stx2A1 and Stx1A1 and variants were determined by using PROC GLM. Only E167K and R172A/R176A variants were significantly different from WT ($P < 0.001$).

Total RNA from Vero cells was analyzed to determine the *in vivo* depurination levels. While there was some difference in depurination levels of the WT Stx1A1 and its variants (Fig. 6B), they were too low to be statistically significant. For Stx2A1 the depurination levels of all mutants were significantly reduced in comparison to WT (Fig. 6B and Table S2).

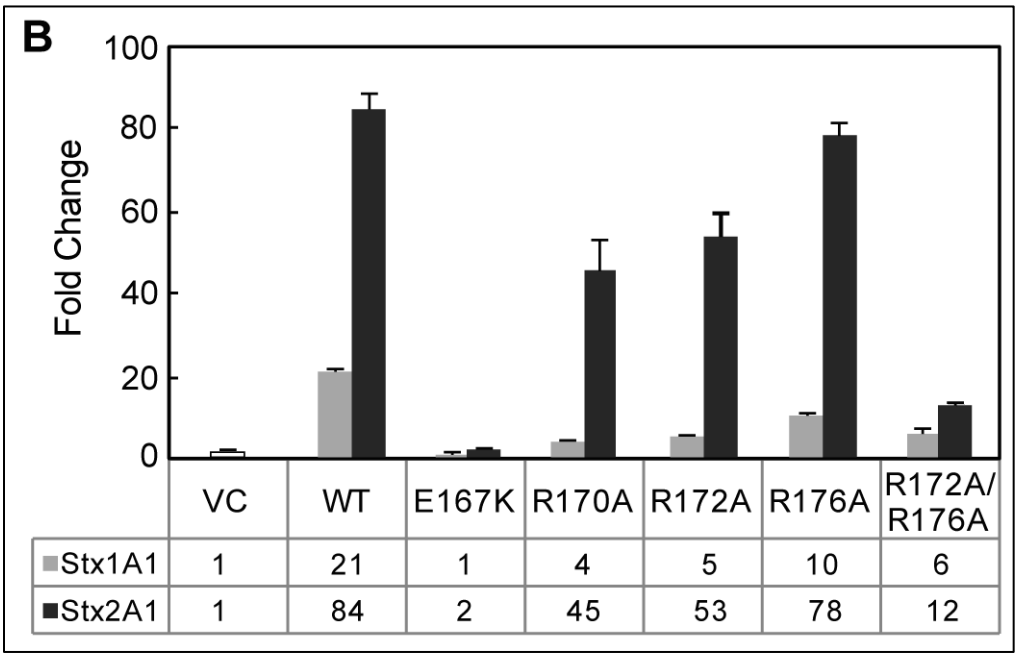

FIG 3.6 (B) Depurination of ribosomes from mammalian cells expressing wild type (WT) or mutant by Stx1A1 and Stx2A1. Total RNA (375 ng) from Vero cells

expressing WT or mutant forms of Stx1A1 (grey bars) or Stx2A1 (black bars) collected at 23 hour post DNA exposure was used to quantify the relative levels of depurination using qRT-PCR. The y-axis shows the fold change in depurination over the control samples (VC). The table shows the fold change in depurination levels in cells transfected with Stx1A1 and Stx2A1 relative to cells transfected with the empty vector. Experiment was repeated at least three times. A representative experiment is shown. Error bars represent S. E. where n=3 technical replicates. Statistical significance of means for WT Stx2A1 and Stx1A1 and variants were determined by using PROC GLM. Means were significantly different between WT Stx2A1 and Stx2A1 variants ($P < 0.001$).

When purified rat liver ribosomes were treated with recombinant WT Stx1A1 and Stx2A1 and variants, Stx1A1 exhibited significant depurination (Fig. 7A and B). As observed with yeast ribosomes (Fig 3), all mutants showed a significant reduction in depurination in comparison to WT at 1 and 3 nM (Fig. 7A and B). Stx1A1 and Stx2A1 R172A/R176A showed a similar level of reduction in depurination at the different concentrations tested. Stx2A1 R172A/R176A had significantly lower depurination in comparison to WT even at 9 nM. These results indicate that mutation of arginines at the distal face of the active site reduce depurination of mammalian ribosomes by Stx1A1 and Stx2A1. Both arginines need to be mutated to reduce the depurination of mammalian ribosomes by Stx2A1 to the same level as Stx1A1. Collectively, this data show that arginines at the distal face of the active site affect ribosome depurination and toxicity of Stx1A1 and Stx2A1 in mammalian cells.

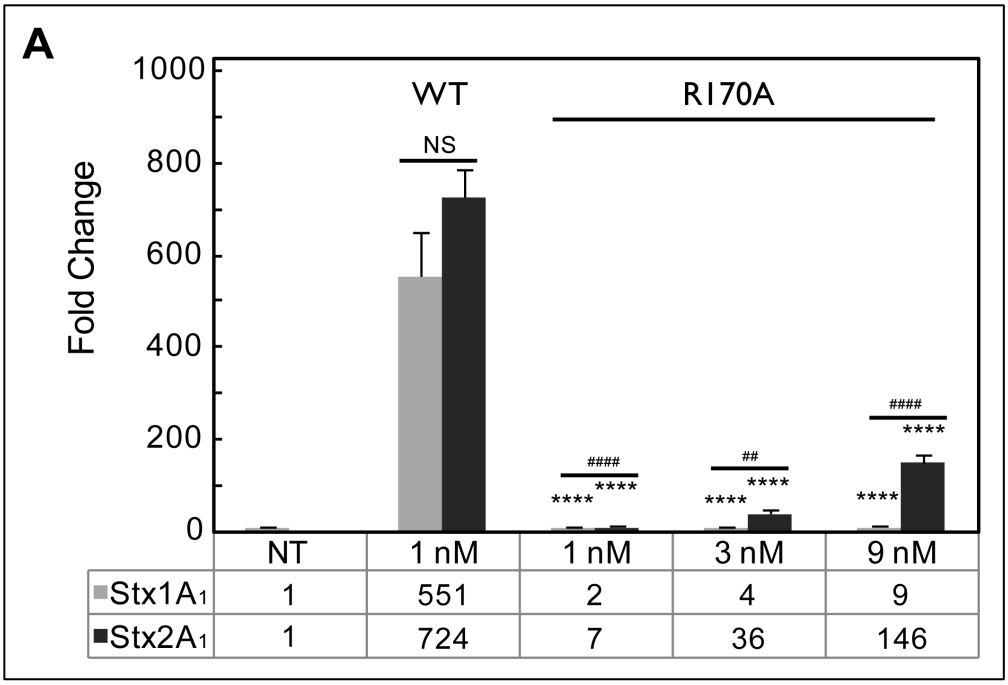

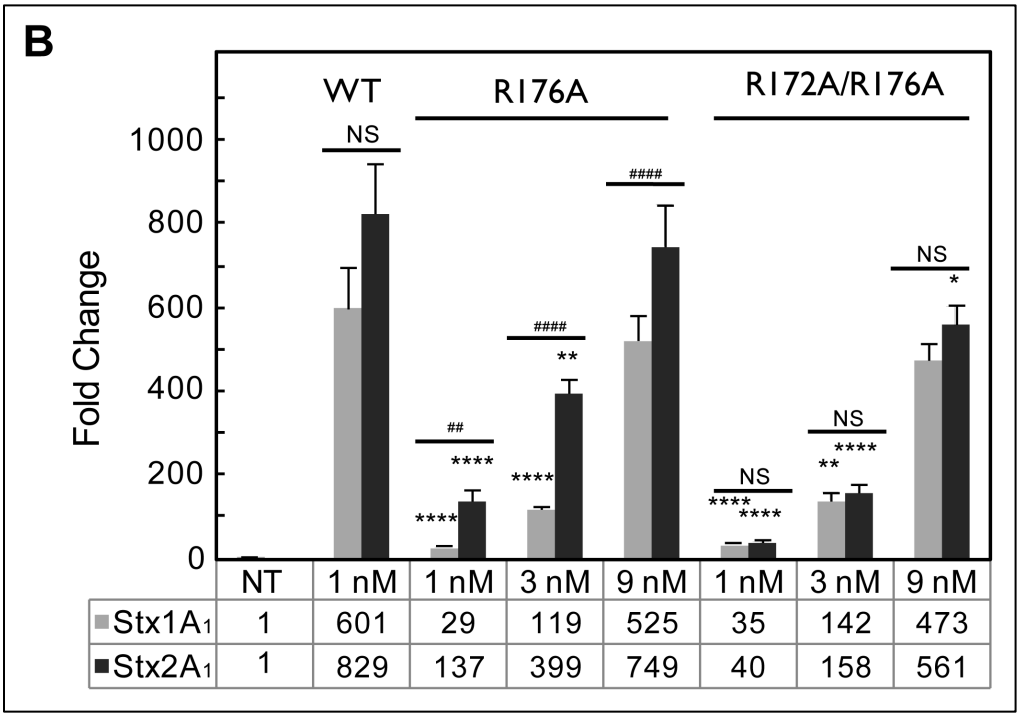

FIG 3.7 (A & B) Depurination of rat liver ribosomes by purified wild type (WT), R170A and R176A 10xHis-tagged Stx1A1 and Stx2A1. Rat liver ribosomes (7 pmol)

were incubated with different concentrations of wild type (WT), R170A, R176A, R172A/R176A 10xHis-tagged Stx1A1 (grey bars) or Stx2A1 (black bars) at 30°C for 10 min. Total rRNA (375 ng) was used to quantify the relative levels of depurination by qRT-PCR. The y-axis shows the fold change in depurination of toxin-treated samples over the control samples without toxin treatment (NT). Error bars represent S. E. where n=3 replicates. Means of WT Stx1A1, Stx2A1 and their variants were significantly different using two-sample t-test (*means compared to respective WT; #means compared between Stx1A1 and Stx2A1 **P< 0.01, ****P< 0.0001, $^{\#\#}$P< 0.01, $^{\#\#\#\#}$P< 0.0001, NS= Not significant).

Arginine mutations affect the interaction of the A1 subunits with mammalian ribosomes. In order to determine if reduced depurination is due to reduced binding to rat liver ribosomes, the interaction of 10xHis-tagged WT Stx1A1 and Stx2A1 and 10xHis-tagged R176A and R172A/R176A variants with rat liver ribosomes was analyzed using Biacore. The A1 chains were captured on a NTA chip at 1800 RU, and rat liver ribosomes were passed over the surface at different concentrations using single-cycle kinetics. The same amount of 10xHis-tagged EGFP was captured on the reference channel as a control (Fig. 8A and B). As observed with yeast ribosomes, R176A and R172A/R176A variants failed to interact with rat liver ribosomes.

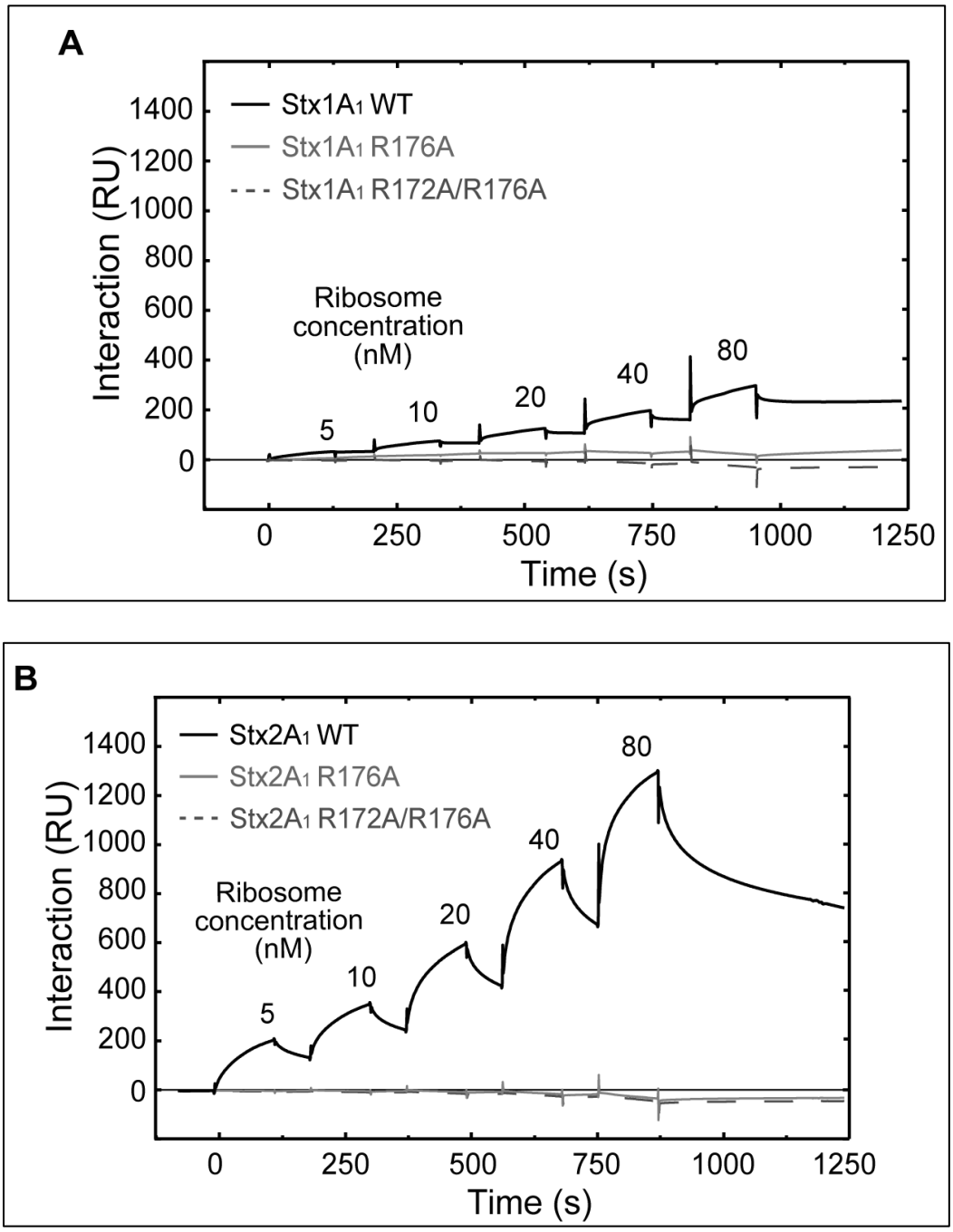

FIG 3.8 (A & B) Interaction of rat liver ribosomes with 10xHis-tagged WT Stx1A1, WT Stx2A1 and 10xHis-tagged R176A and R172A/R176A variants. WT Stx1A1, WT Stx2A1, R176A and R172A/R176A variants were captured on an NTA chip at 1800 RU. Different concentrations of rat liver ribosomes were passed over the surface as analyte.

When interaction of 10xHis-tagged R170A variants was examined with rat liver ribosomes, there was a 1.2 fold reduction in the binding levels of Stx1A1 and Stx2A1 R170A in comparison to WT Stx1A1 and Stx2A1 (Fig. 8C and D). This difference was significant (Table 1). These results demonstrated that Arg170 is critical for interaction of Stx1A1 and Stx2A1 with rat liver ribosomes and highlighted the importance of surface charge in the interaction of the A1 subunits with mammalian ribosomes.

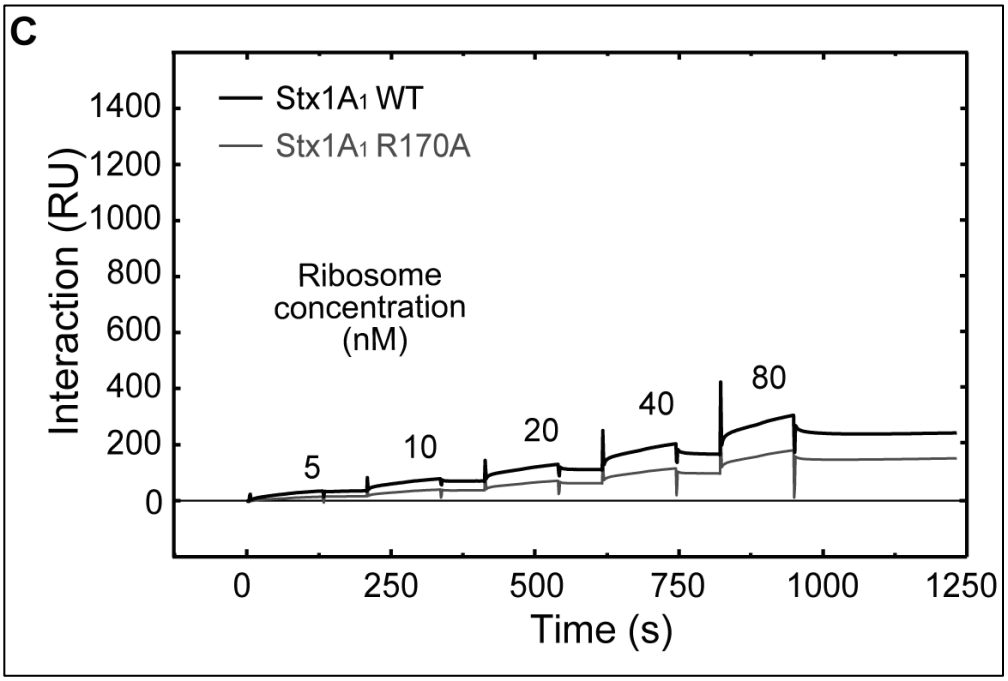

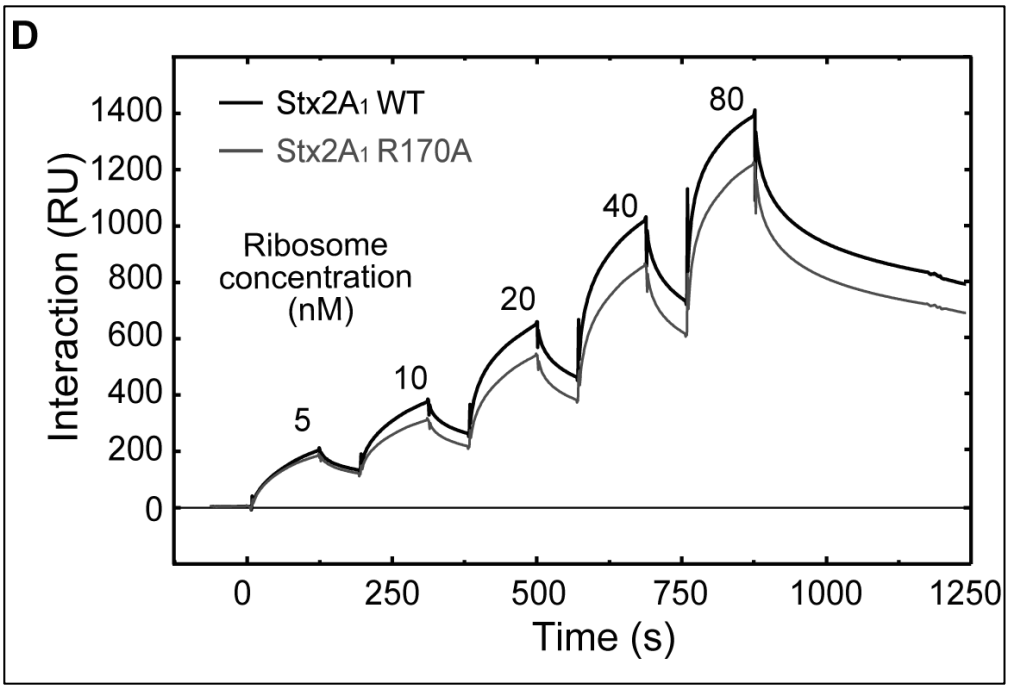

FIG 3.8 (C & D) Interaction of rat liver ribosomes with 10xHis-tagged WT Stx1A1, WT Stx2A1 and 10xHis-tagged R170A. 10xHis-Stx1A1, 10xHis-Stx2A1 and 10xHis-R170A variants were captured on a NTA chip at 1800 RU. Different concentrations of rat liver ribosomes were passed over the surface as analyte as shown.

DISCUSSION

Arginines on the distal face of the active site are critical for the depurination activity and toxicity of Stx1A1 and Stx2A1. Our recent results indicated that there are differences in the biphasic interaction of Stx1A1 and Stx2A1 with the ribosome (Basu, Li et al. 2016). Stx2A1 had a higher affinity for the ribosome and a higher catalytic activity in comparison to Stx1A1 in yeast and in mammalian cells. Examination of electrostatic surfaces of Stx1A1 and Stx2A1 indicated a number of differences (Basu, Li et al. 2016). A ~180° rotation along the y-axis revealed the positively charged zone, which was composed of several arginines and was larger and more exposed in Stx1A1 than in

Stx2A1 (Fig. 1) (Basu, Li et al. 2016). To determine if these differences contribute to the higher affinity of Stx2A1 for the ribosome we mutated Arg172, Arg176 and Arg179 previously shown to be critical for the interaction of Stx1A1 with P11 (McCluskey, Bolewska-Pedyczak et al. 2012) and examined the effect of these mutations on ribosome binding, depurination activity and toxicity. Point mutations at Arg179 did not show any obvious reduction in toxicity and depurination activity in either Stx1A1 or Stx2A1 in yeast (Fig. S1A and B). In contrast, R172A and R176A mutations led to a significant reduction in toxicity (Fig. 2A) and depurination activity (Fig. 2C). These results indicate that the three different arginines have different roles in depurination activity and toxicity of Stx1A1 and Stx2A1. Point mutations at Arg172 or Arg176 showed greater reduction in Stx1A1 than Stx2A1 compared to their respective WT, indicating that they are more critical for the depurination activity and toxicity of Stx1A1 than Stx2A1. These results demonstrate for the first time that arginines on the distal face of the active site are important for the depurination activity and toxicity of Stx1A1 and Stx2A1.

While there was a significant difference in the depurination levels among the Stx1A1 and Stx2A1 mutants in yeast, this difference was not apparent in the cytotoxicity assay, indicating that the absolute level of depurination does often not correlate with cytotoxicity (Yan, Li et al. 2012). In RTA at least two arginines had to be mutated in order to perturb the interaction between the toxin and the stalk pentamer or the ribosome before reduction toxicity was observed (Li, Kahn et al. 2013). Similarly in TCS, single point mutations reduced the interaction with the P2 protein while a triple mutation disrupted the interaction (Chan, Chu et al. 2007). The depurination levels of Stx2A1 single mutants on yeast (Fig. 3B and C) and rat liver ribosomes (Fig. 7A and B) were

consistently higher than Stx1A1 single mutants. Unlike the single mutations, the double and triple arginine mutations had similar effects and caused a more drastic reduction in Stx2A1 than Stx1A1 (Fig. S1 and Fig. 2).

The single arginine mutations were also effective in reducing translation inhibition and depurination in mammalian cells (Fig. 6A and B). However, the double arginine mutant led to a dramatic reduction in translation inhibition and depurination by Stx1A1 and Stx2A1 (Fig. 6A and B). We observed a very low level of depurination by Stx1A1, which may be due to reduced stability of Stx1A1 in mammalian cells. A recent study suggested that the truncation of more than 4-6 residues from the C-terminal end of the A subunits of Stx1 and Stx2 affects the stability of Stx1A more than Stx2A and may lead to a faster degradation in comparison to the WT in HeLa cells (Kymre, Simm et al. 2015). Since in our study A1 subunits are expressed without the A2 subunits, stability of Stx1A1 may be affected. Our results indicate that mutation of more than one arginine is required to cause a substantial reduction in the toxicity and depurination activity of Stx2A1. A plausible reason might be that Stx2A1 has higher catalytic activity than Stx1A1, since it depurinates naked RNA more efficiently than Stx1A1 even in the absence of ribosomal proteins (Fig. 3D and E) (Basu, Li et al. 2016). Further analysis is required to fully understand the basis for this variation.

Conserved arginines on the distal face of the active site are critical for the interaction of Stx1A1 and Stx2A1 with the ribosome and with the stalk pentamer. We previously showed that the interaction of RTA with yeast ribosomes by SPR did not fit 1:1 interaction model, but rather followed a two-step binding model (Li, Chiou et al.

2009). We proposed that the non-stalk-specific electrostatic interactions with the ribosome increase the local concentration of RTA on the ribosome and promote its diffusion to the stalk. Electrostatic interactions with the P-protein stalk stimulate the depurination activity of RTA by orienting RTA towards the SRL (Li, Kahn et al. 2013). Stx1A1 and Stx2A1 interactions with yeast (Fig. 4 and 5) or rat liver ribosomes (Fig. 8) did not follow a 1:1 interaction model, instead fit a biphasic model with an initial fast association-and-dissociation phase followed by a slower association-and-dissociation phase. Stx2A1 had a faster association and dissociation pattern with ribosomes in comparison to Stx1A1, but did not show a significant difference in its interaction with the purified stalk pentamer compared to Stx1A1 (Fig. 4) (Basu, Li et al. 2016). These results suggest that the differences in the interaction of Stx1A1 and Stx2A1 with the ribosome are not due to differences in their interaction with the stalk pentamer.

The R176A and R172A/R176A variants failed to show any interaction with the stalk pentamer or with ribosomes. Although R176A and R172A/R176A mutations affected the depurination of ribosomes by Stx1A1 and Stx2A1 and abolished ribosome binding, they had no effect on their depurination activity when RNA was used as a substrate (Fig. 3D and E). Thus the reduction in depurination activity of the arginine variants towards the ribosome is due to their inability to bind ribosomes and not due to the loss of their catalytic activity. Although R176A and R172A/R176A mutations caused a similar reduction in the affinity of Stx1A1 and Stx2A1 for the ribosomal stalk, they had a differential effect on their depurination activity. These results indicate that conserved arginines at the distal face of the active site are critical for the interaction of Stx1A1 and Stx2A1 with the P-protein stalk. However, the interaction of Stx1A1 and Stx2A1 with the

stalk is not responsible for the differences in the interaction of Stx1A1 and Stx2A1 with the ribosome.

Mutation of an arginine at the active site affects binding affinity of Stx1A1 and Stx2A1 for the ribosome, but not for the stalk pentamer. Early studies using the holotoxins identified Glu167 and Arg170 of the A1 subunits as important for catalytic activity (Hovde, Calderwood et al. 1988, Deresiewicz, Calderwood et al. 1992, Cao, Kurazono et al. 1994, Di, Kyu et al. 2011). The corresponding Arg180 in RTA is proposed to promote cleavage of the adenine by protonating position N3 of the adenine (Schlossman, Withers et al. 1989, Kim and Robertus 1992, Ho, Sturm et al. 2009), while the corresponding Glu177 polarizes a surrounding water molecule to produce a hydroxide ion that aids in the cleavage of adenine. In ricin, conversion of Glu177 to glutamine leads to a 180-fold loss in activity, conversion to an aspartate leads to a 80-fold reduction, while conversion to alanine leads to only a 20-fold loss (Schlossman, Withers et al. 1989, Ready, Kim et al. 1991). It is proposed that the nearby Glu208 can access the SRL due to the small size of the alanine side chain (Frankel, Welsh et al. 1990). The conversion of Glu167 to aspartate only led to a 3-fold reduction in Stx1 (Hovde, Calderwood et al. 1988). However conversion to a positively charged lysine led to a total loss of toxicity. Stx1A1 and Stx2A1 containing the E167K mutation had viability and depurination patterns similar to the empty vector. We were unable to purify this protein, probably as a result of the drastic change in folding of the active site. Conversion of Arg170 to alanine led to 16-fold reduction in the depurination activity of Stx1A1 and a 6-fold reduction in the depurination activity of Stx2A1. Stx1A1 R170A had 4.9-fold lower depurination

activity than Stx2A1 R170A (Fig. 2). We have reported that the region around the active site of Stx2A1 is neutral in comparison to a negatively charged region around the active site of Stx1A1 (Basu, Li et al. 2016). This difference in the surface charge may provide better access of Stx2A1 to the SRL, leading to the observed difference in depurination activity. We examined the effect of the R170A mutation on the interaction of Stx1A1 and Stx2A1 with yeast (Fig. 5A and B) and rat liver ribosomes (Fig. 8C and D). The association and dissociation patterns of this mutant were slightly lower than WT, and the apparent K_D values of both toxins were significantly different than WT (Table 1). We did not observe a significant effect of the R170A mutation on the interaction of either toxin with the purified stalk pentamer (Table 2), but observed differences in their interaction with the ribosome. These results indicate that a charge difference at a site away from the ribosomal stalk binding region affects the binding affinity of the toxins for the ribosome, but not the stalk pentamer, suggesting that Arg170 contributes to the accumulation of the toxins on the ribosome.

In summary, we used site-directed mutagenesis to identify the roles of the arginine residues on the distal face of the active site and at the active site in the interaction of Stx1A1 and Stx2A1 with ribosomes. Our results indicate that mutation of more than one arginine is required to reduce the toxicity and catalytic activity of Stx2A1 significantly in comparison to Stx1A1 in both yeast and mammalian cells. Arg176 and Arg172 play a role in the stalk-dependent interactions of Stx1A1 and Stx2A1 with the ribosome, while Arg170 enhances non-stalk specific interactions with the ribosome. These results demonstrate that conserved arginines at the stalk binding site or at the active site are critical for the interaction of Stx1A1 and Stx2A1 with the ribosome, their

depurination activity and toxicity, but they do not contribute to the higher affinity of Stx2A1 for the ribosome. Differences in surface charge residues in other protein regions likely contribute to the higher affinity of Stx2A1 compared to Stx1A1 for the ribosome. Our results demonstrate that depurination activity and toxicity of Stx1A1 and Stx2A1 are reduced by inhibiting their interactions with the ribosome, identifying toxin-ribosome interactions as a new target for inhibitor design against STEC infection.

REFERENCES

1. Ban, N., R. Beckmann, J. H. Cate, J. D. Dinman, F. Dragon, S. R. Ellis, D. L. Lafontaine, L. Lindahl, A. Liljas, J. M. Lipton, M. A. McAlear, P. B. Moore, H. F. Noller, J. Ortega, V. G. Panse, V. Ramakrishnan, C. M. Spahn, T. A. Steitz, M. Tchorzewski, D. Tollervey, A. J. Warren, J. R. Williamson, D. Wilson, A. Yonath and M. Yusupov (2014). "A new system for naming ribosomal proteins." Curr Opin Struct Biol **24**: 165-169.

2. Basu, D., X.-P. Li, J. N. Kahn, K. L. May, P. C. Kahn and N. E. Tumer (2016). "The A1 Subunit of Shiga Toxin 2 Has Higher Affinity for Ribosomes and Higher Catalytic Activity than the A1 Subunit of Shiga Toxin 1." Infection and immunity **84**(1): 149-161.

3. Bergan, J., A. B. D. Lingelem, R. Simm, T. Skotland and K. Sandvig (2012). "Shiga toxins." Toxicon **60**(6): 1085-1107.

4. Boerlin, P., S. McEwen, F. Boerlin-Petzold, J. Wilson, R. Johnson and C. Gyles (1999). "Associations between virulence factors of Shiga toxin-producing *Escherichia coli* and disease in humans." Journal of Clinical Microbiology **37**(3): 497-503.

5. Cao, C., H. Kurazono, S. Yamasaki, K. Kashiwagi, K. Igarashi and Y. Takeda (1994). "Construction of mutant genes for a non-toxic verotoxin 2 variant

(VT2vp1) of Escherichia coli and characterization of purified mutant toxins." Microbiol Immunol **38**(6): 441-447.

6. Chan, D. S., L.-O. Chu, K.-M. Lee, P. H. Too, K.-W. Ma, K.-H. Sze, G. Zhu, P.-C. Shaw and K.-B. Wong (2007). "Interaction between trichosanthin, a ribosome-inactivating protein, and the ribosomal stalk protein P2 by chemical shift perturbation and mutagenesis analyses." Nucleic acids research **35**(5): 1660-1672.

7. Chan, D. S., L. O. Chu, K. M. Lee, P. H. Too, K. W. Ma, K. H. Sze, G. Zhu, P. C. Shaw and K. B. Wong (2007). "Interaction between trichosanthin, a ribosome-inactivating protein, and the ribosomal stalk protein P2 by chemical shift perturbation and mutagenesis analyses." Nucleic acids research **35**(5): 1660-1672.

8. Chiou, J.-C., X.-P. Li, M. Remacha, J. P. Ballesta and N. E. Tumer (2011). "Shiga toxin 1 is more dependent on the P proteins of the ribosomal stalk for depurination activity than Shiga toxin 2." The international journal of biochemistry & cell biology **43**(12): 1792-1801.

9. Chiou, J. C., X. P. Li, M. Remacha, J. P. Ballesta and N. E. Tumer (2008). "The ribosomal stalk is required for ribosome binding, depurination of the rRNA and cytotoxicity of ricin A chain in Saccharomyces cerevisiae." Mol Microbiol **70**(6): 1441-1452.

10. Choi, A. K., E. C. Wong, K. M. Lee and K. B. Wong (2015). "Structures of eukaryotic ribosomal stalk proteins and its complex with trichosanthin, and their implications in recruiting ribosome-inactivating proteins to the ribosomes." Toxins (Basel) **7**(3): 638-647.

11. Clementi, N., A. Chirkova, B. Puffer, R. Micura and N. Polacek (2010). "Atomic mutagenesis reveals A2660 of 23S ribosomal RNA as key to EF-G GTPase activation." Nature Chemical Biology **6**(5): 344-351.

12. Deresiewicz, R. L., S. B. Calderwood, J. D. Robertus and R. J. Collier (1992). "Mutations affecting the activity of the Shiga-like toxin I A-chain." Biochemistry **31**(12): 3272-3280.

13. Di, R., E. Kyu, V. Shete, H. Saidasan, P. C. Kahn and N. E. Tumer (2011). "Identification of amino acids critical for the cytotoxicity of Shiga toxin 1 and 2 in Saccharomyces cerevisiae." Toxicon **57**(4): 525-539.

14. Diaconu, M., U. Kothe, F. Schlunzen, N. Fischer, J. M. Harms, A. G. Tonevitsky, H. Stark, M. V. Rodnina and M. C. Wahl (2005). "Structural basis for the function of the ribosomal L7/12 stalk in factor binding and GTPase activation." Cell **121**(7): 991-1004.

15. Endo, Y., K. Tsurugi, T. Yutsudo, Y. Takeda, T. Ogasawara and K. Igarashi (1988). "Site of action of a Vero toxin (VT2) from *Escherichia coli* O157: H7 and

of Shiga toxin on eukaryotic ribosomes." European Journal of Biochemistry **171**(1-2): 45-50.

16. Frankel, A., P. Welsh, J. Richardson and J. Robertus (1990). "Role of arginine 180 and glutamic acid 177 of ricin toxin A chain in enzymatic inactivation of ribosomes." Molecular and cellular biology **10**(12): 6257-6263.

17. Gonzalo, P. and J. P. Reboud (2003). "The puzzling lateral flexible stalk of the ribosome." Biol Cell **95**(3-4): 179-193.

18. Grela, P., X. P. Li, M. Tchorzewski and N. E. Tumer (2014). "Functional divergence between the two P1-P2 stalk dimers on the ribosome in their interaction with ricin A chain." Biochem J **460**(1): 59-67.

19. Ho, M.-C., M. B. Sturm, S. C. Almo and V. L. Schramm (2009). "Transition state analogues in structures of ricin and saporin ribosome-inactivating proteins." Proceedings of the National Academy of Sciences **106**(48): 20276-20281.

20. Hovde, C. J., S. B. Calderwood, J. J. Mekalanos and R. J. Collier (1988). "Evidence that glutamic acid 167 is an active-site residue of Shiga-like toxin I." Proc Natl Acad Sci U S A **85**(8): 2568-2572.

21. Kim, Y. and J. D. Robertus (1992). "Analysis of several key active site residues of ricin A chain by mutagenesis and X-ray crystallography." Protein Eng. **5**(8): 775-779.

22. Kimmitt, P. T., C. R. Harwood and M. R. Barer (2000). "Toxin gene expression by shiga toxin-producing Escherichia coli: the role of antibiotics and the bacterial SOS response." Emerging infectious diseases **6**(5): 458.

23. Krokowski, D., A. Boguszewska, D. Abramczyk, A. Liljas, M. Tchorzewski and N. Grankowski (2006). "Yeast ribosomal P0 protein has two separate binding sites for P1/P2 proteins." Mol Microbiol **60**(2): 386-400.

24. Kymre, L., R. Simm, T. Skotland and K. Sandvig (2015). "Different roles of the C-terminal end of Stx1A and Stx2A for AB5 complex integrity and retrograde transport of Stx in HeLa cells." Pathogens and disease **73**(9): ftv083.

25. Li, X.-P., J.-C. Chiou, M. Remacha, J. P. Ballesta and N. E. Tumer (2009). "A two-step binding model proposed for the electrostatic interactions of ricin a chain with ribosomes." Biochemistry **48**(18): 3853-3863.

26. Li, X.-P., P. C. Kahn, J. N. Kahn, P. Grela and N. E. Tumer (2013). "Arginine residues on the opposite side of the active site stimulate the catalysis of ribosome depurination by ricin A chain by interacting with the P-protein stalk." Journal of Biological Chemistry **288**(42): 30270-30284.

27. Li, X. P., J. C. Chiou, M. Remacha, J. P. Ballesta and N. E. Tumer (2009). "A two-step binding model proposed for the electrostatic interactions of ricin a chain with ribosomes." Biochemistry **48**(18): 3853-3863.

28. Li, X. P., P. Grela, D. Krokowski, M. Tchorzewski and N. E. Tumer (2010). "Pentameric organization of the ribosomal stalk accelerates recruitment of ricin a chain to the ribosome for depurination." J Biol Chem **285**(53): 41463-41471.

29. Li, X. P., P. C. Kahn, J. N. Kahn, P. Grela and N. E. Tumer (2013). "Arginine residues on the opposite side of the active site stimulate the catalysis of ribosome depurination by ricin A chain by interacting with the P-protein stalk." J Biol Chem **288**(42): 30270-30284.

30. McCluskey, A., E. Bolewska-Pedyczak, N. Jarvik, G. Chen, S. Sidhu and L. Johannes (2012). "Charged and hydrophobic surfaces on the A chain of Shiga-Like Toxin 1 recognize the C-terminal domain of ribosomal stalk proteins." PLoS One **7**(2): e31191.

31. McCluskey, A. J., G. M. Poon, E. Bolewska-Pedyczak, T. Srikumar, S. M. Jeram, B. Raught and J. Gariepy (2008). "The Catalytic Subunit of Shiga-like Toxin 1 Interacts with Ribosomal Stalk Proteins and is Inhibited by Their Conserved C-Terminal Domain." J Mol Biol **378**(2): 375-386.

32. McGannon, C. M., C. A. Fuller and A. A. Weiss (2010). "Different classes of antibiotics differentially influence Shiga toxin production." Antimicrobial agents and chemotherapy **54**(9): 3790-3798.

33. Pierce, M., J. N. Kahn, J. Chiou and N. E. Tumer (2011). "Development of a quantitative RT-PCR assay to examine the kinetics of ribosome depurination by ribosome inactivating proteins using *Saccharomyces cerevisiae* as a model." RNA **17**(1): 201-210.

34. Ready, M. P., Y. Kim and J. D. Robertus (1991). "Site‐directed mutagenesis of ricin A‐chain and implications for the mechanism of action." Proteins: Structure, Function, and Bioinformatics **10**(3): 270-278.

35. Sandvig, K. and B. van Deurs (2005). "Delivery into cells: lessons learned from plant and bacterial toxins." Gene therapy **12**(11): 865-872.

36. Schlossman, D., D. Withers, P. Welsh, A. Alexander, J. Robertus and A. Frankel (1989). "Role of glutamic acid 177 of the ricin toxin A chain in enzymatic inactivation of ribosomes." Molecular and cellular biology **9**(11): 5012-5021.

37. Shi, X., P. K. Khade, K. Y. Sanbonmatsu and S. Joseph (2012). "Functional role of the sarcin–ricin loop of the 23S rRNA in the elongation cycle of protein synthesis." Journal of Molecular Biology **419**(3): 125-138.

38. Siegler, R. and R. Oakes (2005). "Hemolytic uremic syndrome; pathogenesis, treatment, and outcome." Curr Opin Pediatr **17**(2): 200-204.

39. Spahn, C. M., E. Jan, A. Mulder, R. A. Grassucci, P. Sarnow and J. Frank (2004). "Cryo-EM visualization of a viral internal ribosome entry site bound to human ribosomes: the IRES functions as an RNA-based translation factor." Cell **118**(4): 465-475.

40. Steel, R. G., H. James, D. A. Dickey, H. T. James and A. D. David (1997). "Principles and procedures of statistics: a biometrical approach." McGraw-Hill series in probability and statistics.

41. Tarr, P. I., C. A. Gordon and W. L. Chandler (2005). "Shiga-toxin-producing Escherichia coli and haemolytic uraemic syndrome." The Lancet **365**(9464): 1073-1086.

42. Too, P. H., M. K. Ma, A. N. Mak, Y. T. Wong, C. K. Tung, G. Zhu, S. W. Au, K. B. Wong and P. C. Shaw (2009). "The C-terminal fragment of the ribosomal P protein complexed to trichosanthin reveals the interaction between the ribosome-inactivating protein and the ribosome." Nucleic Acids Res **37**(2): 602-610.

43. Yan, Q., X. P. Li and N. E. Tumer (2012). "N‐glycosylation Does Not Affect the Catalytic Activity of Ricin A Chain but Stimulates Cytotoxicity by Promoting Its Transport Out of the Endoplasmic Reticulum." Traffic **13**(11): 1508-1521.

44. Zhang, T., J. Lei, H. Yang, K. Xu, R. Wang and Z. Zhang (2011). "An improved method for whole protein extraction from yeast Saccharomyces cerevisiae." Yeast **28**(11): 795-798.

SUPPLEMENT:

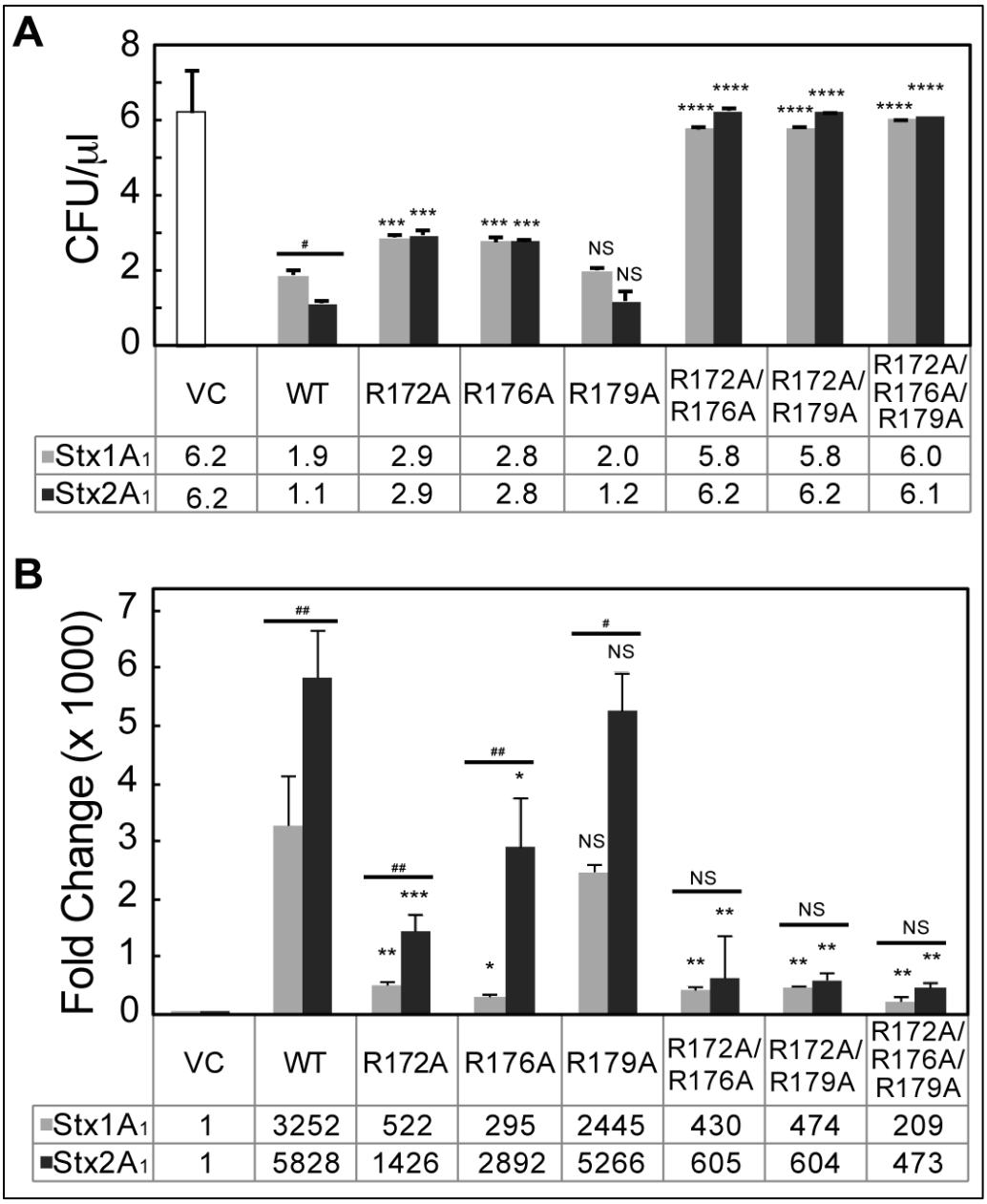

FIG 3. S1. (A) Viability and ribosome depurination in yeast expressing wild type (WT) or mutant Stx1A1 or Stx2A1. Yeast cells transformed with a plasmid carrying wild type (WT) or mutant Stx1A1 or Stx2A1 and yeast cells carrying the empty vector (VC) were grown in SD medium supplemented with 2 % glucose and then transferred to SD medium supplemented with 2 % galactose. At 0 and 4 hours post induction (hpi), a

series of 10-fold dilutions were plated on media containing 2 % glucose and grown at 30°C for 1-2 days. Colony forming units per ml (CFU/ml) were calculated at 4 hpi from at least 3 independent transformants. Error bars represent S. E. where n=3 independent experiments. **(B) Depurination of ribosomes in yeast.** Total RNA (375 ng) isolated from 1 OD_{600} cells expressing wild type (WT) or mutant Stx1A1 (grey bars) or Stx2A1 (black bars) collected at 1 hpi was used to quantify the relative level of depurination using qRT-PCR. The y-axis shows the fold change in depurination of toxin-treated samples over the control samples without toxin (VC). Error bars represent S. E. where n=3 replicates.

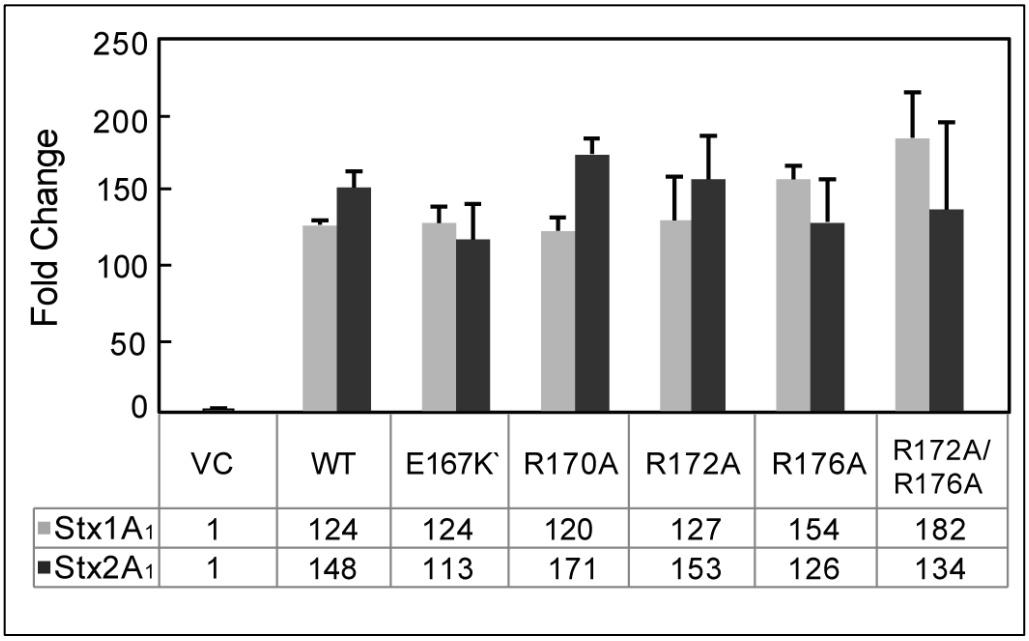

	VC	WT	E167K`	R170A	R172A	R176A	R172A/ R176A
Stx1A1	1	124	124	120	127	154	182
Stx2A1	1	148	113	171	153	126	134

3. S2. Shiga toxin Gene Expression in Vero by qPCR. 375 ng of the total RNA isolated from 6 wells of Vero cells expressing Stx1A1 (grey bars) or Stx2A1 (black bars) collected at 23 hour post DNA exposure were used to quantify the relative levels of Shiga gene expression using qRT-PCR by the comparative CT method (CT). The Stx1A1 primers were Stx1_qPCR_F5' aatgtcgcatagtggaacctca 3' and Stx1_qPCR_R 5' aacatcgctcttgccacagac 3', while the Stx2 primers were Stx2_qPCR_F5' gtatacgatgacgccgggag 3' and Stx2_qPCR_R 5' attcgcccccagttcagagt 3'. β-actin was used as internal control. The y-axis shows the fold change of toxin-gene carrying samples over the control samples without toxin gene (VC). Results (means ± standard errors of the means [SEM]) represent 2 independent biological replicates.

Table 3. S1. EGFP fluorescence Statistical Significance of the Contrasts

Contrast	DF	Contrast SS	Mean Square	F value	Pr > F
Compare Stx1A1 E167K with WT	**1**	**1926072.2**	**1926072.2**	**23.4**	**<0.0001**
Compare Stx1A1 R170A with WT	**1**	**64729.9**	**64729.9**	**0.8**	**0.3764**
Compare Stx1A1 R172A with WT	**1**	**926894.9**	**926894.9**	**11.3**	**0.1009**
Compare Stx1A1 R176A with WT	**1**	**51003.4**	**51003.4**	**0.62**	**0.4322**
Compare Stx1A1 R172A/R176A with WT	**1**	**1119635.7**	**1119635.7**	**13.6**	**0.0003**
Compare Stx2A1 E167K with WT	**1**	**4538565.2**	**4538565.2**	**55.11**	**<0.0001**
Compare Stx2A1 R170A with WT	**1**	**40687.8**	**40687.8**	**0.5**	**0.4829**
Compare Stx2A1 R172A with WT	**1**	**161.7**	**161.7**	**0**	**0.9647**
Compare Stx2A1 R176A with WT	**1**	**207220.4**	**207220.4**	**2.5**	**0.1142**
Compare Stx2A1 R172A/R176A with WT	**1**	**851309.2**	**851309.2**	**10.3**	**0.0015**

*To test the differences of treatment means in data presented in Fig. 6B, PROC GLM in SAS was used to compute contrasts for pairwise comparisons between each variant and their respective WT in $Stx1A_1$ and $Stx2A_1$ (for trait EGFP Fluorescence, *in cell*). The Contrast statement in PROC GLM produces contrast sums of square, mean square, F value, and corresponding p value for each LS-mean difference comparison computed. Reported P values were adjusted for multiple comparisons using the Tukey-Kramer option within PROC GLM. There are highly significant differences between variant and their respective WT in $Stx1A_1$ and $Stx2A_1$.

Table 3. S2. *In cell* depurination Statistical Significance of the Contrasts

Contrast	DF	Contrast SS	Mean Square	F value	Pr > F
Compare Stx1A1 E167K with WT	**1**	**1460.7**	**1460.7**	**0.2**	**0.6597**
Compare Stx1A1 R170A with WT	**1**	**572.5**	**572.5**	**0.08**	**0.7827**
Compare Stx1A1 R172A with WT	**1**	**565.9**	**565.9**	**0.08**	**0.7839**
Compare Stx1A1 R176A with WT	**1**	**157.2**	**157.2**	**0.02**	**0.8851**
Compare Stx1A1 R172A/R176A with WT	**1**	**403.3**	**403.3**	**0.5**	**0.8169**
Compare Stx2A1 E167K with WT	**1**	**557806.8**	**557806.8**	**74.47**	**<0.0001**
Compare Stx2A1 R170A with WT	**1**	**324382.5**	**324382.5**	**43.31**	**<0.0001**
Compare Stx2A1 R172A with WT	**1**	**284548.8**	**284548.8**	**37.99**	**<0.0001**
Compare Stx2A1 R176A with WT	**1**	**87699.3**	**87699.3**	**11.71**	**0.0009**
Compare Stx2A1 R172A/R176A with WT	**1**	**597926.4**	**597926.4**	**79.83**	**<0.0001**

*To test the differences of treatment means in data presented in Fig. 6B, PROC GLM in SAS was used to compute contrasts for pairwise comparisons between each variant and their respective WT in $Stx1A_1$ and $Stx2A_1$ (for trait depurination, *in cell*). The Contrast statement in PROC GLM produces contrast sums of square, mean square, F value, and corresponding p value for each LS-mean difference comparison computed. Reported P values were adjusted for multiple comparisons using the Tukey-Kramer option within PROC GLM. There are highly significant differences between variant and their respective WT in $Stx2A_1$.

CHAPTER 4: Surface charge residues away from the ribosome stalk binding site may play a role in Stx1A1 and Stx2A1 depurination.

RESULTS

Stx1 and Stx2 holotoxins have a 55% and 57% similarity in their A and B subunits respectively and are immunologically distinct (Tesh and O'Brien 1991). Although the active side amino acid residues and the ribosome stalk binding site residues are conserved in both the toxins (Basu, Li et al. 2016), a number of differences are observed when the crystallographic structures of the A1 subunits of the toxins are compared (Fig 4.1). Stx1A1 has a pronounced negatively charged knob near the top of the molecule. It is composed primarily of glutamic acids 60 and 61 with a contribution from aspartic acid 58. There is no such knob in Stx2A1, as the corresponding residues are Y60 and Q61, which occupy a nearly all white vertical band above and to the left of the positively charged zone.

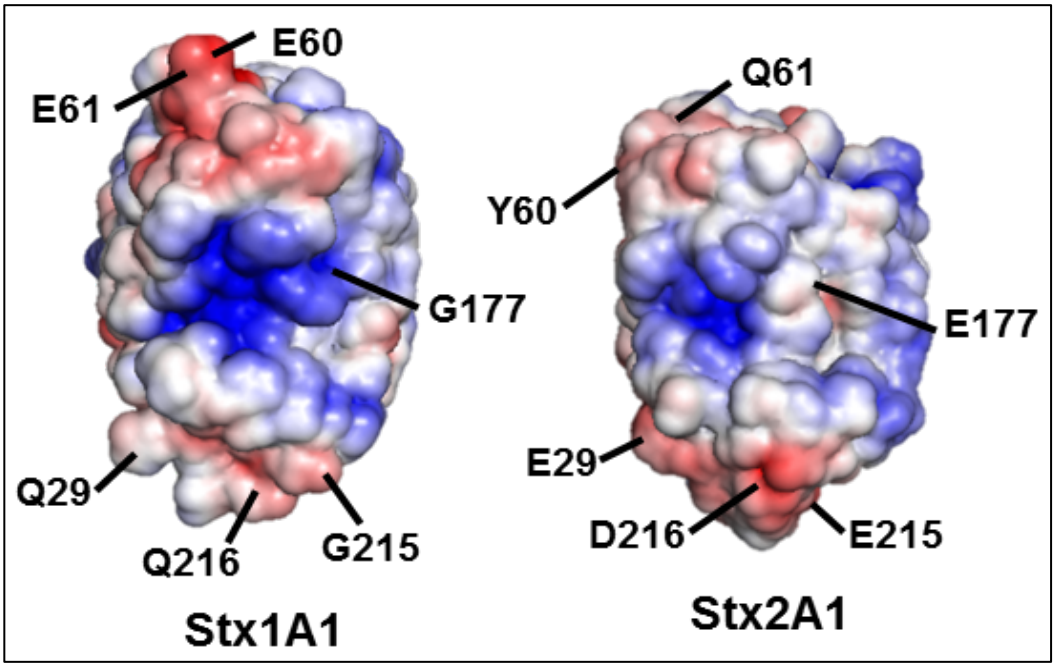

FIG 4.1 Crystallographic structure of Stx1A1 and Stx2A1 showing electrostatic charge distribution. The A1 subunits of Shiga toxin and Shiga toxin 2 were modeled from the Protein Data Bank ID: 1DM0 [Shiga toxin] and 1R4P [Shiga toxin 2]) as described earlier. The surface charge difference between Stx1A1 and Stx2A1 subunit is shown (Red: negative charge; Blue: positive charge; White: neutral).

We were interested to see whether this negative charge on Stx1A1 contributes to its inability to access the negatively charged ribosome and the RNA, in comparison to the neutral charge on Stx2A1. We therefore interchanged the residues between Stx1A1 and Stx2A1, mutating the glutamic acids E60 and E61 in Stx1A1 to Y and Q, and changing the Y60 and Q61 in Stx2A1 to glutamic acids (E). The WT and mutant forms of Stx1A1 and Stx2A1 was then transformed in yeast under the control of GAL1 promoter, and their viability was determined by inducing them in galactose containing liquid media for 4 hours and then plating serial dilutions on media containing glucose. The colony forming unit/μl of each of the WT and mutant strains based on this viability assay is represented in Fig. 4.2A. At 4 hours post induction, the wild type (WT) Stx1A1 and Stx2A1 are significantly different from each other and Stx2A1 is less viable than Stx2A1. The WT as well as the variants were still toxic in comparison to the empty vector. However, while there is a reduction in viability for E60Y/E61Q mutant in Stx1A1 and an increase in viability for Y60EQ61E in Stx2A1, the difference was not statistically significant (Fig. 4.2A).

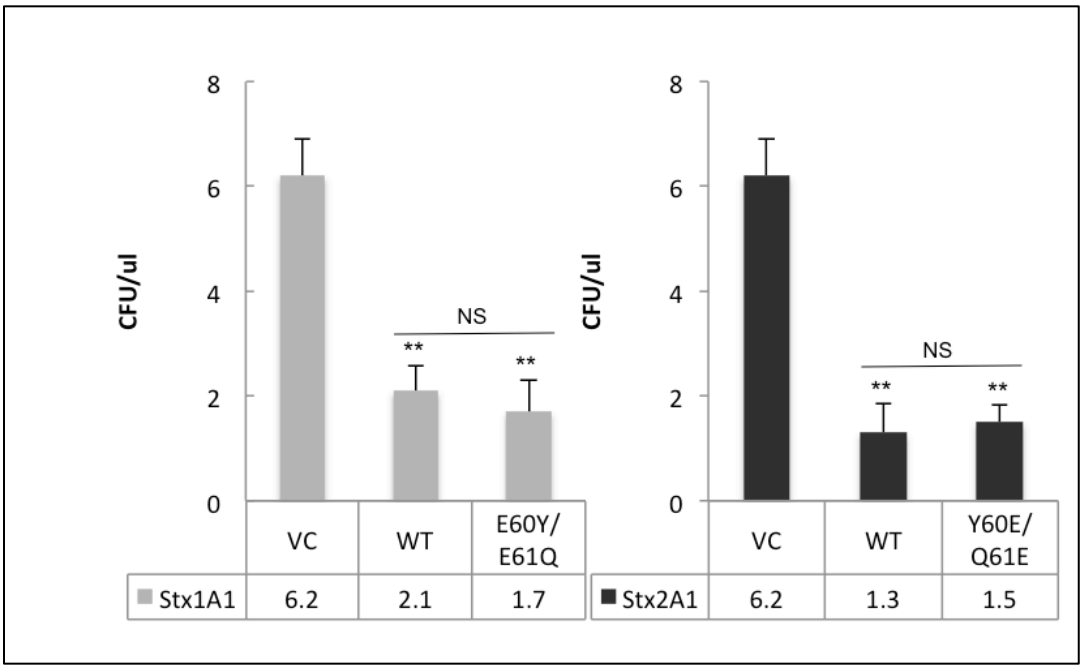

FIG 4.2 (A) Viability in yeast expressing wild type (WT) or mutant Stx1A1 or Stx2A1. Yeast cells transformed with a plasmid carrying wild type (WT) or mutant Stx1A1 or Stx2A1 and yeast cells carrying the empty vector (VC) were grown in SD medium supplemented with 2 % glucose and then transferred to SD medium supplemented with 2 % galactose. At 0 and 4 hours post induction (hpi), a series of 10-fold dilutions were plated on media containing 2 % glucose and grown at 30°C for 1-2 days. Colony forming units per ml (CFU/ml) were calculated at 4 hpi from at least 3 independent transformants. Error bars represent S. E. where n=3 independent experiments. Means of Stx1A1, Stx2A1 and their variants were significantly different using two-sample t-test (*P<0.05, **P< 0.01, NS= Not significant).

The expression of the WT Stx1A1 and Stx2A1 and their variants in yeast was analyzed by immunoblot analysis at 6 hpi with monoclonal antibodies against the V5 epitope (Fig. 4.2B). Total protein was extracted and loaded on a 12% gel and monoclonal

antibodies against phosphoglycerate kinase 1 (Pgk1) were used as a loading control. At 6 hour post induction both the WT and the mutants showed expression in comparison to the empty vector (Fig. 4.2B).

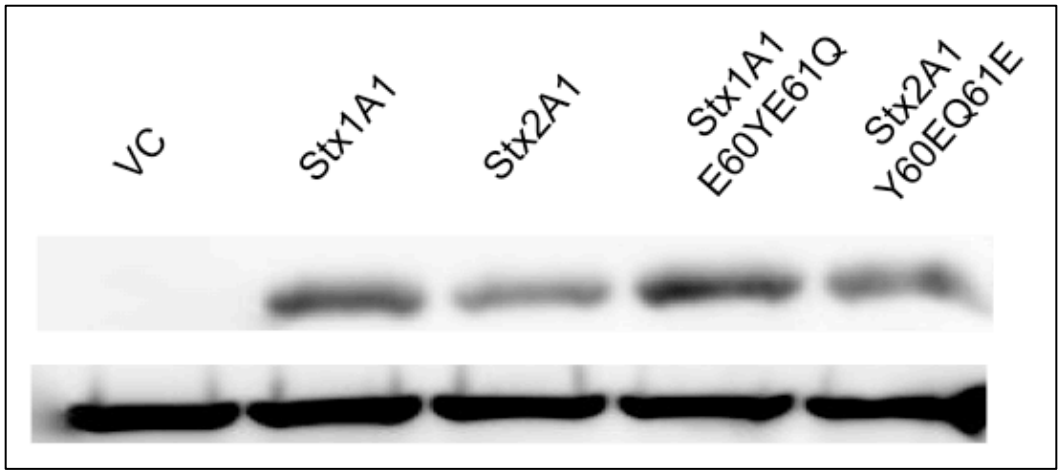

FIG 4.2 (B) Immunoblot analysis of yeast cells transformed with wild type (WT) or mutant of Stx1A1 and Stx2A1. Total protein from 5 OD_{600} cells isolated at 6 hpi was separated on SDS-PAGE and probed with anti-V5. Anti-Pgk1 was used as a loading control.

The depurination in yeast cells of the WT and the variants was measured using a previously described quantitative reverse transcriptase polymerase chain reaction (qRT-PCR) assay (Pierce, Kahn et al. 2011). Total RNA was collected from yeast cells at 1 hpi and their depurination was compared using the comparative CT method (ΔΔCT) relative to yeast harboring the empty vector (Fig. 4.2C). Both the variants E60Y/E61Q mutant in Stx1A1 and Y60EQ61E in Stx2A1, had a significant change in their depurination level in comparison to their respective WT. There was an increase in the depurination level of

E60Y/E61Q mutant in Stx1A1 in comparison to the WT (Fig. 4.2C). On the other hand, there was a decrease in depurination activity of Y60EQ61E in Stx2A1. Collectively, this data suggests that the negatively charged knob on Stx1A1 comprising of two glutamic acids contributes to the lower depurination activities of Stx1A1 in comparison to Stx2A1 (Fig. 4.2C).

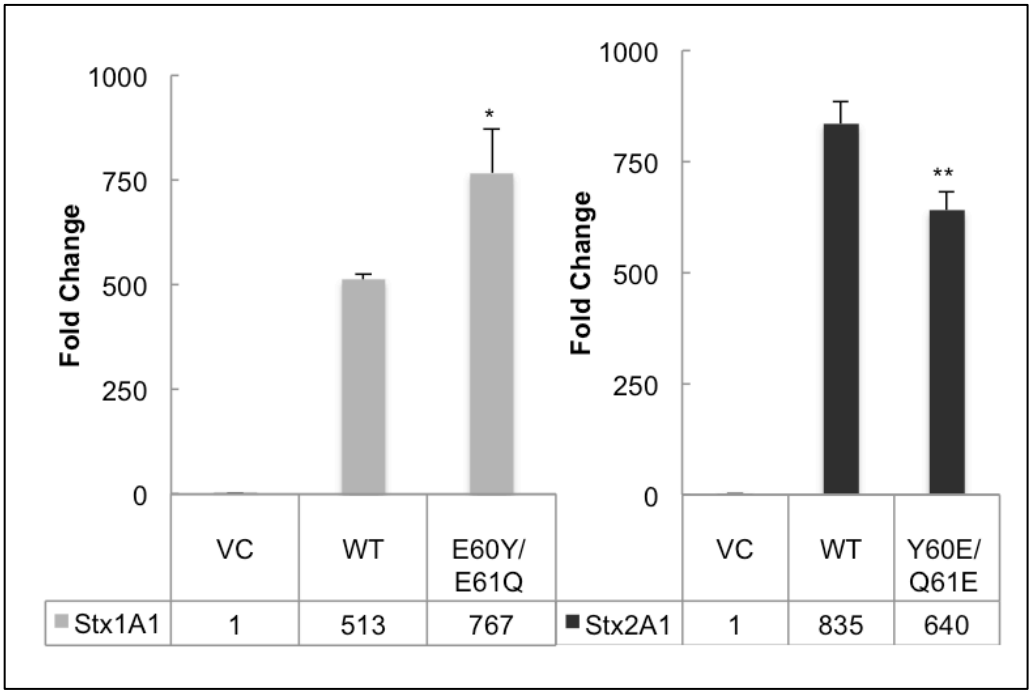

FIG 4.2 (C) Depurination of ribosomes in yeast. Total RNA (375 ng) isolated from 1 OD_{600} cells expressing wild type (WT) or mutant Stx1A1 (grey bars) or Stx2A1 (black bars) collected at 1 hpi was used to quantify the relative level of depurination using qRT-PCR. The y-axis shows the fold change in depurination of toxin-treated samples over the control samples without toxin (VC). Error bars represent S. E. where n=3 replicates. Means of Stx1A1, Stx2A1 and their variants were significantly different using two-sample t-test (*P< 0.05, **P<0.01, NS= Not significant).

DISCUSSION

Therapeutics effective at preventing and/or treating HUS caused by Stx1 and 2 are currently unavailable and only supportive care is used in treatment (Kimmitt, Harwood et al. 2000, Tarr, Gordon et al. 2005, McGannon, Fuller et al. 2010). Thus, a basic understanding of how these toxins function to harm host cells is critical for preventing illnesses following inadvertent or intentional exposure. Although the structures of Stx and Stx2 are similar, the sequence divergence between Stx2A1 and Stx1A1 has some influence on the structure (Basu, Li et al. 2016). Previously we have shown that the A1 subunit of Stx2 is catalytically more active and depurinates both naked RNA as well as ribosomes at a higher rate than the A1 subunit of Stx1A1 (Basu, Li et al. 2016). Stx2A1 also has a higher affinity for the ribosome than Stx1A1 (Basu, Li et al. 2016). We have also discussed (Chapter 3) although the active site residues (E167 and R170) and the ribosome stalk binding site residues (R172, R176, R179) between the toxins are conserved, their surface exposure and the surrounding residues may influence their functions differently. R170A in Stx2A1 still depurinates at a higher level than R170A in Stx1A1, which may be responsible for the higher catalytic activity of Stx2A1 than Stx1A1 as previously reported (Basu, Li et al. 2016). Further, mutations of more than one arginine at the ribosome stalk binding site (R172A/R176A) is required for the reduction of Stx2A1 in comparison to Stx1A1. We were interested to investigate the role of residues away from the active site and ribosome stalk binding site in Stx1A1 and Stx2A1 toxicity. In the published structure of holotoxins of Stx1 and Stx2, some of the loops in the A1 subunits were missing. We have reconstructed the missing loops in the A1 subunits of Stx and Stx2 in the holotoxins as previously described (Di, Kyu et al. 2011).

We observe that the electrostatic surfaces of Stx1A1 and Stx2A1 show a number of differences. Stx1A1 has a pronounced negatively charged knob near the top of the molecule composed of E60 and E61, which is missing in Stx2A1, as the corresponding residues are Y60 and Q61. Near the bottom of the structure on the left Stx2A1 has a negatively charged group, E29, which Stx1A1 lacks, the residue at this position in the Stx1A1 is Q29, which appears as a nearly neutral (white) protuberance. Stx2A1 also has a negatively charged region at the very bottom of the molecule consisting of E215 and D216. Stx1A1 has G215 and Q216 forming a neutral projection at the bottom.

In this study, we interchanged E60 and E61 in Stx1A1 with Y60 and Q61 in Stx2A1 to examine the effect of these mutations on depurination activity and toxicity of Stx1A1 and Stx2A1 by expressing each mutant in yeast and analyzing their viability and depurination activity. As can be seen in Fig. 4.1A, these mutants are still very toxic in comparison to the empty vector. Further, we were unable to detect any significant difference in viability between the E60Y/E61Q in Stx1A1 and Y60E/Q61E in Stx2A1 and their corresponding WTs. However when we measured their depurination rate, there was a significant increase in the depurination of E60Y/E61Q in Stx1A1 and a significant decrease in depurination of Y60E/Q61E in Stx2A1 in comparison to their WT (Fig. 4.2C). Since depurination is an upstream event in comparison to cell death and viability, and it is a more quantitative and sensitive assay in comparison to the viability assay it brings forth the effects of surface charge modifications of Stx1A1 and Stx2A1 in depurination. The negatively charged knob on Stx1A1 plays a role in the depurination activities of Stx1A1, probably by influencing the binding of the Stx1A1 toxin to the negatively charged ribosome and the sarcin/ricin loop (SRL). By converting the glutamic

acids at position 60 and 61 in Stx1A1 to neutral Y and Q, the negatively charged ribosome becomes more accessible. This is further corroborated by the fact that the depurination level of Stx2A1 is reduced when the neutral Y and Q at positions 60 and 61 is changed to the negative glutamic acids. The Stx2A1 mutant is now repelled by the negatively charged ribosome and therefore shows lower depurination. These results indicate that electrostatic interaction of the toxins with the ribosome is critical.

This is the first study that shows residues away from the active site and ribosome stalk binding site, which are not conserved between Stx1A1 and Stx2A1 play a role in Stx1A1 and Stx2A1 viability and depurination. Here we are mutating only 2 residues and therefore the changes observed are small although they are significant. In order to observe a larger difference, more than two residues need to be simultaneously altered in order to change the electrostatic charge distribution sufficiently.

Future work includes purification of E60Y/E61Q and Y60E/Q61E mutants in Stx1A1 and Stx2A1 respectively, and examining their depurination activity on purified monomeric yeast ribosomes and naked RNA. We are also interested to see, how these charge alteration affect the interaction of these toxins with ribosome as well as the stalk pentamer through surface plasmon resonance assay. This will give us valuable information on the role of residues other than those present in the ribosome stalk binding site, in ribosome interactions.

REFERENCES

1. Basu, D., X.-P. Li, J. N. Kahn, K. L. May, P. C. Kahn and N. E. Tumer (2016). "The A1 Subunit of Shiga Toxin 2 Has Higher Affinity for Ribosomes and Higher Catalytic Activity than the A1 Subunit of Shiga Toxin 1." Infection and immunity **84**(1): 149-161.

2. Di, R., E. Kyu, V. Shete, H. Saidasan, P. Kahn and N. Tumer (2011). "Identification of amino acids critical for the cytotoxicity of Shiga toxin 1 and 2 in *Saccharomyces cerevisiae*." Toxicon **57**(4): 525-539.

3. Kimmitt, P. T., C. R. Harwood and M. R. Barer (2000). "Toxin gene expression by shiga toxin-producing Escherichia coli: the role of antibiotics and the bacterial SOS response." Emerging infectious diseases **6**(5): 458.

4. McGannon, C. M., C. A. Fuller and A. A. Weiss (2010). "Different classes of antibiotics differentially influence Shiga toxin production." Antimicrobial agents and chemotherapy **54**(9): 3790-3798.

5. Pierce, M., J. N. Kahn, J. Chiou and N. E. Tumer (2011). "Development of a quantitative RT-PCR assay to examine the kinetics of ribosome depurination by ribosome inactivating proteins using *Saccharomyces cerevisiae* as a model." RNA **17**(1): 201-210.

6. Tarr, P. I., C. A. Gordon and W. L. Chandler (2005). "Shiga-toxin-producing Escherichia coli and haemolytic uraemic syndrome." The Lancet **365**(9464): 1073-1086.

7. Tesh, V. and A. O'Brien (1991). "The pathogenic mechanisms of Shiga toxin and the Shiga-like toxins." Molecular microbiology **5**(8): 1817-1822.